Non-invasive assessment of the conjunctival microcirculation in patients with coronary and valvular heart disease

Author
Mailey , Jonathan

Non-invasive assessment of the conjunctival microcirculation in patients with coronary and valvular heart disease

A thesis presented to The Faculty of Life and Health Sciences of

Ulster University

for the degree of Doctor of Medicine

by

Jonathan Andrew Mailey

MBChB 2012

MRCP 2016

Submitted July 2022

I confirm that the word count of this thesis is less than 60,000 words

Contents

Preface

Cardiovascular disease is a leading cause of both morbidity and mortality worldwide. A large proportion of cardiovascular disease remains symptomatically quiescent until first presentation with either a myocardial infarction or sudden cardiac death. This principle forms the basis for the performance of cardiovascular risk screening to guide clinicians in the initiation of primary preventative therapies. Conventional cardiovascular screening focuses on the identification of pre-existing risk factors. An increasing emphasis is being placed on the use of vascular imaging modalities that can identify evidence of asymptomatic atherosclerotic heart disease, and hence predict risk of a future adverse cardiovascular event.

Our collaborative research group have developed a novel non-invasive approach for imaging the conjunctival microcirculation. The chapters enclosed in this thesis recap the previous work from other members of our research group and describe in full the assessment of the conjunctival microcirculation in distinct cardiovascular diseases; including myocardial infarction, coronary microvascular disease and severe aortic valve stenosis. The indices of conjunctival microvascular function obtained from these cohorts are presented in comparison to age- and sex-matched controls. This thesis therefore highlights the potential utility for conjunctival vascular imaging in both the identification of systemic microvascular dysfunction and in cardiovascular disease primary prevention.

Acknowledgements

I wish to record my thanks to the following individuals:

- Dr Mark Spence has provided support and guidance to me throughout this project. He is an ongoing inspiration and role model to me in both his clinical and academic practice.
- Professor Tara Moore for her leadership, advice and dedication to the project.
- Professor Andrew Nesbit for his guidance and commitment to the project.
- Miss Julie Moore has demonstrated incredible commitment and dedication to this project that has gone over and above what would be expected.
- Ms Min Jing has provided extensive technical input with regard to the computational engineering aspects of this project and her input has been invaluable.

Contributions to this Thesis

In the studies described in this thesis, I was personally responsible for the recruitment of all participants. All blood sampling was performed by myself. Blood sample processing and conjunctival vascular imaging was performed by both myself and Miss Julie Moore. All of the manual differentiation of blood vessel type was performed by myself and the application based semi-automated analysis of conjunctival haemodynamic parameters was performed by Miss Julie Moore.

I confirm that am solely responsible for the writing of all sections of this thesis. The statistical analyses described herein were undertaken by myself with assistance from Miss Julie Moore only with respect to the power calculations reported.

Publications and presentations relevant to this thesis

Publications

1. Brennan PF, McNeil AJ, Jing M, Awuah A, Finlay DD, Blighe K, McLaughlin JAD, Wang R, Moore J, Nesbit MA, Trucco E, Spence MS, Moore TCB. Quantitative assessment of the conjunctival microcirculation using a smartphone and slit-lamp biomicroscope. Microvasc Res. 2019 Nov;126:103907. doi: 10.1016/j.mvr.2019.103907. Epub 2019 Jul 19. PMID: 31330150.

2. Brennan PF, McNeil AJ, Jing M, Awuah A, Moore JS, Mailey J, Finlay DD, Blighe K, McLaughlin JAD, Nesbit MA, Trucco E, Moore TCB, Spence MS. Assessment of the conjunctival microcirculation for patients presenting with acute myocardial infarction compared to healthy controls. Sci Rep. 2021 Apr 7;11(1):7660. doi: 10.1038/s41598-021-87315-7. PMID: 33828174; PMCID: PMC8027463.

3. Brennan PF, Jing M, McNeil AJ, Awuah A, Mailey J, Kelly B, Finlay DD, Blighe K, McLaughlin JAD, Nesbit MA, Trucco E, Lockhart CJ, Moore TCB, Spence MS. Assessment of the conjunctival microcirculation in adult patients with cyanotic congenital heart disease compared to healthy controls. Microvasc Res. 2021 Jul;136:104167. doi: 10.1016/j.mvr.2021.104167. Epub 2021 Apr 7. PMID: 33838207.

4. Awuah A, Moore JS, Nesbit MA, Ruddock MW, Brennan PF, Mailey JA, McNeil AJ, Jing M, Finlay DD, Trucco E, Kurth MJ, Watt J, Lamont JV, Fitzgerald P, Spence MS, McLaughlin JAD, Moore TCB. A novel algorithm for cardiovascular screening using conjunctival microcirculatory parameters and blood biomarkers. Sci Rep. 2022 Apr 21;12(1):6545. doi: 10.1038/s41598-022-10491-7. PMID: 35449196; PMCID: PMC9023476.

Submissions awaiting decision

1. Chapter 3 has been submitted to The American Journal of Cardiology
2. Chapter 4 has been submitted to The American Heart Journal

The content of the above chapters is unchanged from the above journal submissions, with the exception of minor formatting changes only to meet the requirements of Ulster University for thesis submission.

Presentations

1. A Novel Method of Conjunctival Vascular Screening to Detect Hemodynamic Alterations in Patients with Coronary Microvascular Disease
    a. Presented at American Heart Association (AHA) Scientific Sessions 2021

2. INOCA affects more than the coronaries
    a. Presentation at the European Society of Cardiology (ESC) Annual Congress 2022
3. Non-invasive assessment of systemic microvascular function in patients with severe aortic stenosis pre- and post- transcatheter aortic valve intervention
    a. Submitted for presentation to American Heart Association (AHA) Scientific Sessions 2022

Abstract

Cardiovascular (CV) disease often remains asymptomatic until first presentation with a major adverse cardiovascular event. CV risk assessment is therefore recommended in asymptomatic adults to identify individuals with modifiable vascular risk factors. Changes in the microcirculation occur early in atherosclerotic cardiovascular disease and therefore identification of asymptomatic microvascular dysfunction may allow CV risk recategorisation. The microvasculature of the bulbar conjunctiva can be assessed non-invasively using a combination of a smartphone and slit-lamp biomicroscope.

This project sought to determine if differences could be observed in parameters of conjunctival microvascular function in patients with coronary artery or valvular heart disease in comparison to age- and sex-matched control cohorts.

Chapter 3 describes the comparison of 66 patients with acute myocardial infarction (MI) and 61 controls with angiographically non-obstructive coronary arteries and no history of MI or coronary intervention. In the MI cohort, significant reductions were observed in conjunctival axial- and cross-sectional velocity, blood flow and wall shear rate.

Chapter 4 describes the comparison of 43 patients with invasive evidence of coronary microvascular dysfunction (CMD) and 68 controls with no obstructive coronary artery disease, or invasive evidence of CMD. In the CMD cohort, significant reductions were observed in conjunctival arteriole axial- and cross-sectional velocity, blood flow, wall shear rate and wall shear stress.

Chapter 5 describes the comparison of 90 patients with severe aortic stenosis (SAS) undergoing TAVI and 75 controls with no significant valvular heart disease. There were sex-specific differences in conjunctival microvascular haemodynamics in females in the SAS cohort in comparison to controls. In this sub-group significant increases in arteriole axial- and cross-sectional velocity and wall shear rate were observed following TAVI.

This thesis reports alterations in systemic microvascular function in patients with MI, CMD and SAS. These findings suggest the possible utility of conjunctival microvascular screening in CV risk assessment.

Word count = 299

Chapter 1

Background and literature review

The pathophysiology of cardiovascular disease

Cardiovascular disease (CVD) is a broad term encompassing a group of disorders. The World Health Organisation (WHO) use the term CVD to describe coronary artery disease (CAD), valvular heart disease (VHD), peripheral vascular disease (PVD), cerebrovascular disease, systemic hypertension, congenital heart disease, rheumatic heart disease and cardiomyopathies of both hereditary and non-hereditary origin (WHO, 2021). These disorders can occur either in isolation, or in combination with each other. The development of CVD is influenced by a number of factors that can be both modifiable (e.g. smoking, diet. obesity, hypertension and hyperlipidaemia) and non-modifiable (e.g. genetic predisposition).

The majority of CVD arises due to vascular atherosclerosis. This process affects the vascular intima, can involve any arterial bed in the body and is characterized by the deposition of intimal plaques (Hennekens et al, 1993). The underlying process of atherosclerosis is characterized by a chronic inflammatory process of the arterial wall that occurs at predilection sites with disturbed laminar flow (Moore et al, 2011). It is initiated by endothelial dysfunction and structural alterations, including the absence of a confluent luminal elastin layer and the exposure of proteoglycans, which permit subendothelial accumulation of low-density lipoprotein (LDL) (Kwon et al, 2008). These plaques grow with the proliferation of fibrous tissues and the surrounding smooth muscle and bulge inside arteries. Connective

tissue production by fibroblasts and deposition of calcium in the lesion causes sclerosis (Rafieian-Kopaei et al, 2014).

Atherosclerotic plaques progress slowly over time, eventually creating arterial luminal narrowing and hence obstruction to blood flow. Atherosclerosis can therefore manifest clinically with symptoms such as angina (coronary arteries) or intermittent claudication (ileo-femoral arteries) depending on the organ supplied by the affected vascular bed. Atherosclerotic plaques can also become unstable and rupture with resultant thrombosis, vessel occlusion and infarction in the supplied territory (e.g. myocardial infarction or stroke). The rate of atherosclerotic plaque progression is dependent on the individualised patient risk factors detailed above.

Cardiovascular disease epidemiology

The World Health Organisation (WHO) estimate that worldwide, CVD accounts for 17.9 million deaths/year (World Health Statistics, 2020). Cardiovascular disease (CVD) is a major cause of morbidity and premature mortality within the United Kingdom (UK). The modern era of primary and secondary prevention has resulted in a significant decline in mortality, with a 70% reduction in the incidence of death from CVD between 1979 and 2013 (Bhatnagar et al, 2016). Despite this decline, CVD remains the second most common cause of death in the UK

(Townsend et al, 2015). The reduction in CVD mortality has not been accompanied by a reduction in the overall prevalence of the condition. Between 2003/04 and 2014/15 this has remained constant at 3-4% within the UK (Bhatnagar et al, 2016).

Coronary artery disease (CAD) and cerebrovascular disease represent the majority of CVD within the UK, accounting for up to 75% of CVD-related deaths per year (Townsend et al, 2015).

The economic impact of cardiovascular disease

In addition to the health burden of CVD, there is a significant economic cost at both a national and international level. In 2015 costs related to CVD in the UK were estimated at €26 billion (Wilkins et al, 2017). All current CVD prevention guidelines advocate the assessment of total CV risk in order to guide lifestyle, environmental and pharmacological interventions. A report from the National Institute for Health and Care Excellence (NICE) estimated that a UK national programme which reduced CV risk by 1% would prevent 25,000 CVD cases and generate savings of €40 million/year (Collins et al, 2014).

Cardiovascular risk prediction and primary prevention

CVD risk assessment is advocated by current international cardiology guidelines in order to identify individuals at increased risk of future major adverse cardiovascular events (MACE). The European Society of Cardiology (ESC) suggest that screening should be performed in individuals with any major vascular risk factor (i.e. family history of CVD, familial history of hereditary dyslipidaemias, smoking history, systemic hypertension, diabetes mellitus, hypercholesterolaemia, obesity or any other relevant CVD co-morbidity). ESC also suggest considering CVD screening in the general population in men >40 years of age and in women >50 years of age in the absence of established CVD risk factors (Visseren et al, 2021). The main goal of performing risk assessment is to address any modifiable risk factors for CVD, institute guideline recommended pharmacological therapies and hence attempt to improve the patients' longer-term prognosis. CVD screening can be performed either opportunistically (in individuals attending medical services for an alternative reason) or systematically (as part of a formal population screening programme).

Opportunistic screening relies on both individuals coincidentally attending for an alternative purpose and on the motivation of the involved practitioners to engage in this practice. Studies suggest that opportunistic screening is effective at both increasing detection rates of known cardiovascular risk factors and improving risk factor control, however the

net benefit with respect to a reduction in CVD mortality is less certain (Si et al, 2014). Systematic population screening programmes are associated with a significant financial cost to healthcare systems, with much debate as to both the cost-effectiveness and clinical benefit of such strategies (Patel et al, 2020 & Mehta et al, 2014).

Conventional CVD risk assessment in patients without established disease largely focusses on the use of CV risk calculators that take into consideration the patient's age, gender and a variety of known risk factors for CVD. The ESC advocate the Systematic Coronary Risk Estimation 2 (SCORE 2) assessment tool in patients less than 70 years of age and the SCORE 2-OP (older persons) tool in patients greater than 70 years of age (Visseren et al, 2021). Both SCORE 2 and SCORE 2-OP are only applicable to patients without a history of either established CVD; or a condition that automatically confers an intermediate - very high CV risk category (e.g. chronic kidney disease, familial hypercholesterolaemia or diabetes mellitus). Both SCORE 2 and SCORE 2-OP take into consideration the following risk factors:

- Age
- Sex
- Smoking history
- Systolic blood pressure (SBP)
- Non-HDL cholesterol

Figure 1.1. Example of SCORE 2 and SCORE 2-OP CVD risk calculator (Visseren et al, 2021)

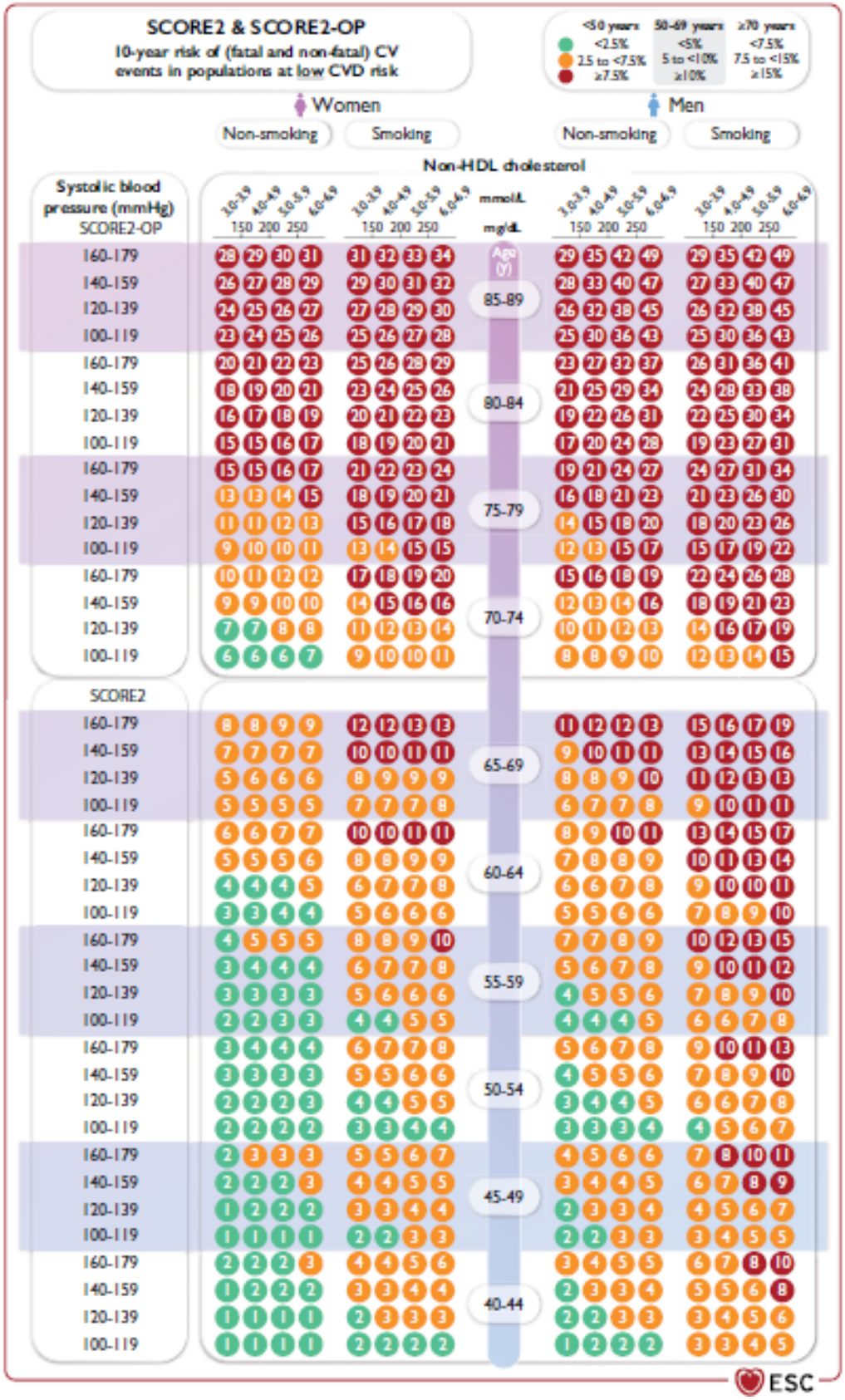

The National Institute for Clinical Excellence (NICE) advocate the use of an alternative risk calculator called Q-RISK 3 (Cardiovascular disease: risk assessment and reduction, including lipid modification, NICE, 2016). Q-RISK 3 considers additional risk factors for CVD in addition to the above incorporated in SCORE 2. These include:

- Ethnicity
- Family history of premature CAD
- Atrial fibrillation
- Migraine
- Rheumatological conditions such as rheumatoid arthritis and systemic lupus erythematosus
- Mental health issues
- Medications that predispose to CVD (atypical antipsychotics and steroids)
- Body mass index (BMI)

Regardless of the particular CVD risk calculator that is used, the result is a percentage estimation of the individual's risk of a MACE (fatal or non-fatal) in the next 10 years. This allows patients to be categorised into low, intermediate, high and very high-risk categories. The first purpose of these categories is to inform the patient in clear and understandable language what their future CV risk is and allow them to identify and adjust modifiable risks, thereby moving them into a lower risk category. The second purpose of the calculators is to provide clinicians with both a guide

for the required intensity of primary preventative therapies and clear targets for modifiable risks such as blood pressure and lipids. These targets should not detract from the importance of patient education regarding the benefits of lifestyle interventions (dietary changes, exercise, weight loss and smoking cessation).

Modifiers to conventional cardiovascular risk assessment

In addition to the conventional CVD risk factors, a variety of additional factors have been associated with increased CV risk, however the process for the integration of these into standardised CV risk assessment is less well established (Visseren et al, 2021). ESC recommend consideration of a potential modifier if it fulfils the following criteria:

- it improves measures of risk prediction
- the public health impact is clear
- it is feasible in routine practice
- information is not only available on how risk increases with the unfavourable result, but also how risk decreases if the modifier is successfully addressed
- the literature on the modifier is not distorted by publication bias

Imaging investigations to augment CV risk assessment

An area of clinical interest in preventative cardiology is the utility of additional radiological investigations to re-classify an individuals' CV risk

category primarily based on the identification of asymptomatic atherosclerotic cardiovascular disease (ASCVD), and thus allow a more targeted and individualised approach to CV prevention. The most extensively researched of these are described below.

Coronary artery calcium scoring

Coronary artery calcium (CAC) scoring involves the acquisition of non-contrast computed tomographic (CT) images of the coronary artery tree. The attenuation of coronary calcification can be automatically highlighted by cardiologists/radiologists in a semi-automated fashion. A total CAC score can then be calculated for the patient. This CAC score is then compared to an age- and sex-matched population. Both any degree of CAC and a higher than average CAC score have been shown to correlate with an increased CV risk in several studies discussed below.

CAC scoring has been incorporated in current ESC prevention guidelines (Visseren et al, 2021) as a consideration (class IIb recommendation) for CV screening. In contrast, results of a large systemic review of the available evidence by the US preventive services task force (Lin et al, 2018) suggested inadequate clinical evidence to date to advise the systemic rollout of population screening with CAC scoring. However, this finding is not due to the failure of clinical evidence to demonstrate the ability of CAC scoring to define CV risk, but rather the lack of evidence

that demonstrates a clear benefit with regards to CVD mortality reduction with lifestyle modifications and primary preventative therapies following CAC assessment. This review included evaluation of 1 randomised control trial and 19 non-randomised studies, which are summarised in **Table 1.1**.

Table 1.1. Summary of trials demonstrating the ability for CT CAC scoring to predict cardiovascular risk and augment conventional risk assessment tools

Study	Objective	Design	Results
Rozanski et al, 2011 (n= 2,137)	Prospective randomised trial comparing the clinical impact of CAC scoring in addition to conventional CV risk assessment	- 2 cohorts (CAC vs no CAC) - Primary end-point- 4 year change in CAD risk factors and Framingham risk score	- CAC scoring associated with a reduction in mean increase in Framingham risk score (0.002 ± 4.9 vs 0.7 ± 5.1, p = 0.003) - CAC scoring associated with reduction in conventional risk factors (SBP, LDL and waist circumference)
Yeboah et al, 2016	Assessment of the predictive value and utility with respect to CV	- Retrospective analysis participants of the MESA study who had	- CAC score was an independent predictor of MACE (HR 2.06, 95% CI 1.86 – 2.29, p<0.001)

(n= 5,185)	risk reclassification of CAC, ABPI, CRP and FHx of ASCVD	undergone the relevant investigations - All participants were asymptomatic with no established CVD and not taking statin therapy	- CAC score modestly improved the discriminative ability of the PCE
Bos et al, 2015 (n= 2,408)	Comparison of atherosclerotic calcification in major vessel beds on the risk of all-cause and cause-specific mortality	- Sub-study from the Rotterdam study - All patients underwent CT and grading of coronary, aortic, extracranial and intracranial vessel calcification - Groups based on severity vessel calcification volume	- Severity of CAC correlated to CV mortality - Dividing patients by quartiles of calcium score, the highest quartile vs lowest quartile predicted a 5-fold increase in CV mortality

Chang et al, 2015 (n=988)	Prospective observational study of CAC scoring, EST and MPI to predict long-term events in patients at low cardiovascular risk	- Patients deemed to have low CV risk by the FRS underwent testing with CAC, EST and MPI - Cardiac events were defined as a composite of cardiac death, non-fatal myocardial infarction, and the need for coronary revascularization	- CAC score significantly improved long-term risk stratification beyond FRS, ETT, and MPI across the spectrum of clinical risk - CAC score ≤10 AU= 0.6% 1yr MACE incidence - CAC score >400 AU= 3.7% 1yr MACE incidence
Elias-Smale et al, 2010 (n= 2,028)	Evaluation of the effect of CAC on 10 year CV risk to derive cut-off values of the CAC score for a general	- Sub-study from the Rotterdam study - Patients divided into low, intermediate and high CV risk based on FRS	- Reclassification by means of CAC scoring was most substantial in persons initially classified as intermediate risk

	population of elderly patients	- Risk reclassified based on CAC score	- 52% of those at intermediate risk were reclassified based on CAC - CAC values >615 or <50 AU were found appropriate to reclassify persons into high or low risk, respectively
Mohlenkamp et al, 2010 (n=4,129)	Determine the ability of CAC score to improve CV risk prediction	- Baseline traditional risk factors and CAC score performed - FRS and National Cholesterol Education Panel ATP III categories used to classify risk	- NRI= 21.7% ($p = 0.0002$) for the FRS - NRI= 30.6% ($p < 0.0001$) for the National Cholesterol Education Panel ATP III categories - IDI using FRS variables and CAC was 1.52% ($p < 0.0001$)

		- Intermediate risk participants reclassified to low if CAC <100 AU and high if ≥400 AU	- Adding CAC scores to the FRS and National Cholesterol Education Panel ATP III categories improved the area under the curve from 0.681 to 0.749 ($p < 0.003$) and from 0.653 to 0.755 ($p = 0.0001$), respectively.
Fudim et al, 2016 (n= 6,742)	Establish the ability for CAC score to reclassify CV risk across multiple genders and ethnicities	- Post-hoc analysis of data from participants of the MESA study - Comparison of the predictive abilities of the ASCVD score with and without the addition of CAC score	- The NRI and IDI suggested that CAC improved the discriminatory abilities of conventional risk assessment in male, female, Caucasian and African American participants, but failed to meet

			statistical significance in Chinese American and Hispanic populations
Geisel et al, 2017 (n=3,108)	Comparison of coronary artery calcification, carotid intima-media thickness and ankle-brachial index for predicting 10-year incident cardiovascular events in the general population	- Patients with no established CVD - Incidence of MACCE assessed - Mean follow-up of 10.3 ± 2.8 years - A cut-off of CAC ≥100 AU used to evaluate CAC scoring	- CAC score was an independent predictor of MACCE adjusting for age and sex (HR 1.27, 95% CI 1.19 – 1.35, p<0.001), conventional CV risk factors (HR 1.24, 95% CI 1.16 – 1.32, p<0.001), and FRS (HR 1.31, 95% CI 1.23 – 1.39, p<0.001)
Greenland et al, 2004	Assessment of CAC score in combination	- Prospective observational population study	- A CAC score >300 AU compared to zero was a predictor of the primary

(n=1,461)	with FRS for CV risk assessment in asymptomatic adults	- Asymptomatic participants - Participants underwent CAC score if at least 1 coronary risk factor - Primary endpoint of non-fatal MI of CV death - A cut-off value of CAC >300 AU used to compare risk	endpoint (HR 3.9, 95% CI 2.1 – 7.3, p<0.001) - CAC score was predictive of CV risk in patients classified as intermediate to high risk by the FRS score
Hoffmann et al, 2016 (n=3,217)	Determination of whether vascular and valvular calcification predicted incident CVD, and all-cause mortality	- Sub-study of the Framingham Heart Study - Participants divided into 4 CAC score groups (0, 1-100, 101-300 and >300 AU)	- CAC significantly improved discriminatory value beyond risk factors for CHD (AUC 0.78-0.82; NRI 32%, 95% CI 11 - 53) but not for CVD - CAC accurately reclassified 85% of the 261 patients who were at

	independent of Framingham risk factors		intermediate (5-10%) 10-year risk for coronary heart disease based on Framingham risk factors to either low risk (n=172; no events observed) or high risk (n=53; observed event rate 8%)
Kavousi et al, 2016 (n=6,739)	To assess the potential utility of CAC testing for CVD risk estimation and stratification among low-risk women.	- Women with 10-year ASCVD risk lower than 7.5% from 5 previous studies - CAC scoring had been performed in all participants - Primary endpoint was MACCE	- In individuals with CAC of 0 AU, the MACCE rate was 1.41 vs 4.33 per 1000 person years in those with CAC >1 AU (multivariable-adjusted HR 2.04, 95% CI 1.44 - 2.90)

Kavousi et al, 2012 (n=5,933)	To assess whether newer risk markers for CHD risk prediction and stratification improve FRS predictions	- All participants asymptomatic with no established CVD - Evaluation of the predictive value of multiple newer in addition to conventional CVD risk factors	- CAC score most significantly improved risk classification in addition to FRS score - c-statistic increase, 0.05 (95% CI, 0.02 to 0.06) - NRI 19.3% overall (39.3% in those at intermediate risk, by FRS)
Malik et al, 2011 (n=6,603)	Evaluation of whether screening patients with diabetes and mellitus and metabolic syndrome using CAC scoring or CIMT	- Population taken from the MESA study database - Evaluation of incidence of presentation with CVD	- Patients with metabolic syndrome and CAC of 0 AU had an annual CVD event rate of 0.2% vs 3.5% in those with CAC ≥400 AU - Patients with diabetes and CAC of 0 AU had an annual CVD event rate of

	improved CVD risk stratification		0.4% vs 4.0% in those with CAC ≥400 AU - Adjusting for age, sex, ethnicity and FRS, CAC was predictive of CHD events (HR 2.0, 95% CI 1.5 – 2.6) in those with diabetes and those with metabolic syndrome (HR 2.2, 95% CI 1.7 – 2.9)
Mohlenkamp et al, 2011 (n=3,966)	Evaluation of whether the combined presence of CAC and CRP improves discrimination and stratification of	- Asymptomatic participants with no established CVD - Primary endpoint was 5 year incidence of coronary related	- CAC independently predicted 91 coronary events [(log(2)(CAC+1) HR 1.25, 95% CI: 1.16 - 1.34, p < 0.0001]; and 130 deaths

	MACE in the general population.	death, non-fatal MI and all-cause mortality	[(log(2)(CAC+1) HR 1.12, 95% CI 1.06 - 1.19] - For coronary events, NRI was 23.8% for CAC (p = 0.0007)
Polak et al, 2017 (n=6,500)	Evaluation of the predictive value of CIMT and CAC scoring in incident CHD prediction	- Data from the MESA study - Median follow-up was 10.2 years - Primary endpoint of the incidence of CHD events - CIMT score added to 2 models (model 1 with conventional risk factors and model 2 with conventional risk factors and CAC score)	- A CIMT score based on normative data incrementally adds to Framingham risk factors and a positive calcium score in predicting first-time CHD in an ethnically diverse cohort. - By adding CIMT to FRS and CAC combined, the AUC increased significantly (p=0.018) from 0.7627

		-	(95% CI 0.7419 - 0.7836) to 0.7714 (95% CI 0.7506 - 0.7923) and the NRI was 5.0%
Rana et al, 2012 (n=1,286)	Comparison of the value of coronary artery calcium and multiple blood biomarkers for prognostication of CV events	- Asymptomatic participants with no known coronary disease - Mean follow-up 4.1 ± 0.4 years - Primary endpoint of combined CVD (cardiac death, myocardial infarction, stroke, and late target vessel revascularization)	- Presence of log CAC beyond FRS was associated with increased hazards for CVD events (HR 1.7, 95% CI 1.4 - 2.0, p <0.001) - The c-statistic increased when log CAC was incorporated into FRS without or with multiple biomarkers score (c-statistic 0.84, p = 0.003 and p = 0.008 respectively).

			- Addition of CAC to risk factors showed significant reclassification (NRI 0.35, 95% CI 0.11 to 0.58, p = 0.007; IDI 0.076, p = 0.0001)
Polonsky et al, 2010 (n=6,814)	To determine whether adding CAC score to a prediction model based on traditional risk factors improves classification of risk	- Sub-study from the MESA study - Participants without known CVD who had undergone CAC scoring recruited - Comparison of 2 prediction models (model 1 with conventional risk factors alone and model 2 with the addition of CAC)	- Model 2 resulted in significant improvements in risk prediction compared with model 1 (NRI 0.25, 95% CI 0.16 - 0.34, p <0.001) - In model 1, 69% of the cohort was classified in the highest or lowest risk categories compared with 77% in model 2

			- An additional 23% of those who experienced events were reclassified as high risk, and an additional 13% without events were reclassified as low risk using model 2
Wong et al, 2009 (n=2,303)	Comparison of CAC and thoracic aortic calcium to predict CV events	- Asymptomatic adults recruited to have CT thorax and subsequent calcium scoring of both coronaries and thoracic aorta - Patients divided into groups of increasing CAC (0, 1-9, 10-99, 100-399 and ≥400 AU)	- The FRS-adjusted hazard ratios across increasing CAC groups (relative to CAC <10 AU) ranged from 3.7 ($p = 0.04$) to 19.6 ($p < 0.001$) for CHD and from 2.8 ($p = 0.07$) to 13.1 ($p < 0.001$) for CVD events

			- CAC, but not thoracic aortic calcium was strongly related to CHD and CVD events
Yeboah et al, 2014 (n=1,343)	Development of a new diabetes CHD risk estimator using traditional risk factors plus CAC, ABPI, CRP, family history of CHD, and CIMT	- Data taken from diabetic patients without clinical CVD in the MESA and Heinz Nixdorf Recall studies	- Among the novel risk markers, CAC best predicted CHD independent of the FRS [log (CAC +25): HR 1.69, 95% CI 1.45 - 1.97, p < 0.0001] - CAC categories: CAC ≤ 25 as reference; >25 and ≤125: HR 2.29, 95% CI 0.87 - 5.95; >125 and ≤400: HR 3.87, 95% CI 1.57-9.57; >400: HR 5.97, 95% CI 2.57-13.84

Yeboah et al, 2012 (n=1,330)	Comparison of the improvement in prediction of incident CVD events of 6 novel CV risk factors (CAC, CIMT, ABPI, brachial flow-mediated dilation, CRP, and family history of CHD) within intermediate-risk participants	- Retrospective analysis of participants of the MESA study deemed to have intermediate CV risk - Probability-weighted Cox proportional hazard models were used to estimate hazard ratios. - AUC and NRI were used to compare incremental contributions of each marker when added to the FRS, plus race/ethnicity - Primary endpoint was a composite of myocardial infarction, angina followed by revascularization,	- CAC was an independent predictor of the primary endpoint (HR 2.60, 95% CI 1.94 - 3.50) - Although addition of the markers individually to the FRS plus race/ethnicity improved AUC, CAC afforded the highest increment (0.623 vs 0.784)

		resuscitated cardiac arrest and CHD related death	

Abbreviations- CAC= coronary artery calcium, CV= cardiovascular, CAD= coronary artery disease, SBP= systolic blood pressure, LDL= low density lipoprotein, ABPI= ankle brachial pressure index, CRP= C-reactive protein, FHx= family history, ASCVD= atherosclerotic cardiovascular disease, MESA=multi-ethnic study of atherosclerosis, MACE= major adverse cardiovascular event, CT= computed tomography, EST= exercise stress test, MPI= myocardial perfusion imaging, FRS= Framingham risk score, AU= Agatston units, HR= hazard ratio, NRI= net reclassification index, IDI= integrated discrimination improvement, MACCE= major adverse cardiovascular or cerebrovascular event, CIMT= carotid intima-media thickness

Computed tomographic coronary angiography

Computed tomographic coronary angiography (CTCA) unlike the more simplistic CAC scoring involves intravenous injection of iodinated contrast, followed by a very precisely timed acquisition of CT chest imaging in time with the cardiac cycle. This allows not only quantification of coronary calcium burden (non-contrast phase), but evaluation of non-calcified coronary atheroma and the degree of coronary luminal obstruction created by atherosclerotic plaques. CTCA has a very clear and well-defined role in the evaluation of symptomatic patients with stable coronary artery disease (Knuuti et al, 2019). CTCA has also been shown to be beneficial in risk stratification in patients with stable angina. The SCOT HEART trial (Newby et al, 2018) demonstrated a reduction in the composite endpoint of CV death or non-fatal myocardial infarction (MI) in patients with chest pain evaluated with CTCA vs standard of care (2.3% vs. 3.9%; hazard ratio, 0.59; [95% CI], 0.41 to 0.84; P=0.004).

Another smaller study evaluated CTCA in 1256 patients undergoing investigation of chest pain. This studied compared the composite endpoint of CV mortality, MI, or unstable angina presentation in those that received CTCA to the estimated risk according to the conventional Framingham risk score (FRS). In this study the primary endpoint occurred in 0.6% and 1.8%, respectively (p=0.01) suggesting the utilisation of CTCA in chronic coronary disease resulted in a reduction in MACE (Hadamitzky et al, 2009).

The role of CTCA in primary prevention is less established, however is under active investigation at present in the SCOT HEART 2 trial evaluating CTCA in addition to conventional risk calculators for the evaluation of asymptomatic patients between 40 and 70 years of age (results awaited, ClinicalTrials.gov identifier: NCT03920176).

Carotid ultrasound

Ultrasonography of the carotid blood vessels can be performed to measure carotid intima-media thickness (CIMT). However, evidence for CIMT as a predictor of CV risk is conflicting. This in part is due to the potential for significant heterogeneity in performance of the technique and interpretation of results. CIMT is therefore currently only recommended as a consideration when CAC scoring is not available (ESC Class IIb recommendation) (Visseren et al, 2021).

In 2007 the American Society of Echocardiography published a consensus document on CIMT, concluding that this modality is a useful adjunct for risk assessment in asymptomatic individuals deemed to have an intermediate CV risk on the basis of conventional screening. This was based upon a comprehensive review of the evidence from 9 prospective studies and 6 observational studies all comprising over 1000 participants (Stein et al, 2007). Contrary to this finding a meta-analysis of a sub-population of 4,220 diabetic patients suggested CIMT was not

advantageous in the prediction of CV risk in this cohort of patients over a median follow-up of 8.7 years (Den Ruijter et al, 2013).

Arterial stiffness

Several studies have highlighted the ability of arterial stiffness measured using either aortic pulse wave velocity or arterial augmentation index to predict CV risk (Vlachopoulos et al, 2010). A study of 108 normotensive vs 82 hypertensive patients demonstrated the ability to perform pulse wave velocity as a surrogate of arterial stiffness using an accurate and repeatable technique (Murphy et al, 2011), however similar to CIMT measurement other studies have highlighted considerable inter-observer variability in measurements, and the widespread use in clinical practice is therefore not recommended (Visseren et al, 2021).

Psycho-social factors

In the general population, adults with either work or private life related stress have a 1.1 - 1.6 fold increase in the risk or CAD or stroke (Kivmaki et al, 2018). Psycho-social stress has both direct biological effects, and has also been correlated to detrimental lifestyle and behavioural factors such as smoking, poor diet, obesity and low compliance rates with medications (Rozanski et al, 2014; Crawshaw et al, 2016, Steinberg et al, 2015 & Rosengren et al 2004). There is a bidirectional association between depression and CAD. Depression has a high prevalence in

patients with CAD and is an independent predictor of poorer outcomes in this patient group (Vaccarino et al, 2018).

A recent prospective study evaluated routine depression screening in 1152 patients hospitalised with an acute coronary syndrome (Kim et al, 2020). This study (median follow-up period 8.4 years) not only demonstrated higher incidences of recurrent MACE in those diagnosed with depression vs those without (43.6% vs 29.6%, $p<0.05$), but initiation of a selective serotonin re-uptake inhibitor in the group with depression was associated with a reduction in recurrent MACE in comparison to those with depression receiving a placebo (40.9% vs 53.6%, $p<0.05$). The results suggest that screening for depression and institution of pharmacological therapies can improve cardiovascular outcomes.

Ethnicity

It is widely acknowledged that CV risk is impacted by ethnic background. The most contemporary data defining the modification of risk on the basis of ethnicity comes from data validating Q-RISK3. It is recommended to multiply CV risk by 1.3 for patients of Indian or Bangladeshi background, 1.7 for Pakistanis, 1.1 for other Asians, 0.85 for individuals from a black Caribbean background and finally 0.7 for those from black African and Chinese backgrounds (Hippisley- Cox et al, 2017).

Family history

A family history of CVD is an easily identifiable indicator of CVD risk. Premature CVD in a 1st degree relative is useful not only with respect to CVD genetic predisposition, but also acts as a surrogate to identify potential exposure to environmental factors that are known CV risks (Bachmann et al, 2017). Family history, however only marginally improves the prediction of CVD risk beyond conventional risk factors, hence is not integrated into the ESC SCORE 2 calculator (Sivapalaratnam et al, 2010; Veronesi et al, 2014; & Yeboah et al, 2012).

Socio-economic determinants

Low socio-economic status is independently associated with adverse long-term CV prognosis (Schultz et al, 2018 & De Mestral et al, 2017). This in part is due to higher rates of other CV risk factors, such as smoking, obesity and poor diet in this population. However, low income also acts as an independent predictor of CV mortality (Marmot et al, 1991 & Khaing et al, 2017).

Biomarkers in blood or urine

The use of biomarkers such as lipoprotein(a) or C-reactive protein (CRP), is currently not recommended on the basis of their limited potential utility in CV risk reclassification (Di Angelantonio et al, 2012 & Kamstrup et al, 2013). There is some data to suggest potential value in natriuretic

peptides or high-sensitivity cardiac troponin measurement (Willeit et al, 2016 & Willeit et al, 2017), however the evidence base at present is not sufficient to justify a recommendation to perform routine screening.

Body composition

Body mass index (BMI) has inherent flaws in assessing body composition given its inability to differentiate individuals with high muscle mass, however both BMI and waist circumference are correlated to CVD (Wormser et al, 2011).

Figure 1.2. Summary table of ESC recommendations for risk classification in specific conditions

Clinical condition	Recommendations	Class[a]	Level[b]
CKD	In all CKD patients, with or without DM, appropriate screening for ASCVD and kidney disease progression, including monitoring changes in albuminuria is recommended.[172]	I	C
Cancer	It is recommended to monitor cardiac dysfunction using imaging techniques and circulating biomarkers before, periodically during, and after cancer treatment.[173]	I	B
	Cardioprotection in high-risk patients (those receiving high cumulative doses or combined radiotherapy) receiving anthracycline chemotherapy may be considered for prevention of LV dysfunction.[174,175]	IIb	B
	Screening for ASCVD risk factors and optimization of the CVD risk profile is recommended in patients on treatment for cancer.	I	C
Mental disorders	It is recommended that mental disorders with either significant functional impairment or decreased use of healthcare systems be considered as influencing total CVD risk.	I	C
Sex-specific conditions	In women with a history of preeclampsia and/or pregnancy-induced hypertension, periodic screening for hypertension and DM should be considered.[184–187]	IIa	B
	In women with a history of polycystic ovary syndrome or gestational DM, periodic screening for DM should be considered.[188–191]	IIa	B
	In women with a history of premature or stillbirth, periodic screening for hypertension and DM may be considered.[192,193]	IIb	B
	Assessment of CVD risk should be considered in men with ED.	IIa	C
COPD	It is recommended that all COPD patients be investigated for ASCVD and ASCVD risk factors.	I	C
Inflammatory conditions	Assessment of total CVD risk may be considered in adults with chronic inflammatory conditions.[176]	IIb	B
	Multiplication of calculated total CVD risk by a factor of 1.5 should be considered in adults with rheumatoid arthritis.[177,178]	IIa	B
Migraine	Presence of migraine with aura should be considered in CVD risk assessment.[179–181]	IIa	B
	Avoidance of combined hormonal contraceptives may be considered in women with migraine with aura.[182,183]	IIb	B
Sleep disorders and OSA	In patients with ASCVD, obesity, and hypertension, regular screening for non-restorative sleep is indicated (e.g. by the question: 'how often have you been bothered by trouble falling or staying asleep, or sleeping too much?').	I	C
	If there are significant sleep problems, which are not responding within 4 weeks to sleep hygiene, referral to a specialist is recommended.	I	C

Coronary microvascular dysfunction

Angina is a clinical syndrome that occurs due to a mismatch in myocardial blood flow and oxygen supply and demand. The result for the patient is the potentially disabling symptoms of chest pain, dyspnoea and exercise limitation. Historical clinical practice has considered that the vast majority of patients experience angina due to the process of atherosclerosis in epicardial coronary arteries, with a resultant fixed luminal obstruction to blood flow. There is however an emerging appreciation that angina also occurs due to coronary vascular dysfunction at both an epicardial and microvascular level (Bairey et al, 2017; Ford et al, 2018; Kaski et al, 2018).

The spatial resolution of invasive coronary angiography does not allow visualisation of coronary arterioles between 20 and 400 µm in diameter (Fulton et al, 1963). CTCA offers a similar spatial resolution of around 500 µm (Ghekiere et al, 2017) and provides no information on either myocardial ischaemia or microvascular function. Coronary angiography and the visual qualitative estimation of coronary atheroma severity therefore has no ability to diagnose coronary vasomotion disorders and results in a large number of patients being investigated for angina receiving both an incorrect diagnosis and inappropriate pharmacological therapies.

It is estimated that as many as half of patients undergoing coronary angiography for the investigation of suspected angina have non-obstructive epicardial coronary arteries (Ford et al, 2018). A proportion of these patients with clinical symptoms of angina and non-obstructive epicardial disease will have a vasomotion disorder of the coronaries to explain their symptoms. This includes microvascular and/or vasospastic angina. The latter can occur both in epicardial vessels and in the microvasculature with an overlapping phenotype. Both vasospasm and microvascular dysfunction can produce the clinical syndromes of ischaemia with non-obstructive coronary arteries (INOCA) and MI with non-obstructive coronary arteries (MINOCA).

Microvascular dysfunction is typically a chronic and under-diagnosed condition (Tavella et al, 2016; Sara et al, 2015; Kobayashi et al, 2015). It is more prevalent in females and has been associated with co-morbidities such as diabetes mellitus and hypertension (Sara et al, 2015; Ford et al, 2019).

Microvascular dysfunction can co-exist with obstructive coronary atherosclerosis, and the earliest manifestations of CVD are observed in the microcirculation (Levy et al, 2001). This has led to the hypothesis that the detection of early microvascular dysfunction may enable CV risk stratification and hence targeted primary preventative therapies, with a resultant reduction in major adverse cardiovascular events (MACE). The

presence of coronary microvascular dysfunction has been strongly associated with an adverse long-term prognosis (Nishi et al, 2019; Jespersen et al, 2012; Maddox et al, 2014).

Coronary physiology

The function of the coronary vasculature is contributed to by the epicardial coronary arteries, intramyocardial branches and the microcirculation (Aziz et al, 2017). Vascular function is in turn determined by tone, tendency to vasoconstriction, vasodilator reserve and resistance. Coronary flow reserve (CFR) is a measure of the coronary circulation's ability to increase blood flow in response to either pharmacological or exercise induced stress (Gould et al, 2018). CFR can be impaired by abnormalities in function in the epicardial conduits and/or the microvasculature. Microvascular resistance in the coronaries is mainly determined by intramural arterioles <100 μm in diameter (Taqueti et al, 2018) and can be measured by the index of microcirculatory resistance (IMR) (Fearon et al, 2003; Fearon et al, 2017; Ng et al, 2006). The resistance reserve ratio (RRR) is a measure of the vasodilatory capacity of the microcirculation expressed as the ratio of basal resistance / IMR, with a RRR <2.0 being considered to be abnormal (Layland et al, 2013).

Abnormalities in coronary microvascular function are a spectrum and therefore it is technically inaccurate to define dysfunction by an absolute

numerical value of either CFR or IMR, however in order to allow microvascular function to be used in algorithmic clinical decision making a cut-off IMR value of ≥25 and CFR <2.0 is considered by most of the literature to be abnormal (Ford et al, 2018). Importantly these values are relevant not just for an algorithmic approach to INOCA management, but have been shown to carry prognostic significance with overall relevance to CVD (Kunadian et al, 2021).

The assessment of coronary microvascular function can be performed invasively at the same time as invasive coronary angiography provided dedicated equipment is available. The procedure is undertaken by insertion of a specialised coronary pressure wire into a distal coronary artery (usually the left anterior descending artery as this subtends the largest percentage of myocardium). The pressure wire has the ability to both measure blood pressure and temperature using two thermistors; one positioned proximally within the coronary guide catheter; and the second distally in the coronary. Measurements of IMR and CFR are made using the principle of thermodilution, whereby if a fluid of differing temperature to blood (i.e. saline at room temperature or below) is injected across the two thermistors, the change in temperature over time can be detected and mean transit time (T_{mn}) of the fluid calculated. Mean transit time is then used to calculate blood flow (Q). Q is measured multiple times and averaged during rest and then following pharmacological stress (usually achieved with an infusion of intravenous adenosine) (Fearon et al, 2017).

A summary of the formulae used to derive the relevant coronary haemodynamics can be found below:

The derivation of IMR is based on Ohm's law, whereby:

$$\text{Resistance (R)} = \text{Voltage (V)} / \text{Current (I)}$$

In the coronary circulation V is analogous to the pressure difference (ΔP) across the coronary microvasculature. ΔP is calculated by subtracting the mean coronary wedge pressure (P_v) from the mean distal coronary arterial pressure (P_d):

$$\Delta P = P_d - P_v$$

Current (I) is equivalent to coronary blood flow (Q), whereby:

$$Q = 1 / \text{Mean transit time } (T_{mn})$$

IMR is thereafter calculated using this formula:

$$\text{IMR} = (P_d - P_v) / \text{Hyperaemic coronary blood flow } (Q_{(Hyp)})$$

P_v is however challenging to measure and usually of negligible value, so the formula can be simplified without creating significant inaccuracy to:

$$IMR = P_d / Q_{(Hyp)}$$

In its simplest form given the inverse relationship of Q and T_{mn}:

$$IMR = P_d \times T_{mn(hyp)}$$

CFR is simply a ratio of hyperaemic to resting coronary flow, thereby:

$$CFR = Q_{(Hyp)} / Q_{(rest)}$$

$$CFR = (1 / T_{mn(hyp)}) / (1 / T_{mn(rest)})$$

$$CFR = T_{mn(rest)} / T_{mn(hyp)}$$

Non-invasive evaluation of coronary microvascular function

Computed tomography (CT) perfusion can diagnose CMD and can simultaneously assess for CAD on the same study. Positron emission tomography (PET) is the most validated modality to evaluate CMD in the absence of obstructive CAD. There are robust prognostic data for this test, and it has good reproducibility and accuracy. Assessment of CMD by CMR is validated against invasive tests and PET and is associated with no radiation exposure. However, it is expensive, is not widely available, and has limited prognostic data at present.

Although many imaging modalities can be used to evaluate for CMD, PET has the most prognostic data at present. Significant future research is needed to compare the relative accuracy and prognostic importance of CMD identified on these imaging modalities, and to assess whether medications and other interventions impact symptoms and outcomes (Matthew et al, 2020).

Pathophysiological basis of coronary vasomotor disorders

Microvascular pathology includes remodelling of the vascular wall, inflammation, alterations in the extravascular (interstitial) matrix and systemic changes including; capillary rarefaction (Lindemann et al, 2018 & Antonios et al, 2001); and arteriolar dysfunction that may be endothelial dependent or independent (Sax et al, 1987 & Ford et al, 2018). Disease processes may differentially affect the function of the epicardial conduit arteries and the microcirculation (Kaski et al, 1991). In patients with INOCA, macrovascular coronary atherosclerosis and risk factors are often prevalent (Siasos et al, 2018). Atherosclerosis is associated with low coronary wall shear stress (Siasos et al, 2018), which is a determinant of major adverse cardiac events (Stone et al, 2018). Myocardial bridging is also prevalent in INOCA probably because of endothelial dysfunction within and distal to affected segments (Rahman et al, 2019). Coronary reactivity testing, such as the injection of intracoronary acetylcholine in patients with a myocardial bridge may provoke transient spasm and chest

pain that reproduces their symptoms. Small vessel disease may be a multi-system disorder (Berry et al, 2019).

Evidence base of benefits from diagnosing coronary microvascular dysfunction

Patients with both microvascular and vasospastic angina are notoriously under-diagnosed and mismanaged. There has been historical reluctance in the interventional cardiology community to perform invasive diagnostic procedures to investigate for these conditions due to a perception that the results do not significantly alter patient's management or prognosis. To date the CORonary MICrovascular Angina (CorMicA) study provides the most robust evidence base to counter this argument.

The CorMicA study sought to establish whether there was a clinical benefit and hence an indication to perform routine invasive pressure wire based coronary physiology in patients with anginal symptoms and/or signs of ischaemia, but no obstructive coronary artery disease during a diagnostic coronary angiogram (Ford et al, 2018). A total of 151 patients in this study were randomised to either receive stratified medical therapy or standard of care following invasive coronary angiography. The stratified medical therapy cohort were managed following invasive assessment of FFR, CFR, IMR and coronary vasoreactivity testing with acetylcholine. The standard of care cohort received a sham procedure followed by treatment

as per the clinician's usual practice following angiography alone. There was no difference in MACE at 6 months (2.6% vs 2.6%, p=1.0), however anginal symptoms as assessed by the Seattle Angina Questionnaire were significantly improved in the stratified medical therapy cohort (mean improvement of 11.7 U; 95% CI 5.0 to 18.4; p=0.001).

Classification of coronary microvascular dysfunction

Coronary microvascular dysfunction (CMD) can occur in isolation or co-exist with other forms of myocardial and coronary disorders. It has therefore previously been suggested that CMD should be categorised according to the clinical setting in which it occurs (see **Table 1.2**) (Crea et al, 2014). There may be considerable overlap in these conditions.

In practice the measurement of CFR and IMR form the basis for the diagnosis of CMD. However, these are independent measurements made to diagnose a condition with a highly heterogeneous underlying pathophysiological mechanism. To account for this and aid the clinical application of these measurements, two distinct endotypes of CMD have been described (functional and structural CMD). This allows patients in whom discordant measurements of CFR and IMR are obtained to be categorised haemodynamically (Rahman et al, 2020). Functional CMD has been defined as an abnormal CFR in the setting of a normal hyperaemic myocardial resistance, whilst structural CMD has been defined as an

abnormal CFR in the setting of an elevated hyperaemic myocardial resistance.

Table 1.2. Summary of the clinical classifications of microvascular dysfunction (adapted from Crea et al, 2014)

	Clinical setting	Main pathogenic mechanism
Type 1 - Absence of myocardial or obstructive epicardial disease	- Microvascular angina	- Endothelial dysfunction - Smooth muscle cell dysfunction - Vascular remodelling
Type 2 - Myocardial disease	- Hypertrophic cardiomyopathy - Dilated cardiomyopathy - Anderson-Fabry disease - Myocarditis - Aortic stenosis	- Vascular remodelling - Smooth muscle cell dysfunction - Extramural compression - Luminal obstruction
Type 3 - Obstructive coronary artery disease	- Stable angina - Acute coronary syndrome	- Vascular remodelling - Smooth muscle cell dysfunction - Luminal obstruction

Type 4 - Iatrogenic	- Percutaneous coronary intervention - Coronary artery bypass grafting	- Luminal obstruction - Autonomic dysfunction

Valvular Heart Disease

Valvular heart disease (VHD) is most commonly the result of progressive degeneration and/or calcification of a previously normal heart valve (Yadgir et al, 2020). This process of degeneration can result in significant narrowing of the valve orifice (valvular stenosis); an inability for the valve to prevent the misdirection of blood flow (valvular regurgitation); or a combination of both stenosis and regurgitation (mixed valvular dysfunction). VHD can also be the result of congenital valvular abnormalities or acquired conditions such as rheumatic heart disease and endocarditis.

The most prevalent form of VHD is aortic stenosis (AS), which represents the most common indication in Europe and North America for surgical or transcatheter valvular intervention. The prevalence of AS has also been steadily increasing due to a combination of the ageing population, availability of echocardiography for diagnosis and the availability of less invasive treatment options prompting clinicians to organise screening investigations more readily (D'Arcy et al, 2016). Severe AS carries a highly

adverse intermediate to long-term prognosis with early studies identifying high rates of sudden cardiac death in the absence of aortic valve replacement (Schwarz et al, 1982 & Ross et al, 1968).

The key diagnostic test for AS is echocardiography. Largely the condition is diagnosed when a trained sonographer identifies the restriction of aortic valve opening and assesses for thickening of valve leaflets and/or calcification. The severity of AS is principally assessed using Doppler assessment of blood flow velocity across the aortic valve. Assessment can also be enhanced by stress tests and cardiac gated CT with valvular calcium scoring.

At present guidelines recommend intervention for AS only following confirmation that the valve fulfils criteria for severe AS (Vahanian et al, 2021). Intervention is currently recommended for symptomatic severe AS or asymptomatic AS with left ventricular systolic dysfunction (LVEF <50%) and should be considered in asymptomatic patients who fulfil any of the following criteria:

- LVEF <55%
- Abnormal blood pressure response to exercise
- Mean gradient >60mmHg or peak velocity >5m/s
- Severe valve calcification and peak velocity progression >0.3m/s/year

- Markedly elevated BNP (>3x age- and sex-corrected normal range)

When indicated the choice of intervention is between surgical aortic valve replacement (SAVR) and transcatheter aortic valve implantation (TAVI). Over the past 10 to 20 years an evidence base has emerged, demonstrating the safety and efficacy of TAVI as a less invasive management strategy for the management of severe AS (Leon et al, 2016; Smith et al, 2011; Reardon et al, 2017; & Mack et al, 2019). This has led to a shift in guidelines recommending TAVI be considered not only preferable in patients at high surgical risk, but also in patients ≥75 years of age provided no anatomical contraindications to transfemoral TAVI exist (Vahanian et al, 2021).

The relationship of aortic stenosis and microvascular dysfunction

In AS disruption to the coronary circulation can occur due to left ventricular hypertrophy (LVH), high left ventricular pressures, low coronary perfusion pressure and extravascular forces that reduce physiological vasodilatory reserve (McConkey et al, 2019). The development of angina in severe AS is associated with an increased risk of sudden cardiac death (Ross et al, 1968 & Lester et al, 1998) and an average life expectancy of 3 years (Aronow et al, 2007). Patients with AS may experience angina in the setting of concomitant coronary disease, but also in the absence of obstructive epicardial disease.

Studies of coronary flow have identified 4 main coronary waves within the cardiac cycle (Davies et al, 2006). Coronary flow waves can be divided into those that are forward or backward travelling from the aorta or microcirculation and those caused by vessel compression or expansion (see **Figure 1.3**). Coronary flow is predominantly influenced by the backward expansion wave (BEW) that occurs during LV diastole.

Figure 1.3. Illustration of the 4 dominant coronary waves and their relationship to the cardiac cycle (McConkey et al, 2019)

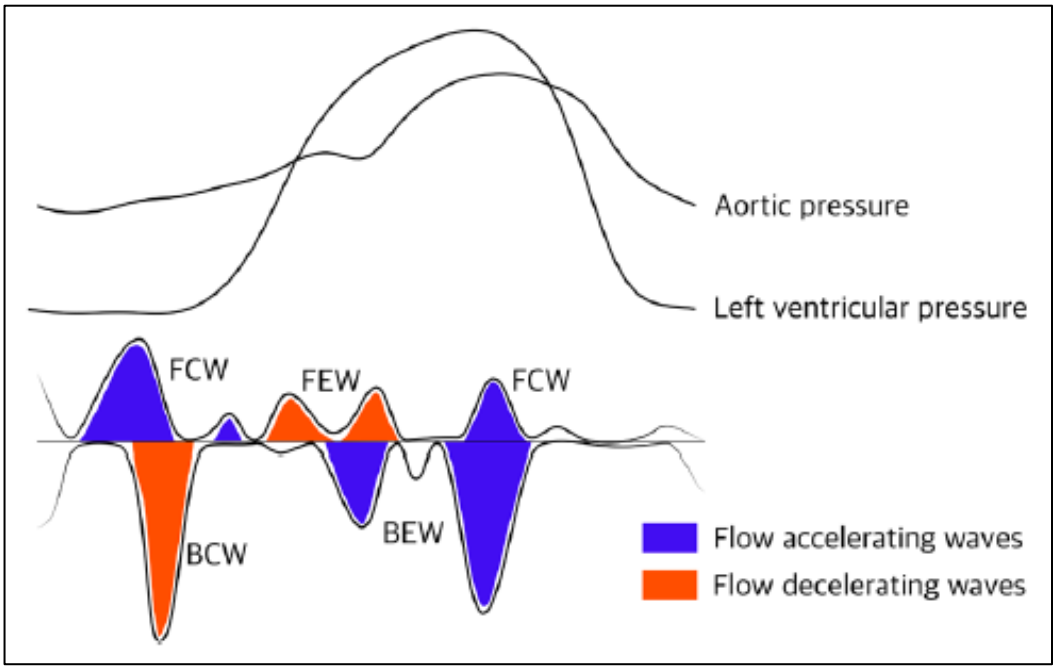

In response to progressive afterload, AS induces LVH to increase contractile force and reduce wall stress (Carabello, 1995). Compressive forces resulting from rising LV pressure determine coronary perfusion pressure and limit coronary circulatory response to increased myocardial

demand (Mahmod et al, 2014). LVH results in an increase in myocardial oxygen demand, however a mismatch in supply-demand occurs due to a reduction in perfusion through the small perforating coronary network created by the combination of an elevation in systolic wall stress and a reduction in capillary density (Rajappan et al, 2002 & Galiuto et al, 2006). Preferential coronary flow shifts from the endocardium to epicardium, with a resultant decrease in subendocardial blood flow and hence ischaemia, cell apoptosis and myocardial fibrosis (Miyagawa et al, 2009).

The severity of AS has been correlated to alterations in CFR (Banovic et al, 2011). An abnormal CFR has also been shown to predict adverse long-term cardiovascular morbidity and mortality in patients with AS (Nemes et al, 2009). Historically it was believed that AS impacted the coronary microcirculation simply due to the development of LVH. Whilst there are similarities in the microvascular impacts of AS and other myocardial and afterload dependent causes of LVH, impairment in microvascular function in AS is not solely dependent on the development or severity of LVH (McConkey et al, 2019).

There appear to be 3 main factors resulting in disrupted coronary flow and reduced coronary flow reserve in aortic stenosis:

1. Microvascular
    a. Capillary rarefaction
    b. Perivascular fibrosis
    c. Reversal of coronary blood flow endo-epicardial gradient
2. Myocardial
    a. Diastolic dysfunction, reduced diastolic perfusion time and disrupted backward expansion wave
    b. Delayed onset of systolic forward flow and reduced peak systolic flow
    c. Increased wall stress, extravascular compressive forces and intra-myocardial compression
    d. Interstitial and replacement myocardial fibrosis
3. Aortic
    a. Low coronary perfusion pressure due to the venturi effect
    b. Increased systemic vascular resistance and resultant reduction in stroke volume
    c. High valvulo-arterial impedance with lower systemic arterial compliance

After TAVI or SAVR there is restoration of myocardial perfusion, oxygenation, energetics and contractility; accompanied by improved microcirculatory function as a result of the relief of mechanical left ventricular outflow obstruction; and eventual LVH regression (Beyerbacht

et al, 2001 & Kenny et al, 1994). Hyperaemic microvascular resistance and CFR have both been shown to improve immediately following aortic valve intervention (Wiegerinick et al, 2015). Theoretically, improvements in microvascular function may be observable in different vascular territories.

Assessing microvascular function in systemic vascular networks

Microvascular networks that offer accessible haemodynamic assessment include the retinal circulation (Zhong et al, 2008), sublingual circulation (Demir et al, 2012), nail-fold circulation (Fagrell et al, 1977) and the conjunctival circulation (Brennan et al, 2019). A recent publication reported the ability for a deep learning and retinal photograph-derived coronary artery calcium (CAC) score to predict cardiovascular events (Rim et al, 2021). In this study 11,770 participants underwent both CT coronary artery calcium (CAC) scoring and retinal photography. Participants were divided into groups based on CAC score (0, 0-100 and >100). This study thereafter developed an automated analysis of retinal photography to develop a RetiCAC score (low, intermediate or high) based on the retinal appearances of the participants in these 3 CAC cohorts. This RetiCAC score was then validated using databases from 2 sources of readily available retinal imaging (Singapore epidemiology of eye diseases study and the UK Biobank). In the Singapore population-based cohort (n=8551), 310 (3·6%) participants had fatal cardiovascular events over 10 years, and the three-strata RetiCAC was significantly associated with increased risk of fatal cardiovascular events (hazard ratio [HR] trend 1·33, 95% CI 1·04–

1·71). In the UK Biobank (n=47 679), 337 (0·7%) participants had fatal cardiovascular events over 10 years. When added to the pooled cohort equation (PCE), the three-strata RetiCAC improved cardiovascular risk stratification in the intermediate-risk group (HR trend 1·28, 95% CI 1·07–1·54) and borderline-risk group (1·62, 1·04–2·54), and the continuous net reclassification index (NRI) was 0·261 (95% CI 0·124–0·364). This study suggests retinal photography has the potential to be used as an alternative to CAC in CV risk estimation.

The conjunctival microcirculation

The conjunctiva of the eye provides protection and lubrication of the eye by the production of mucus and tears. It prevents microbial entrance into the eye and plays a role in immune surveillance. It lines the inside of the eyelids and provides a covering to the sclera. It is also highly vascularized and home to extensive lymphatic vessels (Shumway et al, 2021).

The conjunctiva consists of three distinct anatomical regions: the palpebral conjunctiva (lines the eyelids), bulbar conjunctiva (found on the eyeball over the anterior sclera) and the conjunctival fornices (forms the junction between the palpebral and bulbar conjunctiva) (Shumway et al, 2021). The bulbar conjunctiva can be sub-divided into scleral and limbal parts; receiving blood supply via the anterior ciliary arteries, that in turn originate from the ophthalmic artery (Meyer et al, 1988).

Several previous studies have highlighted the ability to non-invasively assess indices of microvascular function in bulbar conjunctival vessels (see **Table 1.3**). The conjunctival microvasculature readily lends itself to non-invasive imaging as vessels are easily identifiable against the white scleral background and do not require the use of mydriatic agents for pupillary dilatation to facilitate visualisation (unlike the more well studied retinal microvasculature). Conjunctival vascular imaging also does not involve exposure of the patient to ionizing radiation along with the associated long-term cancer risks.

With sufficient magnification and spatial resolution of the imaging apparatus used, conjunctival blood flow can be visualised with the naked eye. This in turn allows for the assessment and subsequent quantification of both static and dynamic microcirculatory parameters.

A literature review was conducted at the commencement of this study. Pubmed was used to search for studies including keywords ‘conjunctiva’ and ‘microvascular’. At the time of writing this thesis, 20 relevant studies were identified that describe the quantification of conjunctival microvascular parameters using a slit-lamp biomicroscope and digital charged camera. These studies are summarised in **Table 1.3** and highlight the various methods used for conjunctival vascular screening and the potential to detect haemodynamic alterations that occur in a variety of ocular, systemic and vascular disease states. Our research group has

therefore hypothesized that the conjunctiva could be used to aid in the non-invasive screening of CVD and potentially have utility in primary prevention in either a systematic or opportunistic manner.

The mode of conjunctival vessel screening described in this thesis has been described in 3 previous publications by Brennan et al in 2019, 2020 and 2021. These studies developed the methodology of this technique and applied it in two well defined, but distinct cardiovascular disease states (myocardial infarction and cyanotic congenital heart disease). The focus of this research has been to further develop this method of conjunctival screening and apply it to the characterisation of microvascular dysfunction in additional distinct CVD states.

Table 1.3. Summary of studies from comprehensive literature review on the quantification of conjunctival microcirculatory function

Study	Summary	Groups	Diameter (μm)	Velocity (mm/s)	Blood flow rate (pl/s)	Wall shear rate (WSR)(s^{-1}) or wall shear stress (WSS) (N/m^2 or $dyne/cm^2$)
Cheung et al, 1999	A comparison of the conjunctival microcirculation in diabetic patients following successful simultaneous pancreas-kidney (SPK) transplantation and a group of controls	Diabetic (DM) controls (n=12) Non-diabetic (NDM) controls (n=12) Diabetics undergoing SPK (n=12)	n/a	<u>DM Controls</u> 1.27 ± 0.45 <u>NDM Controls</u> 2.94 ± 0.57 <u>Post-SPK</u> 1.65 ± 0.42	n/a	n/a

Koutsiaris et al, 2007	Blood flow and wall shear stress quantification in the conjunctival microcirculation of healthy volunteers	Controls (n=17)	4 – 24 (range)	0.53 0.21 - 1.18 (range)	102 5 – 462 (range)	1.54 N/m^2 0.28 – 9.55 N/m^2 (range)
Shahidi et al, 2010	Quantitative assessment of conjunctival microvascular circulation of the human eye	Control (n=1)	15.5 8.7 – 24.3 (range)	0.7 0.2 – 1.2 (range)	111.8 27.3 – 296.9 (range)	n/a
Koutsiaris et al, 2010	Blood velocity pulse quantification in the human conjunctival pre-capillary arterioles	Controls (n=15)	6 – 12 (range)	1.66 ± 0.11 0.52 – 3.26 (range)	n/a	n/a
Cheung et al, 2012	A comparison of conjunctival parameters in subjects using contact lenses in comparison to controls that did not use contact lenses	Contact lens users (n=102) Controls (n=29)	n/a	n/a	n/a	n/a
Koutsiaris et al, 2013	Wall shear rate and stress quantification in the human conjunctival pre-capillary arterioles of healthy volunteers	Controls (n=15)	6 – 12 (range)	1.66 ± 0.11 0.52 – 3.26 (range)	13 – 202 (range)	WSR 587 – 3515 s^{-1} (range)

						WSS 11.7 - 21.1 N/m^2 (range)
Jiang et al, 2014	Comparison of conjunctival microvascular haemodynamics before and after 6 hours of contact lens use	Controls (n=6)	Pre CL 18.8 ± 2.7 Post CL 19.6 ± 2.4 **p= 0.02**	Pre CL 0.60 ± 0.12 Post CL 0.88 ± 0.21 **p= 0.001**	Pre CL 129.8 ± 59.9 Post CL 207.2 ± 81.3 **p= 0.001**	n/a
Kord Valeshabad et al, 2015[1]	Comparison of conjunctival microvascular haemodynamics in patients with different degrees of sickle cell retinopathy based on the presence or absence of focal macular thinning (FMT)	Sickle cell disease patients (n=22)	FMT (n=12) 16 ± 2 No FMT (n=10) 16 ± 2	FMT 0.45 ± 0.11 No FMT 0.64 ± 0.24	n/a	n/a

			p= 0.4	**p= 0.03**		
Kord Valeshabad et al, 2015[2]	Feasibility of the assessment of conjunctival microvascular haemodynamics in unilateral ischemic stroke patients and comparison of parameters based on whether the stroke was on the ipsilateral or contralateral side to eye imaged	Ischaemic stroke (n=12) Controls (n=15)	<u>Contralateral</u> 21.2 ± 3.9 <u>Ipsilateral</u> 20.6 ± 4.4 P= 0.8	<u>Contralateral</u> 0.49 ± 0.16 <u>Ipsilateral</u> 0.35 ± 0.13 **p= 0.02**	n/a	n/a
Koutsiaris et al, 2015	Correlation of axial blood velocity to venular and arteriolar diameter in the human. This study compared the results of venule and arteriole haemodynamics as described previously	Venules (n=17) Arterioles (n=15)	<u>Venules</u> 4 – 24 (range) <u>Arterioles</u> 6 – 12 (range)	<u>Venules</u> 0.53 0.21 - 1.18 (range) <u>Arterioles</u> 1.66 ± 0.11	<u>Venules</u> 102 5 – 462 (range) <u>Arterioles</u> 13 – 202 (range)	<u>Venules</u> 1.54 N/m2 0.28 – 9.55 N/m2 (range) <u>Arterioles</u> 11.7 - 21.1 N/m2 (range)

				0.52 – 3.26 (range)		
Xu et al, 2015	Measurement variability of the bulbar conjunctival microvasculature in healthy subjects using functional slit-lamp biomicroscopy (FSLB)	Controls (n=20)	21.68 ± 2.47	0.62 ± 0.31	166.20 ± 85.78	n/a
Khansari et al, 2016	Automated Assessment of Haemodynamics in the Conjunctival Microvasculature Network in healthy volunteers	Controls (n=15)	<u>Arterioles</u> 15 ± 3 <u>Venules</u> 18 ± 2	<u>Arterioles</u> 0.63 ± 0.17 <u>Venules</u> 0.54 ± 0.13	<u>Arterioles</u> 86 ± 33 <u>Venules</u> 140 ± 55	<u>Arterioles</u> 320 ± 132 s^{-1} <u>Venules</u> 190 ± 46 s^{-1}
Wang et al, 2016	Vessel sampling and blood flow velocity distribution with vessel diameter for characterizing the human bulbar conjunctival microvasculature	Controls (n=5)	30.4 ± 8.4	0.59 ± 0.04	n/a	n/a
Chen et al, 2017	Comparison of conjunctival microvascular haemodynamics before and	Controls (n=22)	n/a	<u>Pre CL</u> 0.51 ± 0.20	n/a	n/a

	after 6 hours of contact lens use			Post CL 0.65 ± 0.22 **p <0.001**		
Khansari et al, 2017	A comparison of conjunctival microvascular haemodynamics in different stages of diabetic retinopathy	Non-diabetic controls (C) (n=34) Diabetics with no retinopathy (NDR) (n=47) Non-proliferative retinopathy (NPDR) (n=45)	C 18 ± 5 NDR 19 ± 4 NPDR 18 ± 4 PDR 18 ± 5	C 0.70 ± 0.23 NDR 0.54 ± 0.22 NPDR 0.62 ± 0.24 PDR 0.64 ± 0.27	C 144 ± 118 NDR 124 ± 98 NPDR 135 ± 90 PDR 146 ± 115	C 8.6 ± 5.0 dyne/cm^2 NDR 5.4 ± 3.2 dyne/cm^2 NPDR 6.2 ± 3.3 dyne/cm^2 PDR 6.6 ± 3.7 dyne/cm^2

		Proliferative retinopathy (PDR) (n=35)	p= 0.9	**p= 0.03**	p= 0.8	**p= 0.003**
Hu et al, 2019	Clinical study on microcirculation changes of the bulbar conjunctiva after contact lens wear	Controls (n=27)	n/a	Pre CL 0.53 ± 0.13 Post CL 0.59 ± 0.13 **p= 0.048**	n/a	n/a
Karanam et al, 2019	Correlation of conjunctival microvascular haemodynamics to conventional cardiovascular risk assessment using Framingham risk assessment	Low risk (n=11) Intermediate risk (n=14) High risk (n=59)	Low 19.5 ± 3.2 Intermediate 21.5 ± 2.0	Low 0.54 ± 0.13 Intermediate 0.44 ± 0.13	Low 133.4 ± 59.6 Intermediate 123.6 ± 39.3	n/a

			High 21.3 ± 2.8 p= 0.9	High 0.42 ± 0.15 p= 0.05	High 121.9 ± 52.6 **p= 0.04**	
Moka et al, 2019	Blood flow velocity comparison in conjunctival capillaries and postcapillary venules between pregnant and non-pregnant women (Figures quoted are capillaries only)	Non-pregnant (n=28) Pregnant- 1st trimester (n=17) Pregnant 3rd trimester (n=16)	n/a	Non-pregnant 0.51 ± 0.17 Pregnant- 1st trimester 0.74 ± 0.20 Pregnant 3rd trimester 0.95 ± 0.45 **p <0.001**	Non-pregnant 15.5 ± 8.2 Pregnant- 1st trimester 25.1 ± 10.4 Pregnant 3rd trimester 31.3 ± 21.3 **p <0.001**	n/a

Shi et al, 2019	Comparison of the conjunctival and retinal microcirculation using a slit-lamp biomicroscope	Controls (n=58)	n/a	0.49 ± 0.13	90	n/a
Jo et al, 2021	Quantification of Blood Flow Velocity in the Human Conjunctival Microvessels Using Deep Learning-Based Stabilization Algorithm	Controls (n=10)	8.17 – 15.62 (range)	0.08 – 0.34 (range)	n/a	n/a

All figures provided are the mean ± standard deviation (where available) unless otherwise stated in the text. In column 7, figures quoted as N/m^2 or $dyne/cm^2$ represent results for wall shear stress and those quoted as s^{-1} represent wall shear rate.

Conjunctival microvascular assessment in healthy subjects

The first step in the development of any non-invasive microcirculatory screening modality is the development of a reliable and calibrated imaging technique. A slit-lamp biomicroscope is a common tool used by both ophthalmologists and optometrists to allow visualisation and assessment of ocular structures. A slit-lamp provides adequate magnification in addition to stabilisation of the head in order to minimise movement of the imaging target. A stabilised image can still be hard to obtain as it also relies on the ability of the individual being screened to focus their gaze in a particular direction and avoid unwanted movements that make assessment challenging.

Several groups have published studies that combined a slit-lamp biomicroscope with a digital charged coupled device camera (summarised in **Table 1.3**) These groups have described the non-invasive assessment of parameters that include diameter (D), velocity (V), blood flow rate (Q), wall shear rate (WSR) and wall shear stress (WSS).

As early as 1999 Cheung et al studied the conjunctival microcirculation in 12 patients with type 1 diabetes mellitus undergoing simultaneous pancreas-kidney transplantation (SPK) in comparison to healthy non-diabetic volunteers (n=12), type 1 diabetic controls who were not transplanted (n=12) and type 1 diabetic patients undergoing solitary kidney

transplant (n=5). The conjunctival evaluation was performed using an intravital microscope at 40x magnification and digital charged coupled device camera (CCD). In this study pre-SPK diabetic patients had significantly larger venules, reduced arteriole:venule ratios and diminished vascular perfusion in comparison with non-diabetics. Significant improvements in diabetic microangiopathy were observed in all 12 patients 18 months post SPK (Cheung et al, 1999).

Koutsiaris et al assessed the conjunctival microcirculation in 17 healthy volunteers using a slit-lamp-CCD combination (Koutsiaris et al, 2007). Using this imaging technique, the group described the first quantification of Q and WSS by applying the known mathematical relationships of vessel diameter and axial velocity (V_a) to Q and WSS. This study evaluated 104 conjunctival microvessels and obtained diameters ranging from 4 to 24 μm, Q ranging from 5 to 462 pl/s and WSS ranging from 0.28 and 9.55 N/m^2. This study is highly relevant to this thesis as the quantification of conjunctival microvascular parameters utilises the mathematical principles it describes. Vessel diameter was obtained following appropriate calibration of the imaging device and application of a pixel : millimetre conversion factor. V_a was obtained using the following formula:

V_a= Distance travelled by RBC (mm) / time

Cross-sectional velocity (V_{cs}) is then derived from V_a using a conversion factor derived from the size of vessel analysed. Time was a constant in the above formula as the group analysed a constant number of video frames per analysis with a set frame rate of the camera.

Q was then estimated using the following formula:

$$Q = V_{cs} (\pi D^2 / 4)$$

WSR was derived using the following formula:

$$WSR = (8V_{cs}) / D$$

WSS is simply the product of WSR and the dynamic viscosity of blood (η). Koutsiaris et al estimated η in this formula in addition to calculated WSR.

In 2010, Koutsiaris et al reported haemodynamic parameters in 30 conjunctival precapillary arterioles of 15 healthy volunteers (Koutsiaris et al, 2010). These vessels ranged from 6 to 12 μm in diameter and V_a ranged from 0.4mm/s (minimum end diastolic value) to 5.84mm/s (maximum peak systolic velocity). The average V_a per vessel ranged from 0.52 to 3.26mm/s. Given the pulsatile nature of blood flow in vessels, each pulsating waveform is characterised by a maximum and a minimum velocity value. In arterioles it is possible to calculate the resistive index (RI)

using these values that correspond to the peak systolic velocity (PSV) and end diastolic velocity (EDV) using the following formula:

$$RI = (PSV - EDV) / PSV$$

RI is a measure of the downstream resistance of the distal microvascular/capillary bed. In this study the mean RI across the 30 precapillary arterioles was 53.1 ± 2.2% (range 35.5 – 81.8%).

In 2015 Xu et al evaluated the repeatability of conjunctival microvascular analysis using functional slit-lamp biomicroscopy (FSLB). In this study the conjunctiva of 20 healthy subjects was imaged by two independent operators and then these measurements repeated every 2 hours to evaluate the haemodynamic variations that occurred over the course of a single day. The coefficient of repeatability (CoR%) and intraclass correlation coefficient (ICC) between the 2 operators suggested excellent correlation and repeatability for both vessel diameter (ICC= 0.989 and CoR%= 4.87%) and axial blood velocity (ICC=0.997 and CoR%= 11.49%). No significant differences were observed in the microvascular parameters obtained between the various time intervals of imaging, suggesting that FSLB imaging of the conjunctiva can be performed at any time throughout the day, without the time itself impacting the results obtained (Xu et al, 2015).

Khansari et al reported the results of an automated method of assessing the conjunctival microvascular network. The conjunctiva provides an abundant number of microvessels to non-invasively study, but the previous groups reporting indices of microvascular function as demonstrated above used a process that was manual or semi-automated and hence more time consuming. This study evaluated conjunctival haemodynamics in 15 healthy subjects. Imaging was performed with a slit-lamp and CCD combination. The automated approach consisted of image registration for correction of eye movement, image segmentation to identify vessels, centreline extraction and bifurcation detection to define centrelines of individual vessel segments, diameter measurement, detection of blood flow, and measurement of axial blood velocity (Khansari et al, 2016). Vessels were differentiated into arterioles or venules based on the direction of blood flow in relation to converging or diverging bifurcations. Repeatability was assessed using this technique by imaging the same area of conjunctiva in 5 healthy subjects multiple times, in order to assess the variation in results obtained. A total of 43 microvessels were analysed for the repeatability assessment with a standard deviation of 0.7 μm for diameter (range: 0.6–1.0 μm) and 0.17 mm/s for axial velocity (range: 0.11 – 0.21 mm/s). This result suggested the technique can be performed efficiently and with sufficient repeatability and reliability of measurements.

Conjunctival microvascular alterations associated with contact lens use

Jiang et al assessed the conjunctival haemodynamic parameters of diameter, blood flow velocity and blood flow rate in 6 human subjects imaged before and after 6 hours of contact lens use. This group observed an increase in mean vessel diameter (18.8 ± 2.7 μm vs 19.6 ± 2.4 μm; p=0.02), blood flow velocity (0.60 ± 0.12 mm/s vs 0.88 ± 0.21 mm/s; p=0.001) and blood flow rate (129.8 ± 59.9 pl/s to 207.2 ± 81.3 pl/s; p=0.001) after 6 hours of contact lens use. This study highlighted alterations in conjunctival microcirculatory function in association with contact lens use.

Hu et al similarly reported increased conjunctival vessel blood flow velocity in association with contact lens use in 27 subjects (mean blood flow velocity before contact lens use was 0.53 ± 0.13mm/s vs 0.59 ± 0.13mm/s following contact lens use; p=0.04). Furthermore, the group demonstrated a positive correlation between ocular discomfort experienced by the contact lens wearers and blood flow velocity.

Cheung et al studied the relationship of contact lens use and conjunctival microcirculatory parameters in 102 long-term contact lens users in comparison to 29 control subjects that did not use contact lenses. This study used a qualitative assessment of abnormalities such as

haemosiderrin deposition, vessel tortuosity, intermittent blood flow and vessel sludging to describe the sum of abnormalities found in each cohort. They observed a significantly higher number of abnormalities in the contact lens vs control cohort and concluded that contact lens use resulted in microvascular abnormalities and remodelling changes due to the inadvertent physical interaction of the lenses with either the underlying conjunctival vessels or the surface of the bulbar conjunctiva.

Whilst the study from Cheung et al does not report quantitative parameters of conjunctival microvascular function, it is relevant to this work as it along with the studies from Jiang et al and Hu et al form the basis for the exclusion of contact lens wearers from this and our groups previous studies.

Conjunctival microvascular assessment in patients with established CVD

In 2015 Kord Valeshabad et al evaluated conjunctival microvascular function in 12 patients following an ischaemic stroke and compared the results to 15 healthy controls. Given the similar vascular origins of conjunctival and cerebral tissues, the study hypothesized that alterations in haemodynamics may be observable between right and left eyes in patients following an ischaemic stroke. The parameters evaluated were diameter and axial velocity. Mean conjunctival vessel diameter did not

differ either between the left and right eyes in either group and did not differ between controls and stroke patients. Mean axial velocity did not differ between the controls and stroke patients, however significantly differed when comparing the eyes on either the ipsilateral or contralateral side of the stroke (contralateral 0.49 ± 0.16 mm/s vs ipsilateral 0.35 ± 0.13 mm/s; p=0.02). This study therefore suggested that conjunctival haemodynamic alterations were observable in relation to the vascular territory responsible for stroke.

Sickle cell disease is a hereditary haemoglobinopathy characterized by the formation of rigid, sickle-shaped erythrocytes (Lei et al, 2012). The condition leads to ischaemia and vascular occlusion and given the systemic nature of the disease, can affect any vascular network. Sickle cell retinopathy (SCR) is typified by a number of vascular events including central/branch retinal artery occlusion, chorioretinal infarctions and proliferative retinopathy (Acacio et al, 1973 & Nagpal et al, 1977). In 2015 Kord Valeshabad et al reported the assessment of the conjunctival microcirculation in 22 subjects diagnosed with SCR (Kord Valeshabad et al, 2015). The 22 patients were sub-divided based on the severity of their sickle cell associated ocular disease based on the presence or absence of focal macular thinning (FMT) indicating more significant disease. Patients with FMT (n=12) as compared to those without FMT (n=10) had no difference in diameter but had significantly lower axial velocity (0.45 ± 0.11 mm/s vs 0.64 ± 0.24 mm/s; p=0.03). The finding of reduced conjunctival venular blood velocity in SCR subjects with FMT supported the studies

hypothesis that systemic haematological abnormalities that cause more severe or frequent retinal microvascular occlusions and consequent retinal thinning also may manifest in alterations of conjunctival microvascular function (Kord Valeshabad et al, 2015).

Karanam et al were the 1st group to directly correlate indices of conjunctival microvascular function to conventional cardiovascular risk scores. They performed FSLB of the conjunctiva in 84 patients with a mean age of 60 years. They divided the population into 3 groups based around their calculated Framingham risk score (low, intermediate or high-risk). Both cross-sectional blood flow velocity and blood flow rate decreased as Framingham risk scores increased. Mean cross-sectional blood flow velocity was 0.37 ± 0.09 mm/s in low-risk subjects, 0.30 ± 0.09 mm/s in intermediate-risk subjects, and 0.29 ± 0.10 mm/s in high-risk subjects, p = 0.04. Mean blood flow rate was 133.4 ± 59.6 pl/s in low-risk subjects,123.6 ± 39.3 pl/s in intermediate-risk subjects, and 121.9 ± 52.6 pl/s in high-risk subjects, p = 0.04 (Karanam et al, 2019).

The impact of diabetes mellitus (DM) on the microcirculation of various tissues throughout the body is well described. Early manifestations of diabetic ocular disease can be observed in the retina. In 2017, Khansari et al therefore evaluated conjunctival microvascular haemodynamics in patients with increasing stages of diabetic microvasculopathy. This study evaluated 161 patients in total (34 controls, 47 with DM but no retinopathy,

45 with a non-proliferative DM retinopathy and 35 with a proliferative DM retinopathy). There were observable reductions in blood flow velocity, blood flow rate and wall shear rate in both arterioles and venules of patients with DM in comparison to controls. However, it did not clearly demonstrate that these measurements accurately correlated with the severity of diabetic ocular disease (Khansari et al, 2017).

Smartphone assessment of the microcirculation

In 2021 estimates suggest that over 6 billion people worldwide own and use a smartphone. This figure represents over 80% of the world's population and smartphone use has nearly doubled in the past 5 years (figures taken from Statista https://www.statista.com/statistics/330695/number-of-smartphone-users-worldwide/). The widespread use of smartphone technology has therefore led to the consideration of implantation of applications for both the diagnosis and monitoring of medical conditions. The most well documented medical use of smartphones is in the monitoring and treatment of patients with diabetes mellitus, with a comprehensive review concluding their use improved treatment targets, such as HbA1c (Garabedian et al, 2015).

With respect to cardiovascular disease the diagnostic utility of smartphones has been most well documented with respect to arrhythmia

screening and more specifically atrial fibrillation (Birkemeyer et al, 2021). Smartphones have also been utilised in the diagnosis of both hypertensive and diabetic retinal diseases (Russo et al, 2015; Raju et al, 2016; Rajalakshmi et al, 2018 & Arima et al, 2019). There is however limited literature on the use of smartphone technology to assess the macro or microcirculations. The benefits of smartphones in microvascular and ocular screening techniques include:

- Camera technology that provides excellent resolution and image quality sufficient for vascular imaging
- Well designed and intuitive user interfaces
- Equipped with technology allowing upload of imaging to computers for image analysis
- Widespread use in society means users are already largely familiar with use and no specific training is required

In 2019 Brennan et al described the first quantification of conjunctival microvascular parameters using a smartphone and slit-lamp biomicroscope combination. This pilot study evaluated the technique in 17 healthy volunteers deemed to be of low cardiovascular risk by conventional cardiovascular risk calculation (Q-RISK 3). Conjunctival imaging was performed using an iPhone 6s coupled with a slit-lamp biomicroscope to measure blood vessel and flow parameters. Quantifiable microvascular indices were obtained from 626 conjunctival vessels. The mean diameter of microvessels was 21.1 μm (range 5.8 - 58 μm). Mean

axial velocity was 0.50 mm/s (range 0.11 – 1.00 mm/s). Mean blood flow rate was 145.61 pl/s (range 7.05 - 1178.81 pl/s). Mean wall shear rate was 157.31 s^{-1} (range 37.37 - 841.66 s^{-1}) (Brennan et al, 2019).

The group later reported statistically significant differences in the measured microcirculatory parameters comparing control and post-MI populations. The parameters examined using this modality were diameter (D), axial velocity (V_a), blood flow (Q) and wall sheer rate (WSR) (Brennan et al, 2021). These findings raise the potential utility of this screening modality to detect preclinical microvascular dysfunction in asymptomatic patients with an estimated low-intermediate CV risk assessed by conventional screening modalities as described above. The main benefits of this modality are that it is relatively inexpensive, does not require intensive training for operators and utilises a readily assessible vascular bed that does not require exposure of the patient to ionizing radiation.

The study described in the subsequent chapters of this thesis is a continuation by our research group of the aforementioned pilot studies conducted by Brennan et al. The design of the previous studies whilst novel, introduce limitations to the conclusions that can be drawn with regard to the utility of this screening modality. The comparison between a group of ‘healthy’ low-risk volunteers and a group of post-MI patients makes two presumptions; firstly that the group of ‘healthy’ patients do not have asymptomatic undiagnosed coronary artery disease (CAD); and

secondly that the differences in both the conjunctival microcirculatory parameters and biomarkers observed were due to the presence of underlying CAD and not as a result of the well-recognised post-MI systemic inflammatory response. This thesis builds on this previous work and evaluates this novel method of microvascular assessment in patients with both stable coronary artery disease and valvular heart disease.

Limitations of slit-lamp biomicroscopy of the conjunctival vessels

The most important initial criteria that any novel screening modality must possess is the ability to obtain results that are reliable, reproducible and are not associated with significant inter- or intra-observer variability. As described in detail above a previous study evaluating conjunctival microvascular screening (Xu et al, 2015) demonstrated both insignificant inter-observer variability and no impact on time of day on results. Khansari et al also demonstrated an acceptable degree of repeatability of a similar conjunctival vascular screening technique (Khansari et al, 2016).

Our research group assessed repeatability by one observer analysing the video sequences for 5 control subjects twice, blinded to the clinical and demographic details of each subject. The repeated measurements were obtained from 38 vessel segments (5–9 per subject). Differences in the four main measured parameters (D, Va, Q, WSR) were compared. Coefficients of repeatability (CR) were calculated using conventional

approaches. The mean difference for D was 0.01 ± 0.04 μm, CR 0.08 μm (95%CI − 0.09 μm to 0.07 μm) and for Va was 0.002 mm/s ± 0.01 mm/s, CR 0.02 mm/s (95%CI − 0.02 mm/s to 0.02 mm/s). The mean difference for Q was 0.03 ± 2.14 pl/s, CR 4.19 pl/s (95%CI − 4.1 pl/s to 4.2 pl/s) and for WSR was 0.78 ± 4.17 s−1, CR 8.18 s−1 (95%CI − 7.4 to 9.0 s−1). These results support acceptable repeatability of vessel segment analysis using our current technical approach (Brennan et al 2021).

Beyond the limitations of quantifying microvascular parameters following image acquisition, the practical limitations of the slit-lamp include:

- Head movement of the patient
- Ocular movement and blinking
- Involuntary movements such as physiological tremor or nystagmus
- Fixed equipment may limit imaging of patients with orthopaedic and rheumatological conditions

Most of these issues can be overcome through a combination of optimising the imaging environment, providing an external fixation target for patients to limit eye movement, delivering appropriate patient instructions and selecting a sequence of images for analysis that minimises movement and blinking artefact. The effect of contact lens use has been described earlier and hence is an exclusion criterion for participation in this study.

Thesis aims and objectives

The aims and objectives of this thesis are as follows:

- To refine the methodology of this modality of conjunctival microvascular assessment, including the development of techniques for vessel differentiation.
- To compare the conjunctival microcirculation in a cohort of patients with a myocardial infarction, to a cohort of controls with no physiologically significant epicardial coronary disease or personal history of major adverse cardiovascular event.
- To compare the conjunctival microcirculation in a cohort of patients with angina, no obstructive epicardial coronary artery disease and evidence of coronary microvascular dysfunction demonstrated by a positive invasive physiological assessment of coronary microvascular function to a cohort of controls with no physiologically significant epicardial or microvascular disease.
- To compare the conjunctival microcirculation in a cohort of patients with severe aortic stenosis to a cohort of control subjects with no haemodynamically significant valvular heart disease.
- To evaluate the impact of transcatheter aortic valve implantation (TAVI) for the treatment of severe aortic stenosis on conjunctival microcirculatory function.

Chapter 2

Optimising a smartphone-based assessment of indices of conjunctival microvascular function

Chapter 2 abstract

Aims

Microvascular dysfunction is one of the earliest pathophysiological manifestations of atherosclerotic cardiovascular disease. The conjunctival microcirculation has previously been studied as an accessible network of vessels to evaluate the impact of systemic conditions on microvascular function. Most of the studies reporting indices of conjunctival microvascular function have done so using a slit-lamp biomicroscope and digital charge coupled camera device. Our research group previously highlighted the utility of smartphone technology as a tool to assess conjunctival microvascular function non-invasively (Brennan et al, 2019). This chapter describes the refinement and optimisation of this semi-automated process and the subsequent study of two cohorts with cardiovascular disease known to be associated with microvascular dysfunction: 1. coronary microvascular disease and 2. severe aortic stenosis.

Methods and Results

The conjunctival imaging platform utilised in this study consisted of an iPhone 11pro coupled with a TopCon SL-D4 slit-lamp biomicroscope using a bespoke adaptor. Video recording was performed using the iPhone camera via a third-party and commercially available recording application. The settings on both smartphone and slit-lamp biomicroscope remained

consistent for all subjects. Following conjunctival imaging, videos were converted to grey-scale binary images for downstream processing. Sequence selection was performed manually prior to an automated analysis by a specifically designed application that measured vessel diameter and subsequently blood flow velocity by tracking visible erythrocyte motion. Vessels were differentiated into arterioles and venules manually based on the direction of blood flow in relation to bifurcations. To validate the results reported we assessed the accuracy and repeatability of this technique for haemodynamic quantification at both the manual and automated stages of this process.

Conclusions

A smartphone in combination with a slit-lamp biomicroscope can provide video imaging of sufficient quality to allow the calculation of conjunctival vessel diameter and other indices of microvascular function (axial/cross-sectional velocity, blood flow rate, wall shear rate and wall shear stress). The repeatability of this technique is sufficient to obtain reliable measures of microvascular function. This technique may have clinical utility in the diagnosis of microvascular disease and in population based cardiovascular disease risk screening.

Introduction

The ocular microvasculature provides a readily accessible network of peripheral blood vessels for the non-invasive assessment of physiological parameters of microvascular function. Unlike retinal vascular assessment, imaging of the bulbar conjunctiva is advantageous as it has no requirement for mydriatic agents to facilitate pupillary dilatation. This enables imaging with no temporary impact to the patient's vision. With sufficient magnification, erythrocyte flow within conjunctival blood vessels can be directly visualised given the small relative thickness of the microvascular adventitia, media and intima. These principles allow the non-invasive and semi-automated assessment of parameters of microvascular function in conjunctival vessels.

As previously described conjunctival vascular imaging has been predominantly performed using a combination of a slit-lamp biomicroscope and digital charged camera (CCD). In 2019 Brennan et al published the first description of the assessment of the conjunctival microvasculature using smartphone technology. This technique was then applied to 2 distinct CVD phenotypes (myocardial infarction and cyanotic congenital heart disease). These pilot studies highlighted the ability to observe alterations in conjunctival microvascular function in these sub-groups of CVD. This study will evaluate this technique of microvascular imaging in patients with both coronary microvascular dysfunction and severe aortic stenosis in comparison to age- and sex-matched controls.

This chapter describes the technical aspects of the development and validation of this method of conjunctival vascular imaging. It will also describe the technological developments that have been made to refine the assessment of the two aforementioned CVD groups.

Key ethical issues

This project received ethical approval from ORECNI and the West Midlands South Birmingham Research Ethics Committee (REC Reference 15/WM/0431 and IRAS project ID 166742).

Informed consent

All subjects were provided with both written and verbal information prior to consenting formally to participation in the study. The written information had been reviewed and approved by the ethics committee prior to commencement of the study. Adequate time was given to allow subjects to consider this information and hence provide an informed decision regarding their participation. Written information was provided in English only, therefore any subjects that were not fluent in the English language were provided verbal information regarding the study via an independent translator. This was only applicable to one participant in the study. All subjects then provided written informed consent to participation.

Confidentiality and data handling

All subjects were recruited and information collected in a confidential environment. Paper copies of questionnaires and signed consent forms were stored in a locked filing cabinet in a dedicated research office in the Royal Victoria Hospital, Belfast. This data was under the custodial care of the principal investigator of the study. Subjects were given a unique study code and electronic data was stored in a fully anonymised format. This electronic database was kept encrypted and password protected on hospital and university computers. Both paper and electronic data was only accessible by researchers involved with this study. All patients provided both verbal and written consent to researchers accessing their Northern Ireland Electronic Care Record (NIECR) to ensure the accuracy of baseline characteristics collected and to allow clinical follow-up of patients following discharge.

Blood sampling and storage

All blood samples were collected by a member of the clinical research team. All researchers involved with blood collection had undergone previous phlebotomy training and had been signed off as competent in the required skills. Routine bloods were processed by the Belfast Trust laboratory department. 20ml of blood was also sampled from each patient and a series of novel cardiovascular biomarkers analysed. These biomarkers form the basis for a thesis presented by another PhD student and the results are not reported in this thesis.

Participant recruitment

All interventional cardiologists in the Royal Victoria Hospital, Belfast were informed of the commencement of this clinical study and provided a summary of the study design and protocol. Patients were identified by the treating clinicians and researchers were then provided basic details of subjects during their hospitalisation for this treatment. Subjects were then approached and consented to participation by researchers. The study adhered to the Declaration of Helsinki.

Sample storage

All human samples were stored within the Royal Victoria Hospital, Belfast or University of Ulster, Belfast. All samples were handled and stored in accordance with the 2004 Human Tissue Act (HTA).

The impact of COVID-19

Prior to the commencement of this study, COVID-19 had become endemic in Northern Ireland. In order to avoid unnecessary social contact for study subjects and researchers, recruitment was only performed during either an elective or unscheduled hospital presentation that was required for the treatment of their medical condition. Subjects were not invited to attend hospital solely for data collection, blood sampling or conjunctival imaging. During the design of the study, the aortic stenosis group were planned to have repeat blood sampling and conjunctival imaging performed at a 3-

month follow-up appointment. This was to tie in with clinical post-procedural follow-up. The Belfast Trust subsequently replaced these “face-to-face” consultations with a telephone appointment. Following a risk assessment, our research group chose not to collect 3-month follow-up data in this sub-group, thereby avoiding unnecessary hospital contact for these subjects. These decisions were in line with national COVID-19 guidelines in addition to the Belfast Trust and University of Ulster’s policies during the recruitment period.

Statistical analysis

A formal power calculation was performed using the results from our research group’s previous study evaluating the conjunctival microcirculation in patients with a myocardial infarction (MI) in comparison to a group of controls (Brennan et al, 2021). In this study a total of 132 patients were enrolled (66 MI vs 66 controls), with a mean of 36 conjunctival vessels analysed per patient. We estimated for a 10% reduction in the between group means of both the aortic stenosis and coronary microvascular disease cohorts of our study. We calculated that a sample size of 100 patients (3600 conjunctival vessels) in both the aortic stenosis and coronary microvascular disease cohorts would provide the study with a power of at least 80% to reject the null hypothesis of no between-group differences in conjunctival microvascular parameters.

To mitigate the confounding effects of age and sex specific differences on microvascular function, matching was performed throughout the recruitment period. This posed obvious challenges as recruitment was aimed at all comers with valvular and coronary heart disease to our institution that met our eligibility criteria.

For statistical analysis, Statistical Package for the Social Sciences (SPSS) for Apple iOS version 27 (property of IBM) was used. Continuous variables were described using the mean and standard deviation of the mean. Kolmogorov–Smirnov testing was used to assess the normality of the continuous variables. Categorical variables were expressed as a number and percentage of the total category number to which the variable belonged.

Normally distributed continuous variables were compared between the two populations using the independent-samples t-test. Non-normally distributed continuous variables were compared using a non-parametric test (Mann–Whitney U test). Categorical comparisons were made between the two groups using Pearson Chi-Square or Fisher's exact test.

Imaging using a slit-lamp biomicroscope and smartphone combination

Equipment for image acquisition

In order to obtain video imaging of the conjunctival microvasculature of sufficient quality to allow for the quantification of microvascular parameters, a combination of hardware that provides sufficient illumination and magnification of the vessels is required. This study utilised similar technology described by our research group previously (Brennan et al, 2019), but with an upgrade to the smartphone used in line with technological developments since that study. The equipment used for conjunctival vascular imaging included:

1. Topcon SL-D4 Slit-lamp Biomicroscope (Topcon Medical Systems Inc., Oakland, NJ, USA) **(Figure 2.1)**
2. Apple iPhone 11 Pro Smartphone (Apple Inc., Cupertino, CA, USA) **(Figure 2.2)**
3. Digital Photomicrography Slit-lamp Lens Adapter (Zarf Enterprises Inc., Spokane, WA, USA) **(Figure 2.3)**

Figure 2.4 demonstrates how this equipment was combined for vascular imaging.

Figure 2.1. Topcon SL-D4 Slit-lamp Biomicroscope (Topcon Medical Systems Inc., Oakland, NJ, USA)

Figure 2.2. Apple iPhone 11 Pro Smartphone (Apple Inc., Cupertino, CA, USA)

Figure 2.3. Digital Photomicrography Slit-lamp Lens Adapter (Zarf Enterprises Inc., Spokane, WA, USA)

Figure 2.4. Demonstration of the combination of the component parts of the conjunctival imaging apparatus

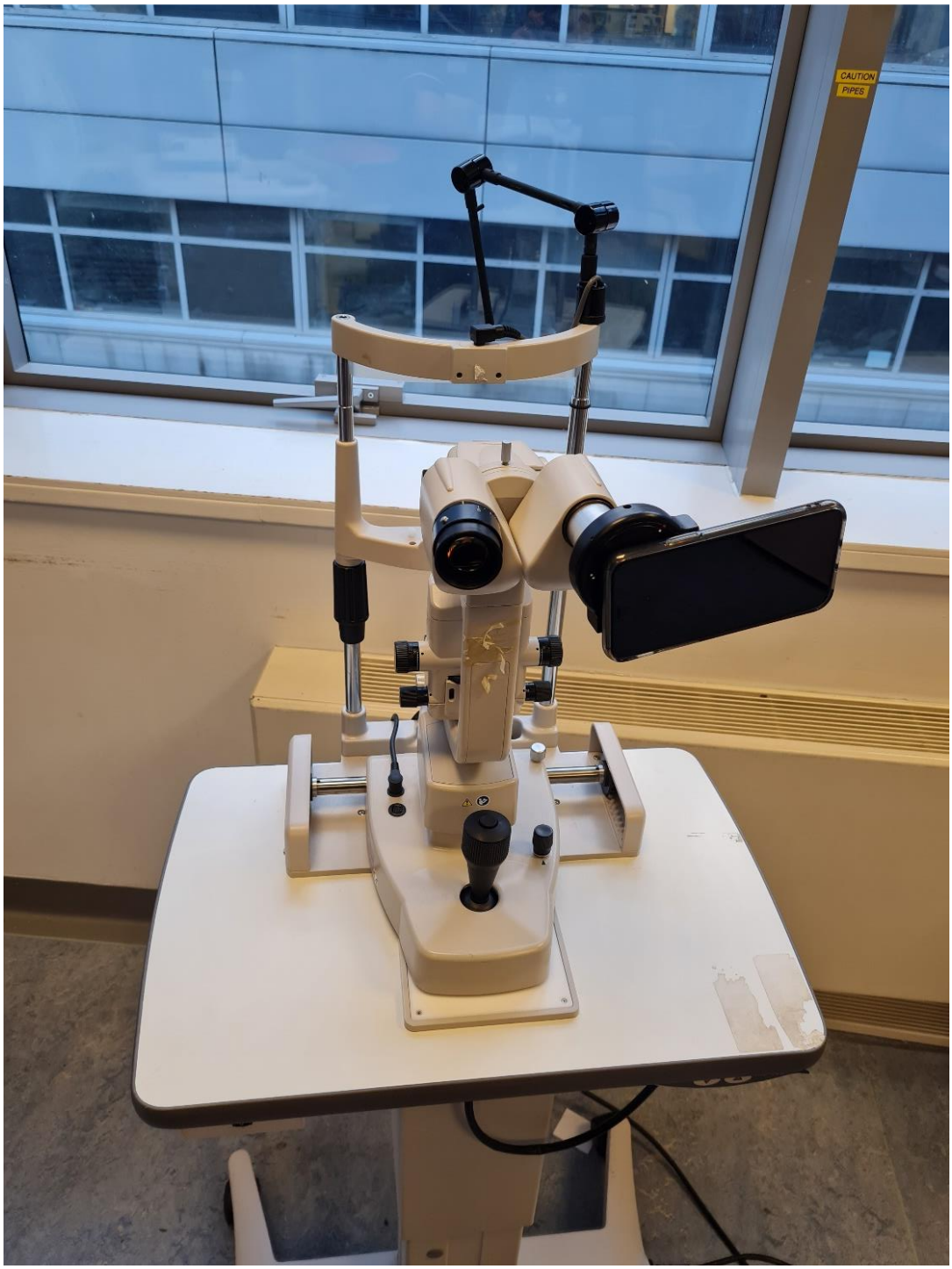

Image Acquisition

The Topcon SL-D4 (Topcon Medical Systems Inc., Oakland, NJ, USA) slit-lamp biomicroscope (**Figure 2.1)** was used for both illumination and magnification of the bulbar conjunctival microvasculature. This provided a 40x magnification of the micro-vessels. Images were then also magnified by the smartphone camera by a further factor of 2x. This allowed sufficient image quality without the size of the field of view and number of blood vessels visualised. The slit-lamp and iPhone were coupled using a bespoke adapter developed by Zarf Enterprises (**Figure 2.3).**

A smartphone was selected for video imaging as it is a portable recording device with an excellent and straightforward user interface. In addition, it allows high speed data transfer to other devices for downstream video processing and analysis. The downside to the “ease-of-use” of this technology is that the pre-installed video recording software gives little control over relevant camera properties (focus, ISO, shutter speed, aperture and compression). Most of these settings are controlled by the device to provide automatic image optimisation for the standard user, however this means that videos are recorded under a multitude of different video settings and hence vessel measurements would not be reproducible. In this study we overcame this by using a commercially available third-party application “ProMovie Recorder” (www.promovieapp.com). This enabled conjunctival imaging to be performed in line with a set imaging protocol (see below), which provided

consistent imaging settings with respect to zoom, ISO, focus, shutter speed and exposure. This allowed calculation of a pixel to millimetre conversion factor for the video settings applied. This conversion factor was then used for the downstream measurement of vessel diameter and blood flow velocity, in addition to the calculation of other parameters of microcirculatory function.

Equipment calibration to facilitate quantification of indices of microvascular function

Calibration was performed using a PYSER-SGI (100x0.01=1mm) calibration reticle. This reticle was positioned in the imaging field of the slit-lamp and brought into focus. 5 videos were acquired at both 1080 x 1920 and 3840 x 2160 pixels resolution (see **Figure 2.5**). Videos were then used to obtain a pixel to millimetre calibration factor for the 3 iPhone cameras at both resolution settings according to the following protocol:

1. Video loaded into a video processing utility for Microsoft (virtualdub)
2. 60 frames of video selected on the basis of 2 criteria:
    a. Least movement during recorded period
    b. Imaging sharp and in focus
3. PNG image sequence exported to documents file and then imported as image sequence to Java-based image processing program (Image J)
4. Average image from sequence in Image J using projection Z plugin

5. Straight line distance measured in pixels along the 1mm calibration reticle

This process allowed the number of pixels per millimetre (mm) in each video to be calculated. This was then averaged across the 5 videos obtained to give a pixel to mm conversion factor for both recorded resolutions. The standard wide camera on the iPhone was chosen to standardise imaging. Using this camera, the pixel to mm conversion factor was calculated as 454.8 ± 22.4 pixels/mm on 1080 x 1920p resolution and 3840 x 2160p= 894.7 ± 53.6 pixels/mm. This conversion factor was applied during image processing to enable the calculation of distance, vessel diameter and velocity of blood flow (as described in detail below).

Figure 2.5. Photograph at 80x magnification of the reticle used for the calibration process.

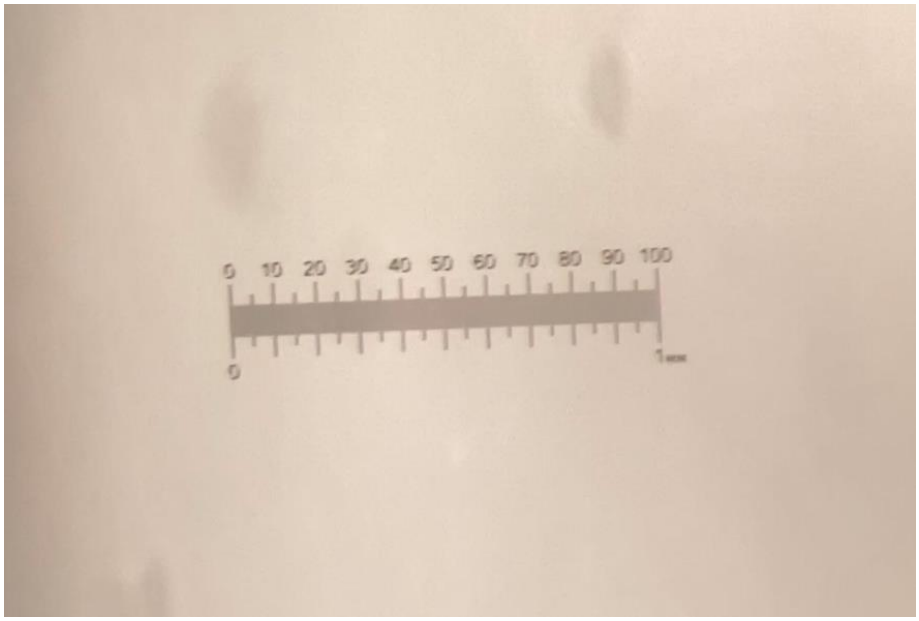

Protocol for conjunctival image acquisition

1. All imaging was performed with surrounding external lighting dimmed and the primary source of ocular illumination provided by the slit-lamp biomicroscope.
2. The 12 megapixel rear facing wide lens on the iPhone 11 pro was used to acquire videos.
3. The iPhone was connected to the slit-lamp biomicroscope using the previously described bespoke adaptor **(Figure 2.3).**
4. Magnification on the slit-lamp was set at a factor of 40x.
5. An external fixation target was used to minimise blinking and eye movement.
6. Videos were captured using the camera application “Promovie Recorder”. The fixed camera settings used were as follows:
    a. Aspect ratio 16 : 9
    b. Resolution 3840 x 2160 pixels
    c. Frame rate 60 frames per second
    d. Maximal available compression bitrate (120Mbps)
    e. Camera zoom 2x magnification
    f. Focus 0.5
    g. ISO set to the minimum level (30)
    h. Shutter speed set to minimum level (61)
7. In each subject 5 to 10 second videos were obtained from both the nasal and temporal fields of each eye (a total of 4 videos per subject)

8. Videos were saved under a unique anonymised study number prior to being electronically transferred to a University laptop for image processing

Image processing

A summary of the image processing steps used in sequence to determine microvascular indices and hence assess conjunctival microvascular function is shown in **Figure 2.6**.

Figure 2.6. Stepwise schematic of image processing

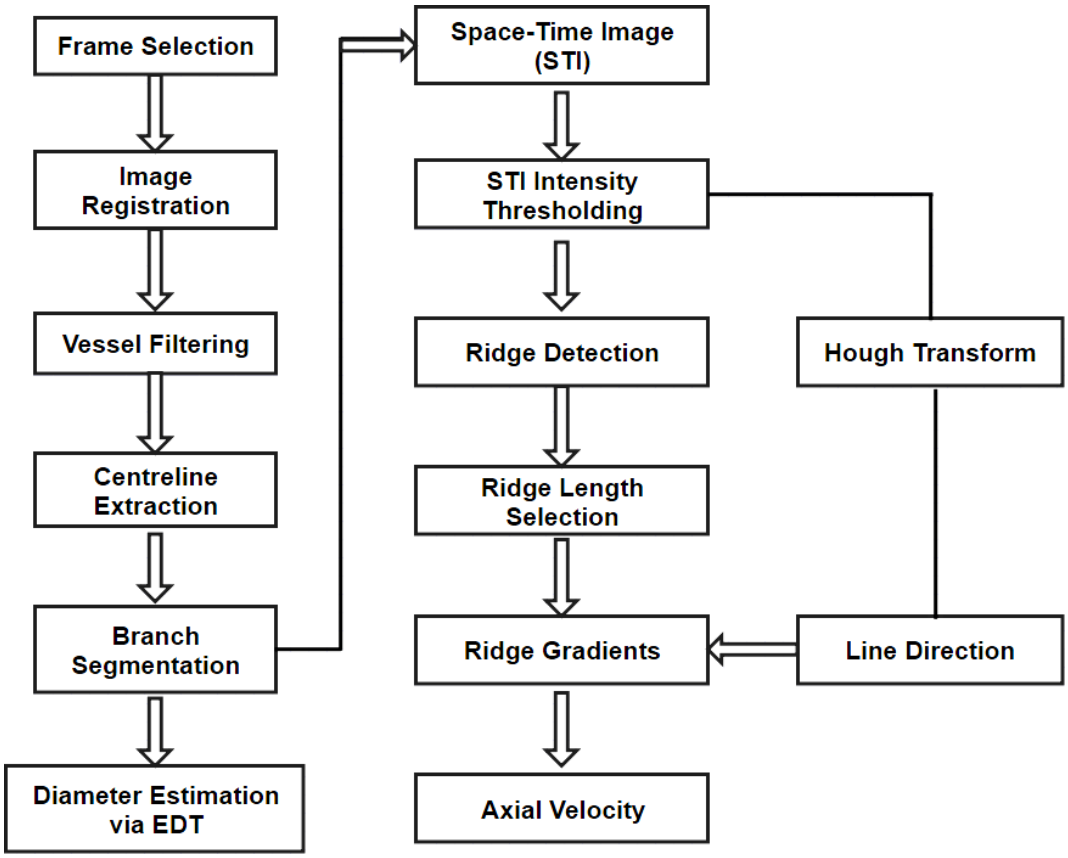

Following image acquisition, an initial manual visual inspection of the videos was performed. This allowed for consecutive frames of the highest quality to be selected for subsequent analysis by researchers. The criteria applied to select these frames included:

- Conjunctival microvasculature in focus
- No eye blinking
- Minimal eye movement
- Field of view did not drift by more than 25% of the width of the frame

Figure 2.7. Conjunctival imaging prior to sequence selection and video stabilisation process

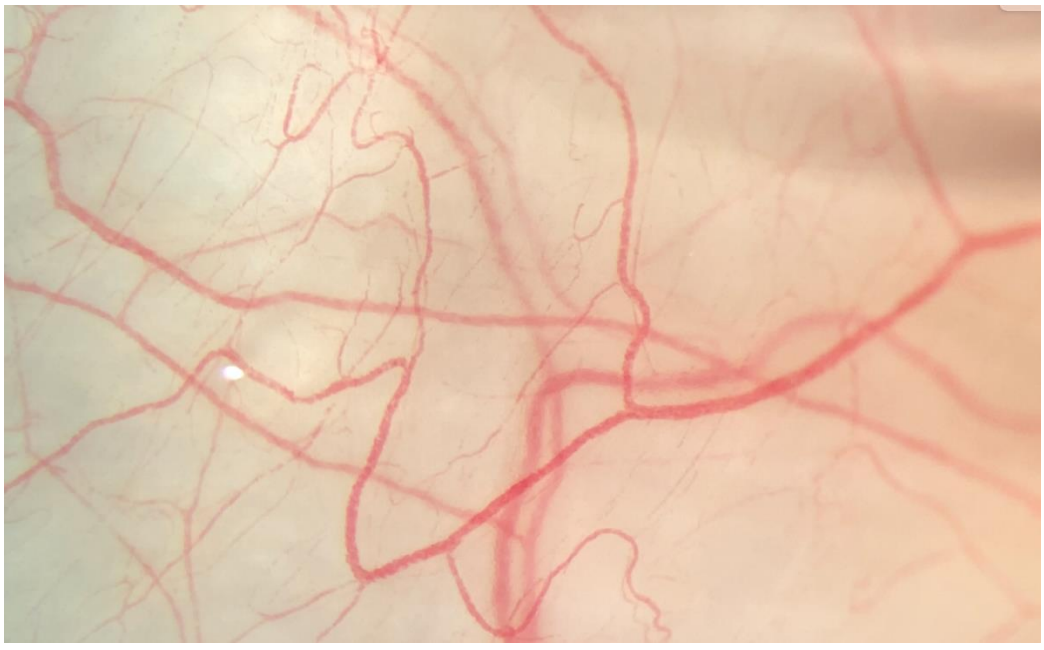

The colour videos were converted into grey scale (**Figure 2.8**) and any underexposed or out of focus regions were excluded. The sharpest frame in the selected sequence was then chosen as a reference frame and all other frames registered to it through an affine registration procedure (Forsberg, 2013). A vessel enhancement filter was then applied to the mean registered images (Jerman et al, 2016) to enhance the performance of the Frangi filter (Frangi et al, 1998). A binary map of the conjunctival vasculature and corresponding centrelines was obtained via standard skeletisation techniques (**Figure 2.9**). This allowed small spurious branches to be removed and for the detection of the end and branch points of the vessels. The connected vessel network was broken into individual vessel segments by setting the branch points' neighbouring pixels to zero. Any vessel segments longer than 30 pixels were selected for further assessment.

Figure 2.8. Stabilised grey scale video

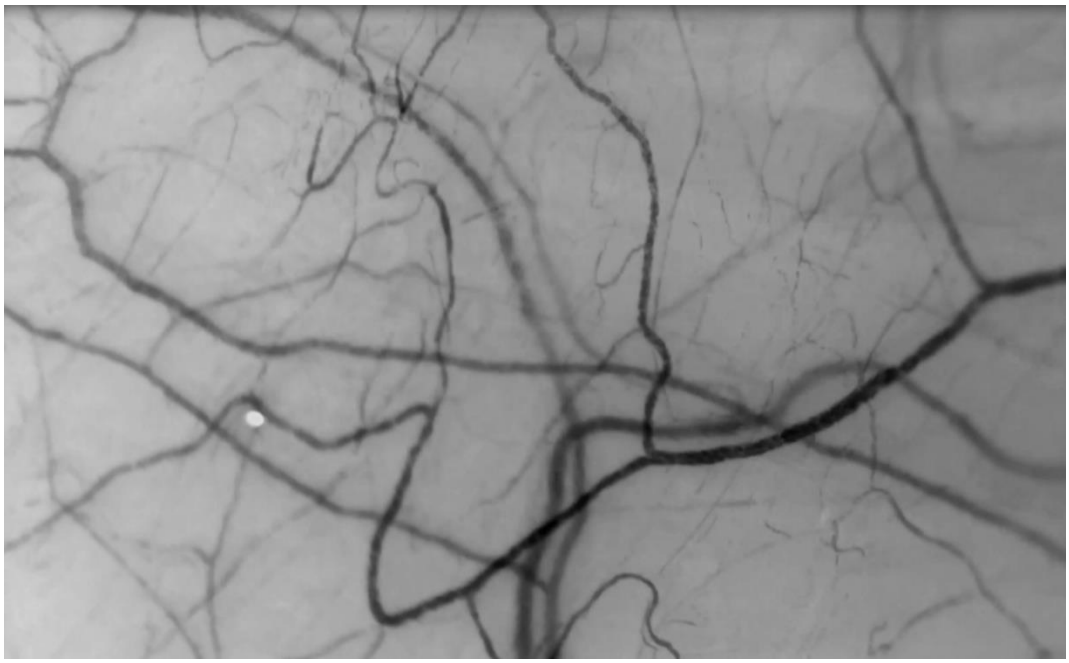

Figure 2.9. Grey scale video with centrelines

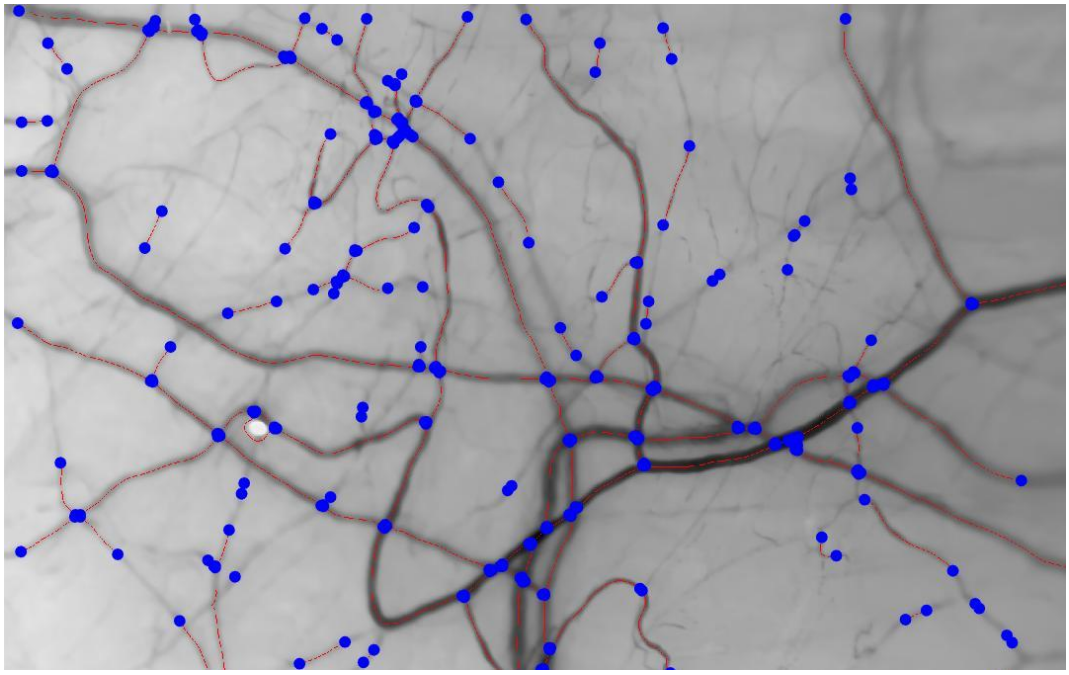

Estimation of vessel diameter

The Euclidean Distance Transform (EDT) was used for vessel diameter estimation. This method can be applied to binary images to measure the straight-line distance in pixels between two points on the image. This measurement in pixels is then converted to millimetres using the previously calibrated pixel to mm conversion factor for the constant camera settings applied in the recording protocol. Using this method, the vessel centreline is used to obtain the central EDT values and thus the radius along the vessel axis. The average of the diameters along the analysed vessel length was used to provide the final vessel diameter estimation.

Estimation of axial velocity

The axial velocity of blood flow within the vessels imaged was estimated using spatial-temporal image (STI) graphs generated for each analysed vessel segment (**Figure 2.10**). In these STI graphs a change in signal intensity is reflective of erythrocyte movement through the blood vessel. The graphs provide a plot of signal intensity against vessel segment length on the y-axis and the frame number on the x-axis. All imaging was recorded at a consistent setting of 60 frames per second, meaning 1 frame= 0.01667 seconds. Therefore, the slope of the change in signal intensity can be used to track erythrocytes, calculate the change in distance of an erythrocyte in mm/frame, which can then be converted to axial velocity in mm/s. These STI graphs can then be matched to an

annotated grey-scale conjunctival vessel map (**Figure 2.11**). The process of generating these STI graphs is automated using specially designed software. Afterwards the process requires a manual review to differentiate which graphs are of sufficient quality to enable erythrocyte tracking and hence estimation of the axial velocity.

Figure 2.10. STI graphs

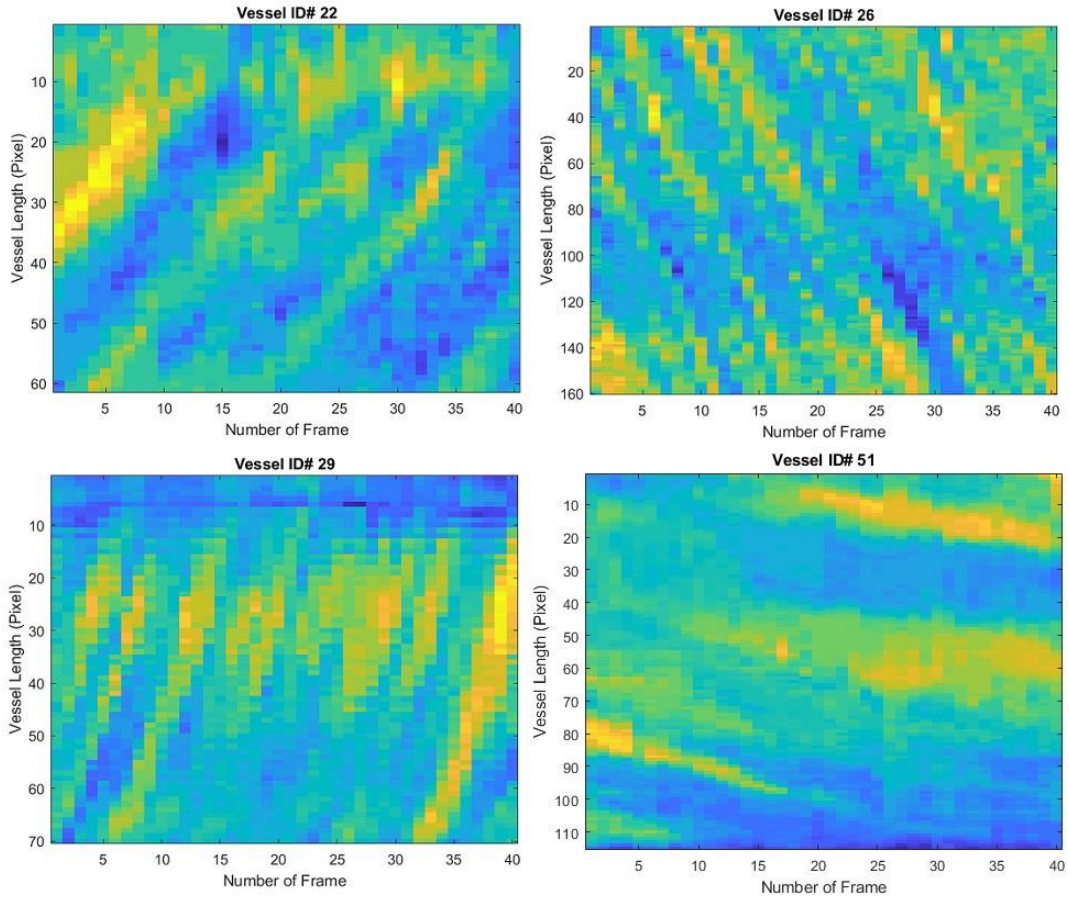

Figure 2.11. Grey scale video after segmentation

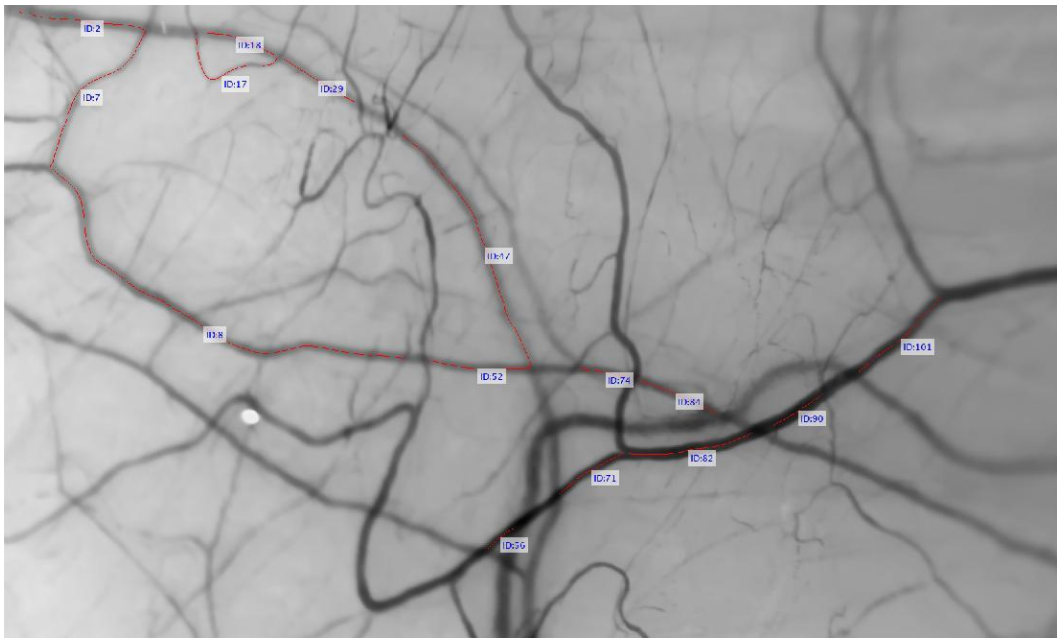

Quantifying additional conjunctival microvascular parameters

Cross-sectional velocity, blood flow rate, wall shear rate and wall shear stress were estimated using the formulae described below. These calculations are performed using the results for diameter and axial velocity described in previous publications (Khansari et al, 2016 & Koutsiaris et al, 2007). These estimates were on the basis of external vessel diameter and not true luminal diameter, however it is not possible to measure luminal diameter using this technique and the thickness of the vessel wall in the microvasculature was presumed to be negligible.

Cross-sectional velocity (V_{cs})

V_{cs} is impacted by the diameter of the vessel in which blood is travelling. In this study it was calculated according to these formulae:

Diameter / human erythrocyte diameter (D_c) ≤ 0.6:

$$V_{cs} = V_a$$

Diameter / human erythrocyte diameter (D_c) > 0.6:*

$$V_{cs} = V_a / 1.58 \times (1 - e^{-\sqrt{2D_c}})$$

* In these equations D_c was taken to be a constant, equal to 7.65 μm.

Blood flow rate (Q)

Q has a linear relationship to V_{cs} and is exponentially related to diameter according to this formula:

$$Q = V_{cs} (\pi D^2 / 4)$$

Wall shear rate (WSR)

WSR has a linear relationship to V_{cs} and an inverse relationship to diameter according to this formula:

$$WSR = (8V_{cs}) / D$$

Wall shear stress

Wall shear stress (WSS) is calculated as the product of wall shear rate (WSR) and whole blood viscosity (η):

$$WSS = WSR \times \eta$$

Newton's law defines the relationship between shear stress and the shear rate of a fluid subjected to mechanical stress. The ratio of shear stress to shear rate is a constant for a given temperature and pressure, and hence in Newtonian fluids the viscosity is independent of the shear rate (Qureshi et al, 2013). Blood does not follow Newton's law of viscosity, and hence is described as a non-Newtonian fluid. The primary determinants of η are plasma viscosity (η_p) (in turn primarily influenced by total protein concentration), haematocrit (HCT) and the mechanical properties of red blood cells (Baskurt et al, 2003).

In this study it was not possible to measure η directly on participants as expensive specialised laboratory equipment is required. The Quemada model for estimation of η was therefore chosen to obtain results and in turn estimate WSS (Quemada, 1981). This model takes into consideration HCT, η_p and WSR as defined in the equation below:

$$\eta = \eta_\rho \left(1 - \frac{1}{2} \frac{\kappa_0 + \kappa_\infty \sqrt{\frac{\dot{\gamma}}{\gamma_c}}}{1 + \sqrt{\frac{\dot{\gamma}}{\gamma_c}}} H_t \right)^{-2}$$

In this equation k_0, k_∞ and γ_c are constants (4.33, 2.07 and 1.88 respectively). HCT and η_p were obtained from blood sampling during the recruitment process and WSR estimated for the individual vessels as described previously in this chapter.

Assessing repeatability of conjunctival parameter quantification

The aforementioned process to quantify physiological parameters of microcirculatory function needs to consider several possible areas that may impact the reproducibility of results:

1. Time of day conjunctival imaging performed
2. Impact of operator on imaging and results
3. Participant use of antithrombotic and anti-hypertensive medications
4. Conjunctival video stabilisation and sequence selection
5. Downstream image processing and microvascular parameter quantification

1. Time of day conjunctival imaging performed

A previous study evaluated the impact that time of day had on conjunctival haemodynamics. In this study the conjunctiva of 20 healthy subjects were imaged by two independent operators and then measurements were repeated every 2 hours to evaluate the variations that occurred over the course of a single day. No significant differences were observed in the microvascular haemodynamics obtained between the various time

intervals of imaging, suggesting that slit-lamp imaging of the conjunctiva can be performed at any time throughout the day, without the time itself impacting the results obtained (Xu et al, 2015).

On the basis of the results from this study, imaging of the conjunctiva was not performed at a pre-specified time of day, instead this was dictated by timing in relation to the administration of peri-procedural medications (see below for more detail).

2. Impact of operator on imaging and results

In the above described study from Xu et al in 2015, the coefficient of repeatability (CoR%) and intraclass correlation coefficient (ICC) between the 2 operators suggested excellent correlation and repeatability for both vessel diameter (ICC= 0.989 and CoR%= 4.87%) and axial blood velocity (ICC=0.997 and CoR%= 11.49%). This study highlighted minimal inter-observer variability between assessors and therefore we chose for conjunctival imaging within this study to be performed by more than one researcher.

3. Participant use of antithrombotic and anti-hypertensive medications

All participants in the microvascular disease cohort of this study were recruited following the performance of a coronary angiogram and pressure

wire evaluation of coronary physiology. This involves the administration of intra-arterial nitroglycerine and unfractionated heparin in addition to intravenous adenosine. Adenosine and nitroglycerine have very short half-lives (10-30 seconds and 1.5-7.5 minutes respectively) (Pantely et al, 1990 & Kim et al, 2022). Unfractionated heparin has a longer half-life (30 minutes) (Blann et al, 2002). In order to mitigate the impact of these medications on the conjunctival microcirculation and avoid any potentially confounding effect, participants were recruited a minimum of 4 hours following their procedure in order to ensure these medications would not impact results. Likewise in the aortic stenosis cohort of our study, participants had conjunctival imaging performed prior to their procedure and more than 6 hours following TAVI to avoid peri-procedural medications confounding results.

Participants in this study were all-comers and therefore were on regular anti-thrombotic and anti-hypertensive medications for the treatment of co-morbid conditions. This is acknowledged as a limitation, but an analysis of the between group medication differences and their impact on results is presented in the subsequent data chapters of this thesis.

4. Conjunctival video stabilisation and sequence selection

The process of video stabilisation and conversion of images to a binary format for analysis is semi-automated. Researchers review the 5 - 10

second conjunctival videos and select 1 second (60 frames) for subsequent analysis described previously in this chapter. This process therefore is subject to operator variation. Whilst this may influence results, this is performed to select the sequence with the best image quality and hence we believe provides the most accurate assessment of microvascular parameters. In the future this process will ideally become fully automated. Following sequence selection, the process of video stabilisation is entirely automated and provided the same sequence is selected introduces no variability.

5. Downstream image processing and microvascular parameter quantification

The repeatability of the methodology to obtain results following video stabilisation was assessed both using the previous iPhone 6s imaging platform and has been repeated for the upgraded iPhone 11pro system.

iPhone 6s

One researcher analysed 5 video sequences for control subjects twice. The researcher was blinded to the clinical and demographic details of each subject. The repeated measurements were obtained from 38 vessel segments (5–9 per video). Differences in the four main measured parameters (D, V_a, Q, WSR) were compared. Coefficients of repeatability (CR) were calculated. The mean difference for D was 0.01 ± 0.04 μm, CR

0.08 µm (95% CI − 0.09 µm to 0.07 µm) and for V_a was 0.002 mm/s ± 0.01 mm/s, CR 0.02 mm/s (95% CI − 0.02 mm/s to 0.02 mm/s). The mean difference for Q was 0.03 ± 2.14 pl/s, CR 4.19 pl/s (95% CI − 4.1 pl/s to 4.2 pl/s) and for WSR was 0.78 ± 4.17 s^{-1}, CR 8.18 s^{-1} (95% CI − 7.4 to 9.0 s^{-1}) (Brennan et al, 2021).

iPhone 11pro

A total of 16 videos recorded from 4 participants were analysed twice by the same operator independent of clinical details or the participant cohort. A total of 221 vessels were analysed. Differences in the four main measured parameters (D, V_a, Q, WSR) were compared. Stabilised vessel maps were then reviewed by another independent operator to ensure the same vessels were compared. For each vessel the mean difference in 5 measured parameters (D, V_a, V_{cs}, Q and WSR) was calculated. The mean difference for D was 0.02 ± 0.31 µm, V_a was 0.002 ± 0.02 mm/s, V_{cs} was 0.001 ± 0.02 mm/s, Q was 0.08 ± 11.31 pl/s and WSR was 0.98 ± 8.39 s^{-1}. Intraclass correlation coefficient suggested excellent repeatability across all parameters (D 0.999, 95% CI 0.999 – 0.999; V_a 0.986, 95% CI 0.981 – 0.989; V_{cs} 0.985, 95% CI 0.980 – 0.988; Q 0.997, 95% CI 0.996 – 0.998; and WSR 0.988, 95% CI 0.985 – 0.991).

The differentiation of arterioles and venules

Classification of blood vessel type was performed on the basis of blood flow direction in relation to vessel bifurcations. This method of vessel differentiation has been described previously by Khansari et al in 2016 and 2017. Vessels were defined as arterioles if blood flow was towards a diverging bifurcation; venules if blood flow was towards a converging bifurcation; and undifferentiated if no bifurcation was present in the imaging field to allow vessel differentiation.

Figure 2.12. Figure illustrating the principle used for arteriolar and venular differentiation based on blood flow direction in relation to vessel bifurcations

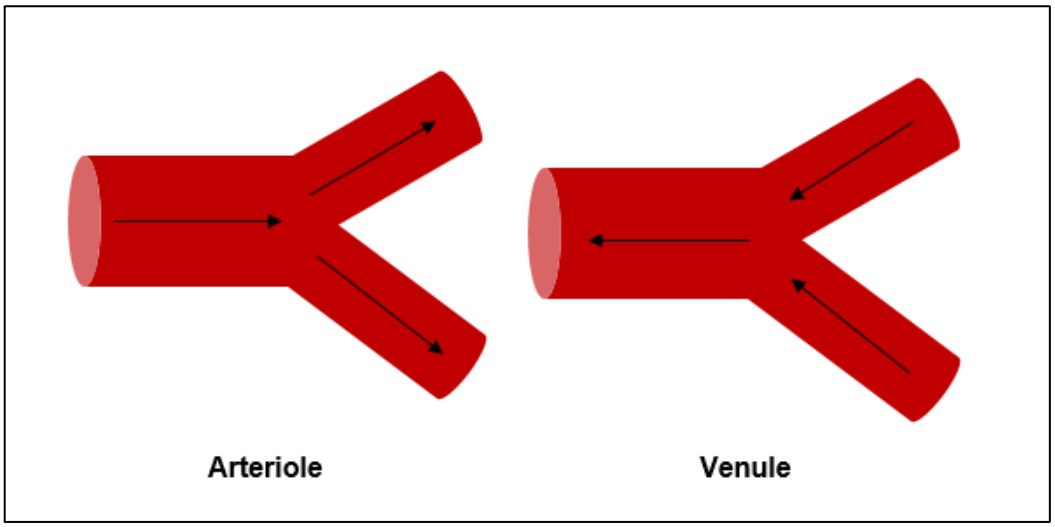

This method of vessel differentiation has 2 main limitations:

1. It is not automated and requires individual review of each measured vessel segment which is time-consuming
2. Repeatability is variable as there is a degree of subjectivity with regards to vessel allocation

In order to assess the repeatability of this method we compared the results of vessel differentiation performed by four independent assessors with varying experience in the interpretation of vascular imaging. These included 2 interventional cardiologists with several years of previous experience, 1 junior doctor with limited experience and 1 PhD student with no experience. All 4 assessors interpreted a total of 28 conjunctival videos with a mean of 7.7 ± 2.1 vessels per video (total = 216 vessels).

Fleiss' kappa was run to determine the agreement between assessors. There was moderate agreement between all 4 assessors (κ = 0.488, 95% CI, 0.446 to 0.529, $p < .0005$). Individual kappa for arterioles, venules and undifferentiated vessels was 0.428, 0.854 and 0.579 respectively. Excluding the assessor with no experience in vascular imaging there was good agreement between the remaining 3 assessors (κ= 0.695, 95% CI, 0.632 to 0.757, $p < .0005$). There was very good agreement between the 2 assessors with several years of experience in vascular imaging (κ = 0.839, 95% CI, 0.734 to 0.943, $p < .0005$).

Given the above results, all vessel differentiation was performed by an interventional cardiologist with several years of experience in the interpretation of vascular imaging.

Conclusion

Using a pre-defined and consistent imaging protocol, a smartphone in combination with a slit-lamp biomicroscope can provide video imaging of sufficient quality to allow conjunctival microvascular diameter to be calculated in addition to other indices of microvascular function (axial/cross-sectional velocity, blood flow rate, wall shear rate and wall shear stress). The repeatability of this technique is sufficient to obtain reliable measures of microvascular function that may have clinical utility in the diagnosis of microvascular disease; or in the augmentation of population based atherosclerotic cardiovascular disease risk screening.

Chapter 3

Assessment of indices of conjunctival microvascular function in patients with and without obstructive coronary artery disease

ABSTRACT

Background

Atherosclerotic heart disease often remains asymptomatic until presentation with a major adverse cardiovascular event. Primary preventive therapies improve outcomes, but conventional screening often misattributes risk. Vascular imaging can be utilised to detect atherosclerosis, but often involves ionising radiation. The conjunctiva is a readily accessible vascular network allowing non-invasive hemodynamic evaluation.

Aim

To compare conjunctival microcirculatory function in patients with and without obstructive coronary artery disease.

Methods

We compared the conjunctival microcirculation of myocardial infarction patients (MI-cohort) to controls with no obstructive coronary artery disease (NO-CAD cohort). Conjunctival imaging was performed using a smartphone and slit-lamp biomicroscope combination. Microvascular indices of axial (V_a) and cross-sectional (V_{cs}) velocity; blood flow rate (Q); and wall shear rate (WSR) were compared in all conjunctival vessels between 5 and 45 μm in diameter.

Results

A total of 127 patients were recruited (66 MI vs 61 NO-CAD) and 3602 conjunctival vessels analysed (2414 MI vs 1188 NO-CAD). Mean V_a, V_{cs} and Q were significantly lower in the MI vs NO-CAD cohort (V_a 0.50 ± 0.17 mm/s vs 0.55 ± 0.15 mm/s, **p <0.001**; V_{cs} 0.35 ± 0.12 mm/s vs 0.38 ± 0.10 mm/s, **p <0.001**; Q 154 ± 116 pl/s vs 198 ± 130 pl/s, **p < 0.001**). To correct for differences in mean vessel diameter, WSR was compared in 10 - 36 µm vessels (3268/3602 vessels) and was lower in the MI-cohort (134 ± 64s^{-1} vs 140 ± 63s^{-1}, **p=0.002**).

Conclusions

Conjunctival microcirculatory alterations can be observed in patients with obstructive coronary artery disease. The conjunctival microvasculature merits further evaluation in cardiovascular risk screening.

GRAPHICAL ABSTRACT

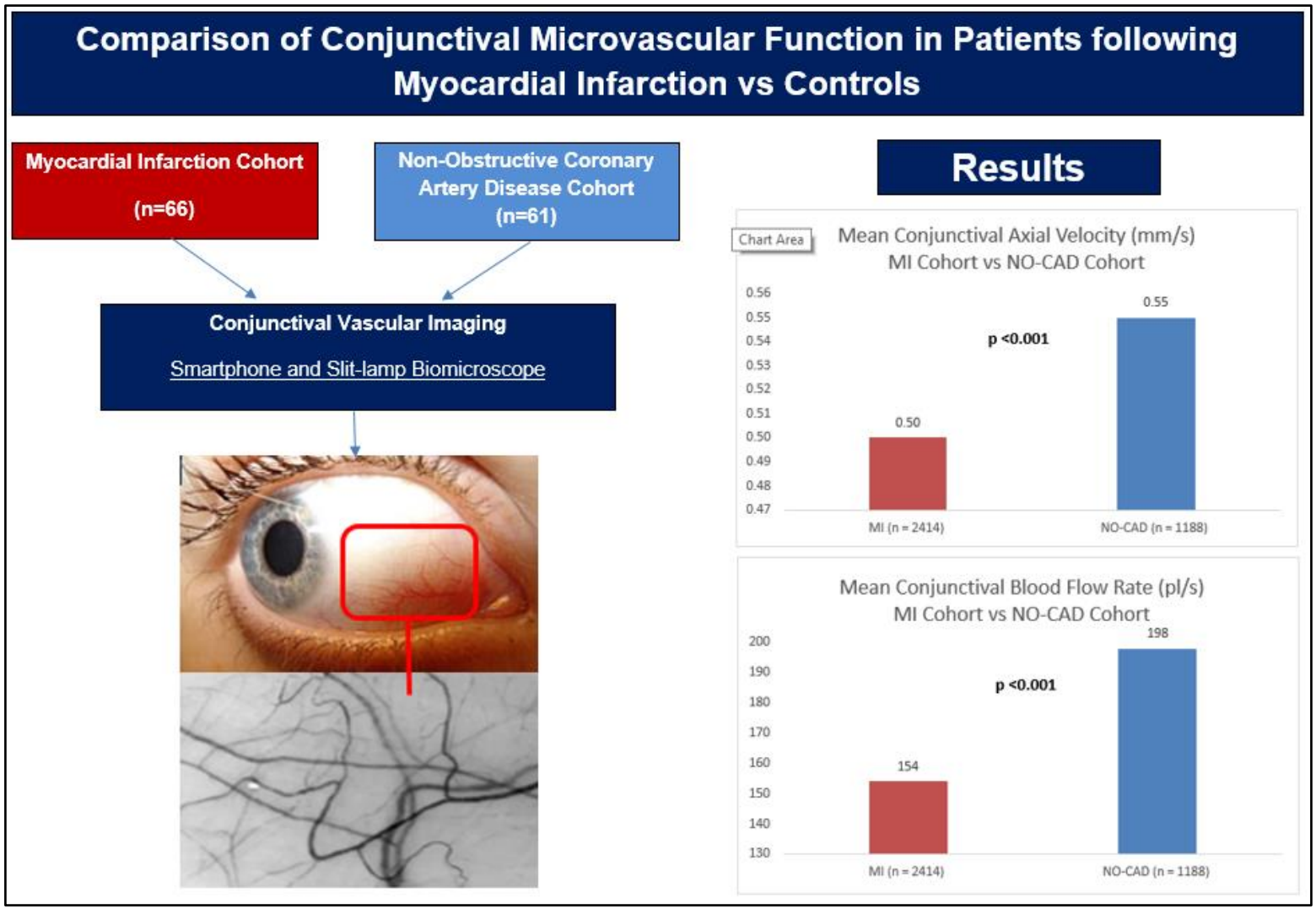

Highlights

- The conjunctival microvasculature can be assessed non-invasively using a combination of a smartphone and slit-lamp biomicroscope
- Haemodynamic abnormalities in microvascular function can be detected in the conjunctiva of patients presenting with myocardial infarction
- The non-invasive detection of conjunctival microvascular dysfunction may have potential utility in cardiovascular risk assessment and preventive cardiology

INTRODUCTION

Cardiovascular disease (CVD) represents a significant cause of morbidity and mortality worldwide (Visseren et al, 2021). Coronary artery disease (CAD) represents the most prevalent form of CVD (Roth et al, 2021). A large proportion of patients with CAD remain asymptomatic until first presentation with a major adverse cardiac event (MACE). This observation forms the basis for guideline recommendations to perform CVD screening in asymptomatic adults (Visseren et al, 2021). Several studies have highlighted that the majority of atherosclerotic plaque rupture events and resultant myocardial infarctions (MI) arise from non-obstructive plaques (Libby et al, 2005, Little et al, 1988, Falk et al 1995, Ambrose et al, 1988, Giroud et al, 1992, Fuster et al, 1994 & Shah et al, 2007). The recent HUYGENS study (Nicholls et al, 2021) highlighted the ability for statins and PCSK9 inhibitors to positively remodel vulnerable plaques, highlighting the potential value of such evidence-based medications in CV risk reduction. Identification of individuals who will benefit from targeted primary preventative therapies remains a challenging issue.

The European Society of Cardiology (ESC) recommend the use of SCORE 2 for screening in adults aged 40-69 years of age and SCORE 2-OP in adults ≥70 years of age (Visseren et al, 2021). The National Institute for Clinical Excellence (NICE) recommend the use of QRISK III (Duerden et al, 2015). These CVD risk calculators rely on the identification of

conventional CVD risk factors to estimate the long-term probability of either a fatal or non-fatal MACE.

Conventional screening modalities estimate a large proportion of patients to be in a low-intermediate CV risk category. It is therefore recommended to establish other modifiers of CV risk, such as the presence of diabetes mellitus, chronic kidney disease, familial dyslipidaemias or through the demonstration of established asymptomatic CVD (Visseren et al, 2021). The latter can be observed through performance of computed tomography (CT) coronary artery calcium scoring to detect atherosclerotic plaques and grade total burden of CAD in comparison to individuals of a similar age and sex (Lin et al, 2018, Peters et al, 2012, Vliegenthart et al, 2005 & Hadamitzky et al, 2013). A recent study evaluating CT coronary angiography (CTCA) demonstrated a high prevalence of asymptomatic atherosclerotic coronary disease in the evaluated population, with as many as 42.1% of participants having silent atherosclerosis (Bergström et al, 2021). Other modalities such as carotid ultrasound or the measurement of arterial stiffness using pulse wave velocity have been studied, but not found to be beneficial in CV risk screening to date (Den Ruijter et al, 2012 & Vlachopoulos et al, 2010). CT as a screening modality; whilst being highly sensitive, is limited by availability, cost and exposure of the patient to ionizing radiation. These factors limit the widespread introduction of CT for population CV screening programmes.

The presence of coronary microvascular dysfunction not only can result in symptoms of angina, but is also prognostically adverse (Maddox et al, 2014 & Ford et al, 2018). Microvascular dysfunction occurs in the initial manifestations of CVD (Stokes et al, 2005). Detection of microvascular dysfunction, therefore, has the potential to augment conventional CVD screening and allow early initiation of guideline based medical therapies to reduce MACE. The diagnosis of coronary microvascular disease involves invasive coronary angiography and exposure of the patient to procedural risks. However, several previous studies have demonstrated the ability to non-invasively assess the microvasculature of the retinal, sublingual and nail-fold circulation (Zhong et al, 2018, Demir et al, 2012 & Fagrell et al, 1997). Recently, a novel cardiovascular disease risk stratification system using retinal photography was found to be comparable to conventional CT coronary artery calcium scoring in predicting MACE over a 5-year follow-up period using UK Biobanks and cohorts from South Korea and Singapore (n > 70,000) (Rim et al, 2021).

Our research group previously reported the ability to non-invasively assess the conjunctival microcirculation using an iPhone coupled with a slit-lamp biomicroscope (Brennan et al, 2021). Statistically significant differences were observed in indices of conjunctival microvascular function when comparing a cohort of patients admitted to hospital with a myocardial infarction (MI) and a cohort of age and sex-matched controls estimated to be at low CV risk using the Q-Risk 3 score. In this study mean axial velocity for the controls was 0.53 ± 0.15 mm/s compared to

0.49 ± 0.17 mm/s for the MI patients ($p < 0.001$). Wall shear rate was higher for controls than MI patients (162 ± 93 s−1 vs 145 ± 88 s−1, $p < 0.001$). Blood volume flow did not differ significantly for the controls and MI patients (153 ± 124 pl/s vs 154 ± 125 pl/s, $p = 0.84$). However, this was largely due to differences in the mean vessel diameter between the groups (controls 21.41 ± 7.57 vs MI 22.32 ± 7.66 μm). This study highlighted the potential for conjunctival imaging to be utilised for CV risk assessment in asymptomatic patients. However, it was limited by the absence of coronary imaging in the low-risk cohort to identify patients with asymptomatic CAD potentially confounding the results obtained.

In this study we compare indices of conjunctival microvascular function in the previously reported MI cohort to a group of patients with no obstructive epicardial coronary artery disease detected during an invasive coronary angiogram, and no personal history of either MI or percutaneous coronary intervention (PCI).

METHODS

We conducted a prospective study (Integrated Research Application System study number 166742) comparing a group of patients with a recent MI (MI cohort) to a group of patients with no obstructive coronary artery disease (NO-CAD cohort) as demonstrated by a coronary

angiogram and physiological evaluation of any intermediate coronary stenoses.

All subjects provided written informed consent for participation in this study. The protocol was approved by the Research Ethics committee in the Belfast Health and Social Care Trust (BHSCT) and Ulster University (UU) and was carried out in accordance with the Declaration of Helsinki.

Baseline clinical data and characteristics were obtained using the recruitment questionnaire, inpatient clinical notes (MI cohort), hospital cardiology database and the patient's electronic healthcare record.

MI cohort

Patients were deemed eligible for inclusion in the MI cohort if they were an inpatient with a type 1 MI as defined by the European society of cardiology (ESC) 4th universal definition of myocardial infarction (Thygesen et al, 2018). The MI cohort was comprised of patients presenting with both ST-elevation myocardial infarction (STEMI) and non ST-elevation myocardial infarction (NSTEMI).

NO-CAD cohort

Patients were deemed eligible for inclusion in the NO-CAD cohort if they had no past medical history of MI or previous coronary revascularisation by either PCI or coronary artery bypass grafting (CABG). All patients in this cohort were recruited following an invasive coronary angiogram that excluded obstructive epicardial coronary disease. At the time of angiography any intermediate coronary lesions were physiologically assessed by pressure wire evaluation. Patients were included in this cohort only if fractional flow reserve (FFR) in any intermediate lesions was ≥0.80 (i.e. considered to be physiologically non-obstructive).

The majority of patients in this cohort were admitted electively (72%) for the investigation of stable symptoms of chest pain or dyspnoea. The remainder underwent inpatient coronary angiography due to presentation to the hospital emergency department with chest pain. Inpatients were only recruited to this cohort if their presenting symptoms were deemed to be non-cardiac in origin by the referring clinician, with no identifiable cardiovascular cause for admission (i.e. no elevation in serum troponin, no ECG changes and no echocardiographic findings of hemodynamically significant valvular abnormalities or impairment in biventricular function).

Exclusion criteria

Exclusion criteria for both groups included pregnancy, age less than 18 years old, inability to consent and history of recent conjunctival inflammation or current use of contact lenses.

Conjunctival Microvascular Assessment

Conjunctival imaging was performed using a commercially available Topcon SL-D4 (Topcon Medical Systems Inc., USA), an iPhone smartphone (Apple, Inc, USA) and a bespoke adapter (Zarf Enterprises Inc., USA) (see **Figure 3.1**). We acquired 5–10 s videos of the conjunctival microcirculation in both nasal and temporal views, thus generating four videos per subject. All videos then underwent a process of stabilisation, image registration and then semi-automated analysis of microvascular parameters. The imaging platform is calibrated to define a pixel to millimetre (mm) conversion factor. This conversion factor is then used to estimate vessel diameter (D). Axial (V_a) and cross-sectional (V_{cs}) velocity are then estimated using this conversion factor coupled with an app that allows blood flow tracking and hence calculation of distance travelled over a 1 second stabilised video clip. Blood flow (Q) and wall shear rate (WSR) are then estimated from the results of D and V_{cs}. This technique has been described in 3 previous studies (Brennan et al 2019 & 2021). **Figure 3.2** gives an example of a video frame showing the conjunctival microvascular network obtained from our imaging platform, following the process of video stabilisation. Conjunctival vessel diameter, V_a, V_{cs}, Q and WSR were

assessed in vessels with observable blood flow. We analysed and report results for vessels between 5 and 45 μm in diameter.

Figure 3.1. The iPhone 6s, TopCon SL-D4 imaging system with the Zarf bespoke adapter (red arrow) and TopCon external fixation target (green arrow)

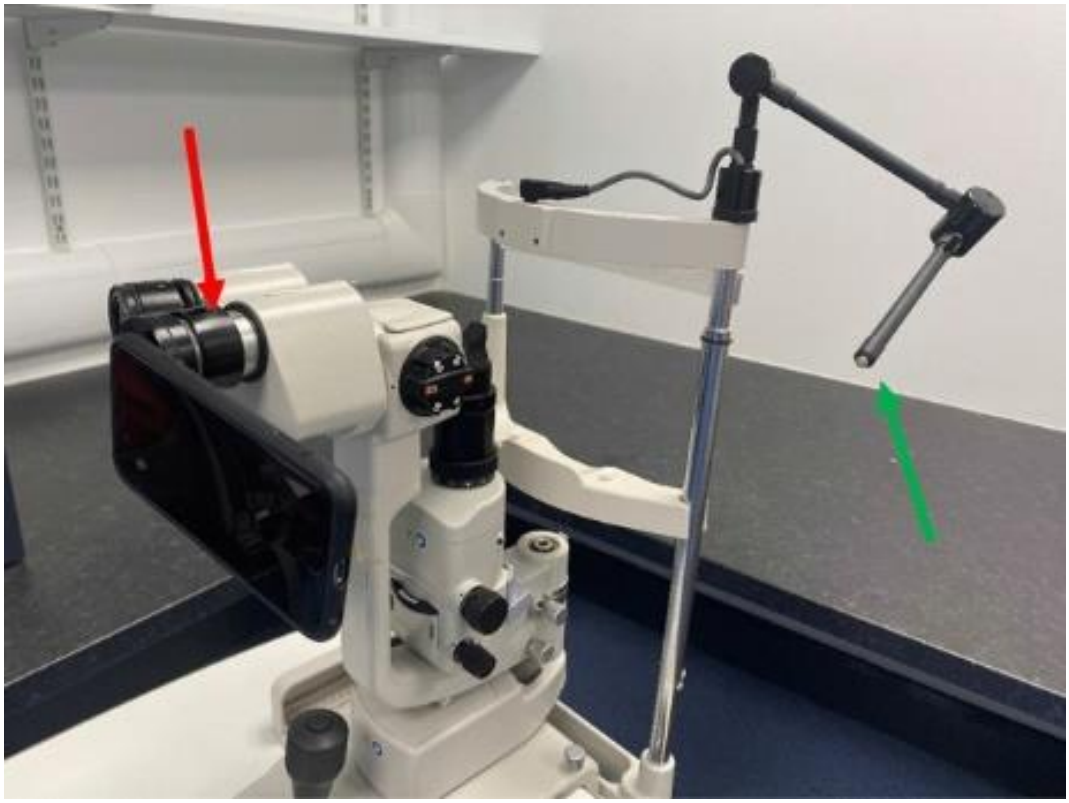

Figure 3.2. Stabilised video frame of conjunctival microvascular network

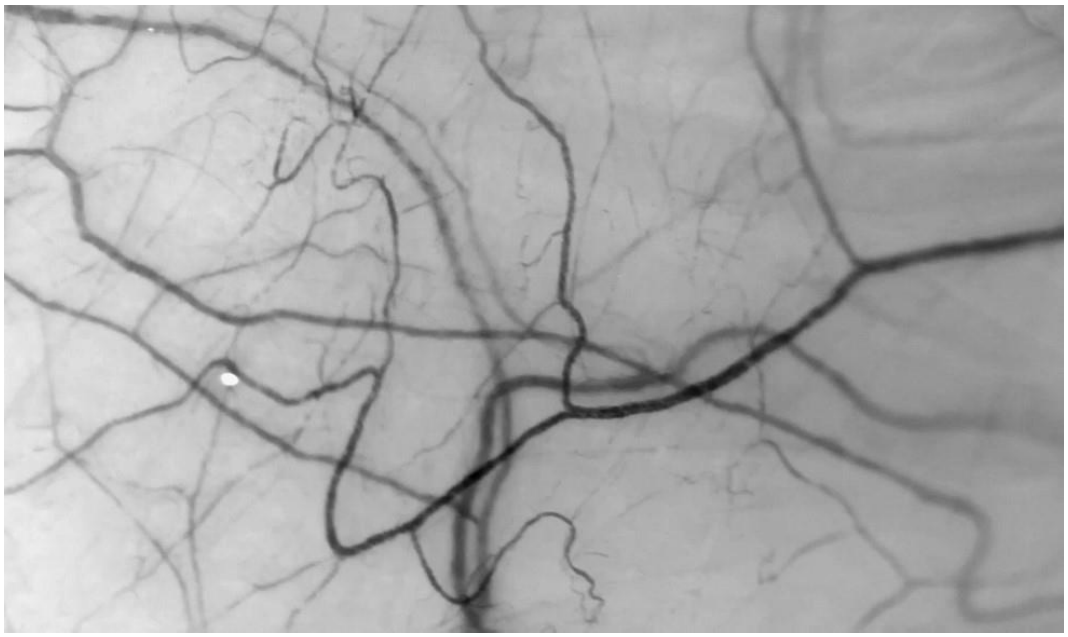

Given the significant impact that vessel diameter creates on the parameters of Q [defined as $Q=V_{cs}(\pi r^2)$] and WSR (defined as $WSR=8V_{cs}/D$), it is important to standardise the range of vessels analysed in order to evaluate microvascular indices in vessels of comparable size. To avoid significant outliers in vessel diameter skewing the results we therefore conducted a sub-analysis of conjunctival vessels between 10 and 36 μm in diameter. This range was selected as it excluded 5% of vessels at both the upper and lower end of the diameter range (n=3268). Vessels in this diameter range were then classified into 4 distinct diameter groups (D 10 - 17μm, D 17 - 23μm, D 23 - 29μm and D 29 - 36μm).

Statistical Analysis

For statistical analysis SPSS for Apple iOS version 26 (property of IBM) was used. Continuous variables were described using the mean, standard deviation of the mean and 95% confidence intervals (CI). Kolmogorov–Smirnov testing was used to assess normality of the continuous variables. Categorical variables were expressed as a number and percentage of the total category number to which the variable belonged.

Normally distributed variables were compared between the two populations using the independent-samples t-test. Non-normally distributed continuous variables were compared using a non-parametric test (Mann–Whitney U test). Categorical comparisons were made between the two groups using Pearson Chi-Square or Fisher's exact test.

RESULTS

Baseline Characteristics

Between 31st January 2018 and 1st October 2021, 127 patients were recruited to this study. A total of 61 patients were included in the NO-CAD cohort and 66 patients were included in the MI cohort. The mean ages were 63 ± 10 years and 57 ± 11 years respectively in these cohorts (**p=0.003**). A higher proportion of patients in the MI cohort were male (78.8% vs 49.2%, **p<0.001**). There was no statistically significant difference in the prevalence of systemic hypertension, diabetes mellitus

and smoking between the groups (p=0.12, p=0.21 and 0.07, respectively). **Table 3.1** provides a comparative summary of the patients' baseline characteristics. Of note, the prevalence of conventional cardiovascular risk factors (hypertension, smoking and diabetes mellitus) was higher in the NO-CAD cohort than would be anticipated in the general population.

Table 3.1. Baseline characteristics

Characteristic	**NO-CAD (n = 61)**	**MI (n = 66)**	**p value**
Age- *yrs ± SD*	63 ± 10	57 ± 11	**0.003**
Male sex- *n (%)*	30 (49.2)	52 (78.8)	**<0.001**
BMI- *kg/m^2 ± SD*	30.2 ± 5.6	28.6 ± 4.7	0.10
Prior PCI- *n (%)*	0 (0.0)	9 (13.6)	**0.003**
Prior MI- *n (%)*	0 (0.0)	9 (13.6)	**0.003**
Hypertension- *n (%)*	37 (60.7)	31 (47.0)	0.12
Diabetes mellitus- *n (%)*	20 (32.8)	15 (22.7)	0.21
Smoking history- *n (%)*	30 (49.2)	43 (65.2)	0.07
HbA1c- *mmol/mol ± SD*	46.0 ± 16.0	45.4 ± 17.0	0.66
Creatinine clearance- *ml/min ± SD*	97 ± 41	104 ± 36	0.07
Haemoglobin- *g/l ± SD*	137 ± 14	144 ± 16	**0.04**
Total cholesterol- *mmol/l ± SD*	3.7 ± 0.9	4.6 ± 1.5	**<0.001**

At the time of recruitment, both patient cohorts were normotensive, but the NO-CAD cohort had a higher mean systolic blood pressure (126.3 ± 13.6mmHg vs 120.4 ± 16.4mmHg, **p=0.03**).

All patients in the MI cohort underwent invasive coronary angiography. 4 (6.1%) of these patients were managed medically and the remaining 62 (93.9%) patients underwent either percutaneous or surgical revascularisation. All patients that underwent surgical revascularisation were recruited and had conjunctival imaging performed prior to surgery.

Indices of conjunctival microvascular function

Conjunctival video imaging was obtained for all patients. There were no adverse clinical events during conjunctival imaging. All image processing and subsequent quantitative microvascular assessment was performed by study investigators blinded to the clinical characteristics at the time of the analysis to prevent bias.

A total of 3602 vessel segments were analysable across the two cohorts (1188 in the NO-CAD cohort vs 2414 in the MI cohort). A mean of 28.3 vessel segments were assessable per patient. A comparison of conjunctival microcirculatory parameters is summarised in **Table 3.2,** and the range of results presented in **Figure 3.3.** Statistically significant differences were observed between cohorts for mean D, V_a, V_{cs} and Q.

There is however considerable overlap in the range of parameters in the MI vs NO-CAD cohort. This creates obvious challenges when trying to define a normal reference range for conjunctival microvascular parameters and impacts the sensitivity and specificity of this imaging modality as a screening investigation.

Table 3.2. Comparison of conjunctival microcirculatory parameters

Parameter	**NO-CAD (n = 1188)**	**MI (n = 2414)**	**p value**
Diameter- *µm ± SD*	24.7 ± 7.8	22.4 ± 7.5	**< 0.001**
Axial velocity- *mm/s ± SD*	0.55 ± 0.15	0.50 ± 0.17	**< 0.001**
Cross-sectional velocity- *mm/s ± SD*	0.38 ± 0.10	0.35 ± 0.12	**< 0.001**
Blood flow rate- *pl/s ± SD*	198 ± 130	154 ± 116	**< 0.001**
Wall shear rate- s^{-1} *± SD*	140 ± 74	144 ± 88	0.78

Figure 3.3. Boxplots comparing indices of conjunctival microvascular function in the MI and NO-CAD cohorts

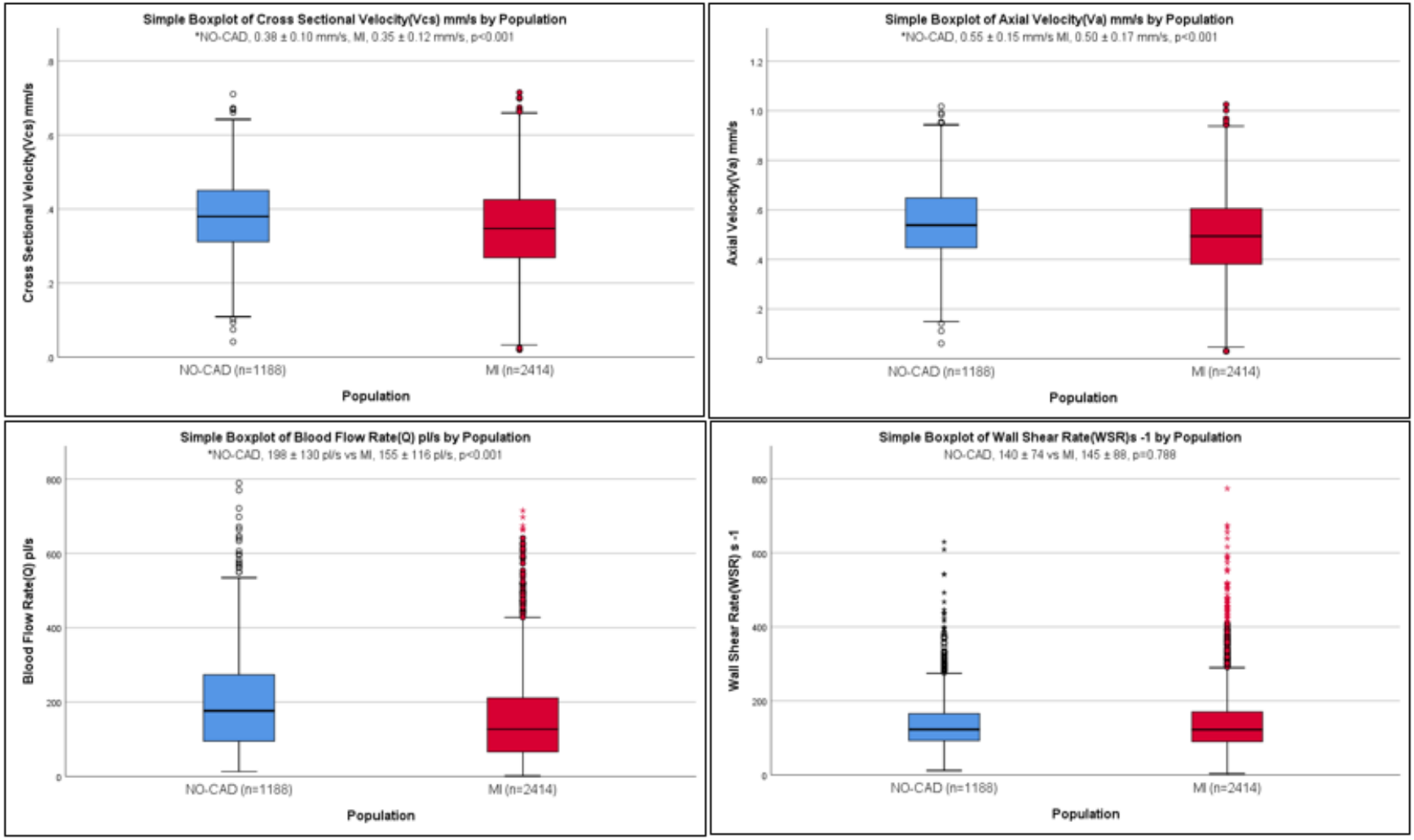

There was no difference in wall shear rate (WSR) between cohorts; however, WSR is inversely related to diameter. The lack of difference therefore related to the difference observed in mean diameter, which was significantly lower in the MI cohort (24.73 ± 7.79 vs 22.41 ± 7.46; **p < 0.001**). As described above, to compensate for this discrepancy in mean diameter, we conducted a sub-analysis of microvascular indices in vessels between 10 and 36 μm in diameter (n=3268/3602). In this sub-analysis, significant differences were observed in all conjunctival parameters (V_a 0.50 ± 0.17 mm/s vs 0.55 ± 0.15 mm/s, **p <0.001**; V_{cs} 0.35 ± 0.11 mm/s vs 0.38 ± 0.10 mm/s, **p <0.001**; Q 152 ± 100 pl/s vs 183 ± 108 pl/s, **p < 0.001;** and WSR 134 ± 64 s^{-1} vs 140 ± 63 s^{-1}, **p=0.002**).

A further analysis comparing the cohorts by 4 previously described sizing groups revealed significant reductions in V_a, V_{cs}, Q and WSR across all groups (see **Table 3.3**).

Figure 3.4 demonstrates a comparison of conjunctival vessel axial and cross-sectional velocity in patients with and without an established history of several conventional vascular risk factors (diabetes mellitus, hypertension, hypercholesterolemia and smoking history). There were no significant differences in mean axial or cross-sectional velocity in any of these groups. This finding suggests the observed differences in microvascular parameters in this study are secondary to the underlying

atherosclerotic coronary disease in the MI cohort rather than the presence of other co-morbidities that may impact microvascular function.

Table 3.3. Comparison of conjunctival microcirculatory parameters based on vessel group

10 – 17 µm			
Parameter	**NO-CAD (n = 189)**	**MI (n = 466)**	**p-value**
Diameter- *µm ± SD*	14.0 ± 1.9	13.8 ± 1.9	0.26
Axial velocity- *mm/s ± SD*	0.53 ± 0.13	0.47 ± 0.15	**< 0.001**
Cross-sectional velocity- *mm/s ± SD*	0.39 ± 0.10	0.35 ± 0.12	**< 0.001**
Blood flow rate- *pl/s ± SD*	61.3 ± 22.0	52.9 ± 22.2	**< 0.001**
Wall shear rate- s^{-1} *± SD*	230 ± 67	207 ± 78	**< 0.001**
17 – 23 µm			
Parameter	**NO-CAD (n = 282)**	**MI (n = 667)**	**p-value**
Diameter- *µm ± SD*	20.1 ± 1.8	20.2 ± 1.7	0.18
Axial velocity- *mm/s ± SD*	0.54 ± 0.14	0.48 ± 0.16	**<0.001**
Cross-sectional velocity- *mm/s ± SD*	0.38 ± 0.10	0.34 ± 0.11	**<0.001**
Blood flow rate- *pl/s ± SD*	121 ± 39	109 ± 42	**<0.001**
Wall shear rate- s^{-1} *± SD*	151 ± 42	134 ± 47	**<0.001**
23 – 29 µm			
Parameter	**NO-CAD (n = 319)**	**MI (n = 685)**	**p-value**
Diameter- *µm ± SD*	26.0 ± 1.7	25.9 ± 1.7	0.30

Axial velocity- *mm/s ± SD*	0.55 ± 0.15	0.51 ± 0.17	**<0.001**
Cross-sectional velocity- *mm/s ± SD*	0.37 ± 0.10	0.35 ± 0.12	**<0.001**
Blood flow rate- *pl/s ± SD*	199 ± 60	285 ± 69	**<0.001**
Wall shear rate- s^{-1} ± *SD*	116 ± 32	108 ± 36	**<0.001**
29 – 36 µm			
Parameter	**NO-CAD (n = 282)**	**MI (n = 378)**	**p-value**
Diameter- *µm ± SD*	32.0 ± 1.9	31.7 ± 1.9	0.05
Axial velocity- *mm/s ± SD*	0.57 ± 0.16	0.54 ± 0.16	**0.01**
Cross-sectional velocity- *mm/s ± SD*	0.38 ± 0.11	0.36 ± 0.11	**0.01**
Blood flow rate- *pl/s ± SD*	308 ± 98	287 ± 98	**0.001**
Wall shear rate- s^{-1} ± *SD*	96 ± 28	91 ± 27	**0.03**

Figure 3.4. A comparison of axial and cross-sectional velocity in patients with and without relevant conventional vascular risk factors (diabetes mellitus, hypertension, hypercholesterolemia and smoking history)

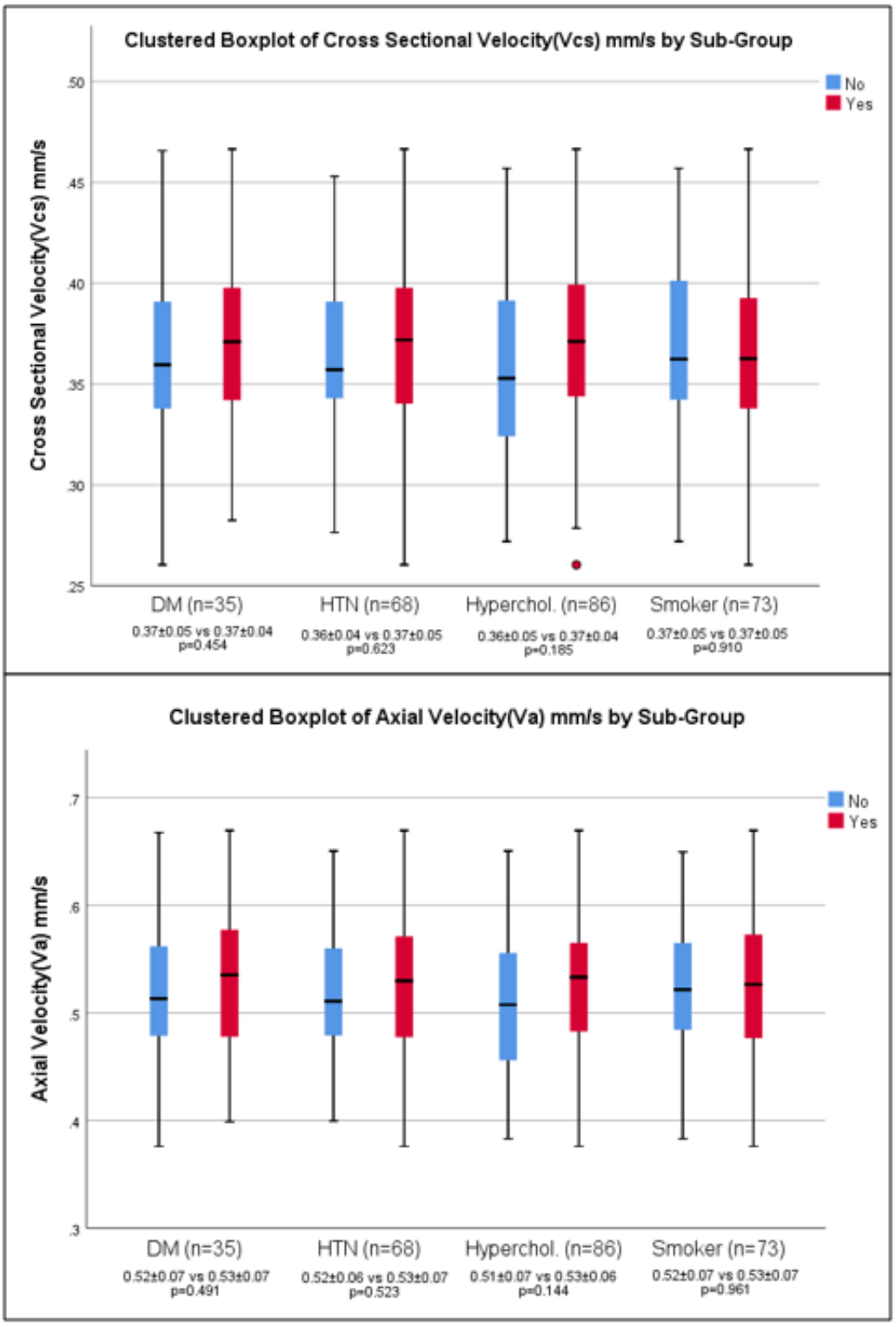

DISCUSSION

This study demonstrates statistically significant differences in conjunctival microcirculatory function of a group of patients with established CAD and therefore proven to be at very high CV risk in comparison to a group with no obstructive coronary artery disease or previous major adverse cardiovascular event. The underlying pathophysiological mechanisms involved in the development of atherosclerotic vascular disease can be observed earliest in the microcirculation (Stokes et al, 2005). The ability to detect microvascular dysfunction has the potential to identify asymptomatic patients who may benefit from aggressive primary preventative therapies. The conjunctiva is an easily accessible site to non-invasively assess for microvascular dysfunction without exposing patients to ionising radiation.

Coronary microvascular dysfunction can result in symptoms of angina or dyspnoea that can considerably impact quality of life. Its presence has also been shown to confer an adverse CV prognosis long-term (Bairey Merz et al, 2017, Ford et al, 2018 & Kaski et al, 2018). The diagnosis of coronary microvascular dysfunction is performed invasively based on demonstrating a reduction in coronary blood velocity, and hence a reduction in blood flow rate using pressure wire evaluation and thermodilution techniques. Importantly, this study demonstrates that conjunctival vessels share these same physiological alterations in patients with established atherosclerotic CAD. Further evaluation of this

conjunctival microvascular screening modality in patients with invasively assessed coronary microvascular dysfunction would be of clinical interest.

A reduction in both microvascular axial/cross-sectional velocity and blood flow have previously been reported in association with CVD (Cheung et al, 2001, Sadr-Ameli et al, 2014, Kord Valeshabad et al, 2015 & Khansari et al, 2017). In our study these parameters significantly differed across all vessel sizing groups, consistent with these measurements having a significant correlation with the presence of atherosclerotic disease.

The microvascular alterations observed in this study were more marked than those previously reported in a comparison of the MI cohort to patients deemed to have low CV risk (as estimated by convention CV risk calculators) in the absence coronary imaging (26). This furthers the argument that conjunctival microvascular dysfunction correlates with CAD and warrants dedicated evaluation to predict CV risk.

LIMITATIONS

The MI cohort were recruited within a few days of their clinical event. This study therefore compares microvascular indices in stable patients with individuals following an acute event, in whom both a reduction in cardiac output and systemic inflammatory response may be present. The NO-CAD cohort also encompassed a wide range of coronary pathology. Despite

these patients having non-obstructive coronaries, there was a spectrum ranging from those with no coronary atheroma, to those with at least moderate coronary atheroma in the absence of physiologically significant luminal obstruction. Some included NO-CAD patients therefore might be considered not to be conventionally at low CV risk nor free from coronary atherosclerosis.

In this study we do not differentiate between conjunctival arterioles and venules, which would potentially add to the discriminatory ability of this vascular screening modality. Future research into the benefit of conjunctival vascular screening should focus on evaluation of the technique in stable symptomatic and asymptomatic coronary disease, in order to evaluate the potential utility to augment conventional CV risk assessment.

CONCLUSION

This study highlights the ability of an iPhone coupled with slit-lamp biomicroscope to detect differences in conjunctival microcirculatory function between patients with and without obstructive coronary artery disease. The differences observed between these populations were more significant than those reported previously in a low-risk population without coronary imaging. These findings warrant further investigation in future research. Importantly, a definition of abnormal vs normal conjunctival

parameters needs to be established for the purpose of CV risk categorisation. These results suggest the potential for this conjunctival imaging modality to be utilized for the detection of asymptomatic CVD to augment conventional CV screening.

Chapter 4

Assessment of indices of conjunctival microvascular function in patients with coronary microvascular dysfunction

ABSTRACT

Objective

Coronary microvascular dysfunction (CMD) is a cause of ischaemia with non-obstructive coronary arteries (INOCA). It is notoriously underdiagnosed due to the need for invasive microvascular function testing. We hypothesised that systemic microvascular dysfunction could be demonstrated non-invasively in the microcirculation of the bulbar conjunctiva in patients with CMD.

Methods

Patients undergoing coronary angiography for the investigation of chest pain or dyspnoea, with physiologically insignificant epicardial disease (fractional flow reserve ≥0.80) were recruited. All patients underwent invasive coronary microvascular function testing. We compared a cohort of patients with evidence of CMD (IMR ≥25 or CFR <2.0); to a group of controls (IMR <25 and CFR ≥2.0). Conjunctival imaging was performed using a previously validated combination of a smartphone and slit-lamp biomicroscope. This technique allows measurement of vessel diameter and other indices of microvascular function by tracking erythrocyte motion.

Results

A total of 111 patients were included (43 CMD and 68 controls). There were no differences in baseline demographics, co-morbidities or epicardial coronary disease severity. The mean number of vessel segments analysed per patient was 21.0 ± 12.8 (3.2 ± 3.5 arterioles and 14.8 ± 10.8 venules). In the CMD cohort, significant reductions were observed in axial/cross-sectional velocity, blood flow, wall shear rate and stress. The most marked differences were observed in arterioles.

Conclusion

The changes in microvascular function linked to CMD can be observed non-invasively in the bulbar conjunctiva. Conjunctival vascular imaging may have utility as a non-invasive tool to both diagnose CMD and augment conventional cardiovascular risk assessment.

Keywords

INOCA; microvascular angina; microvascular dysfunction; conjunctiva; cardiovascular screening

Key Messages

What is already known on this topic?

- Coronary microvascular dysfunction is highly prevalent and associated with an adverse long-term cardiovascular prognosis

What this study adds?

- This is the first study to demonstrate alterations in systemic microvascular function in a cohort of patients with coronary microvascular disease

How this study might affect research, practice or policy?

- The non-invasive demonstration of microvascular disease may have utility for cardiovascular risk assessment and screening

GRAPHICAL ABSTRACT

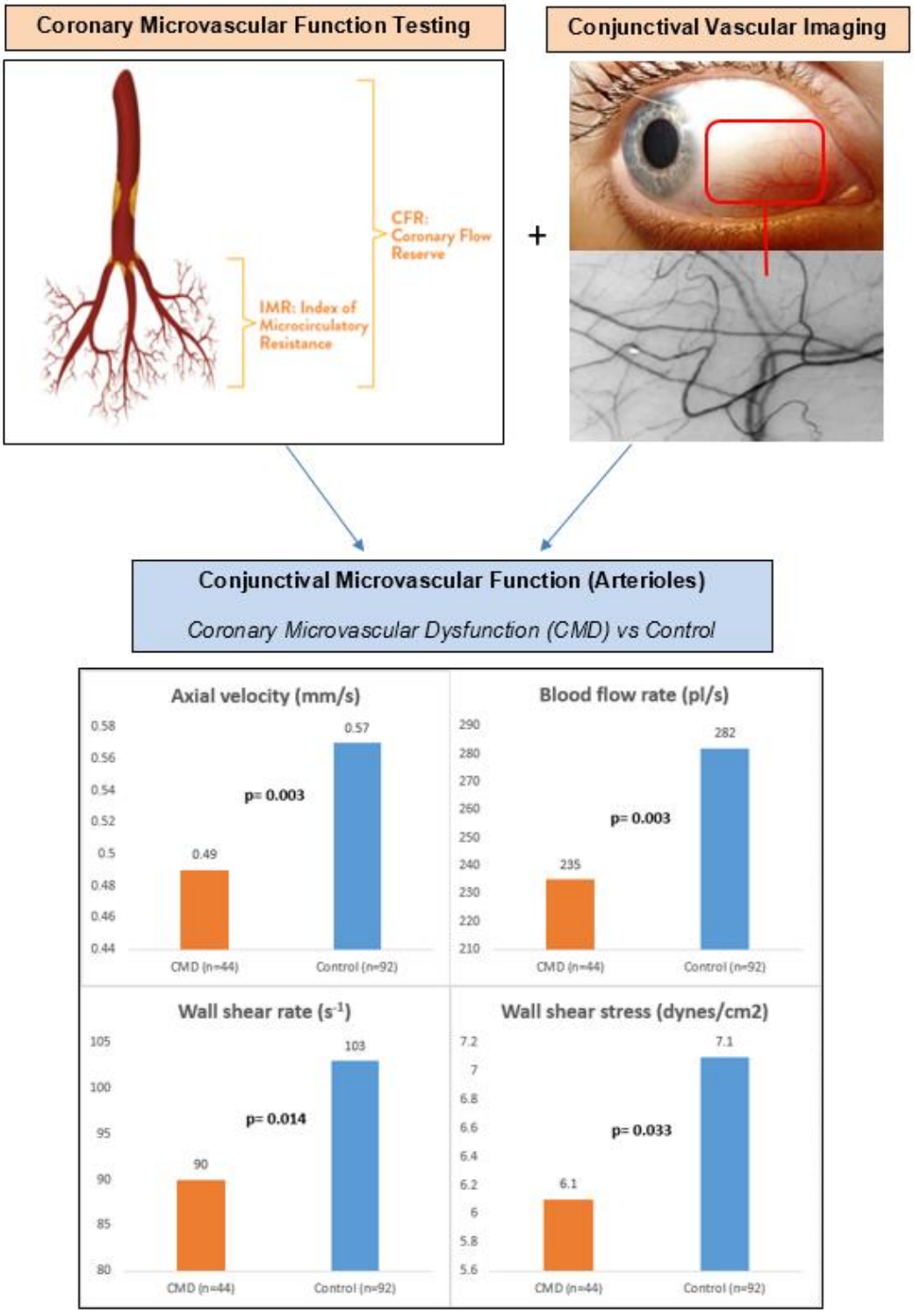

INTRODUCTION

It is estimated that approximately 112 million people globally experience angina pectoris (GBD 2015 Mortality and Causes of Death Collaborators). Between 40 and 50% of patients undergoing invasive coronary angiography for the investigation of angina have no obstructive epicardial disease (Patel et al, 2010 & Ford et al 2018). In the setting of abnormal functional ischaemic testing these symptoms are commonly due to ischaemia with non-obstructive coronary arteries (INOCA). The most frequently encountered sub-types of INOCA are coronary microvascular dysfunction (CMD) and epicardial vasospastic angina (VSA) (Camici et al, 2007). These conditions are notoriously underdiagnosed leading to recurrent angina, impaired quality of life, unplanned hospitalizations, repeated coronary angiography and adverse long-term cardiovascular outcomes (Kunadian et al, 2021 & Jespersen et al 2011 & 2013). The CorMicA trial highlighted the importance of invasive coronary function testing in INOCA with significant reductions in angina and improvement in quality of life with stratified medical therapy in the intervention arm of the study vs standard of care (Ford et al 2018). The intervention in this study led to a mean improvement of 11.7 U in the Seattle Angina Questionnaire summary score at 6 months (95% confidence interval [CI]: 5.0 to 18.4; $p = 0.001$). In addition, the intervention led to improvements in the mean quality-of-life score (EQ-5D index 0.10 U; 95% CI: 0.01 to 0.18; $p = 0.024$) and visual analogue score (14.5 U; 95% CI: 7.8 to 21.3; $p < 0.001$) (Ford et al 2018).

CMD can occur due to structural remodelling of the microvasculature (fixed reduction in microcirculatory conductance) and/or functional vasomotor disorders affecting the coronary arterioles (dynamic arteriolar obstruction) (Ong et al, 2017 & Mejía-Rentería et al, 2017). VSA is caused by abnormal dynamic epicardial coronary obstruction. There can be overlap between VSA and CMD sub-types, particularly with functional CMD.

Significant epicardial coronary artery disease can be excluded non-invasively using CT coronary angiography (CTCA) and ischaemia demonstrated with a functional imaging test. However, the gold-standard for the diagnosis of CMD remains invasive coronary angiography to exclude obstructive epicardial CAD and perform a physiological evaluation of microvascular function including vasoreactivity testing. Current European Society of Cardiology (ESC) guidelines for the diagnosis and management of chronic coronary syndromes suggest that invasive coronary function testing should be considered in patients with suspected CMD (IIa recommendation) (Knuuti et al, 2020). The downside to invasive angiography is the exposure of the patient to infrequent, but potentially life-threatening iatrogenic complications (Tavakol et al, 2012).

Whilst a link between systemic microvascular dysfunction and INOCA has been suggested from previous studies (Ford et al, 2018), it remains to be definitively shown. We hypothesized that if microvascular dysfunction in an

alternative vascular network could be demonstrated non-invasively in patients with CMD, this would have potential clinical utility in both the non-invasive diagnosis of CMD and the enhancement of conventional cardiovascular risk assessment tools such as SCORE, ASSIGN and Q-RISK III. A diagnostic algorithm for CMD that utilises a non-invasive assessment of systemic microvascular dysfunction has clear advantages. It would avoid the cost and time requirement for invasive coronary angiography and benefit the patient by avoiding discomfort, anxiety and potential procedural complications.

The conjunctival microcirculation is a readily assessable microvascular network in which physiological parameters can be non-invasively evaluated (Brennan et al 2019 & 2021). Microvascular dysfunction has previously been observed in the bulbar conjunctiva in a variety of cardiovascular disorders (Brennan et al, 2021 & Kord Valeshabad 2015). In this study we compare physiological parameters of conjunctival microvascular function in symptomatic subjects with and without invasive evidence of CMD.

METHODS

We conducted a prospective study (Integrated Research Application System study number 166742) comparing conjunctival microcirculatory function in a group of patients with coronary microvascular dysfunction

(CMD cohort) (n=43) as a cause of INOCA to a group of patients with non-obstructive coronary artery disease and normal indices of coronary microvascular function (Control cohort) (n=68).

All subjects provided written informed consent for participation in this study. The experimental protocol was approved by the Research Ethics committee in the Belfast Health and Social Care Trust (BHSCT) and Ulster University (UU). The study was carried out in accordance with the Declaration of Helsinki.

Baseline clinical data and characteristics were obtained using a recruitment questionnaire, clinical notes, hospital cardiology database (Cardiovascular Information System Tomcat, Phillips, Eindhoven, Netherlands) and each patient's electronic healthcare record.

Inclusion criteria

All subjects were recruited following invasive coronary angiography for the investigation of symptoms of chest pain (angina) and/or dyspnoea (angina equivalent). Only patients with both angiographically and physiologically non-obstructive epicardial coronary disease were eligible for recruitment. Non-obstructive coronary disease was defined angiographically by the absence of any epicardial stenosis >50% and physiologically as a fractional flow reserve (FFR) ≥0.80 in the context of any intermediate

stenosis (50-70%). All subjects underwent an evaluation of coronary microvascular function with measures of coronary flow reserve (CFR) and index of microcirculatory resistance (IMR) calculated using standard thermodilution techniques and commercially available software. Subjects were only considered eligible if measurements of mean transit time during both rest and maximal hyperaemia were deemed to be repeatable (<20% variation in measurements).

Exclusion criteria

1. Inability to consent
2. Age less than 18 years of age
3. Pregnancy at time of recruitment
4. History of conjunctival inflammation or contact lens use in the 24 hours prior to recruitment
5. Presentation that fulfilled the ESC 4th universal definition of myocardial infarction (Thygesen et al, 2018)
6. Haemodynamically significant valvular heart disease
7. Left ventricular ejection fraction <40%
8. Heart failure with preserved ejection fraction
9. Previous coronary artery bypass grafting (CABG)

CMD cohort

All subjects fulfilled the COVADIS diagnostic criteria for CMD (Ong et al, 2017). Thus, all patients, in addition to symptoms suggestive of INOCA, had objective evidence of CMD with an elevated IMR (≥25), a reduced CFR (<2.0) or the combination of both of these abnormalities in microvascular function.

Control cohort

Subjects without evidence of CMD were recruited to the control arm of the study. Both indices of coronary microvascular function were normal in this cohort (IMR <25 and CFR ≥2.0).

Conjunctival Microvascular Assessment

Conjunctival imaging was performed using a Topcon SL-D4 (Topcon Medical Systems Inc., USA), iPhone 11pro smartphone (Apple, Inc, USA) and a bespoke adapter (Zarf Enterprises Inc., USA) to allow coupling of these devices (**Figure 4.1**). This technique has previously been described (Brennan et al 2019 & 2021). We acquired 5–10 s digital video recordings of the microcirculation in both nasal and temporal fields of the bulbar conjunctiva, thus generating four video recordings per subject. All video recordings were converted to grayscale and underwent a process of sequence selection and stabilisation (**Figure 4.2**). The stabilised sequences were then analysed to obtain measurements of vessel

diameter and other physiological parameters of microvascular function using the principle of erythrocyte tracking, to quantify blood flow velocity.

Figure 4.1. Smartphone and slit-lamp biomicroscope imaging system with the adapter and external fixation target

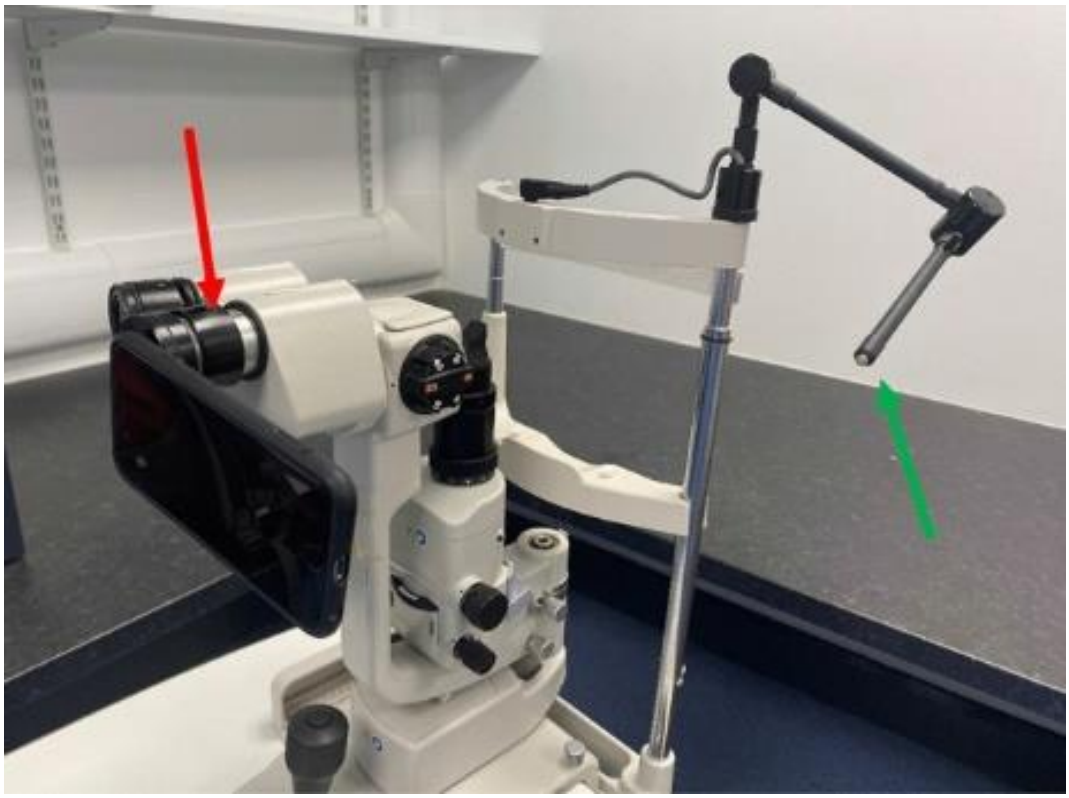

Figure 4.2. Stabilised conjunctival image obtained at 80 times magnification

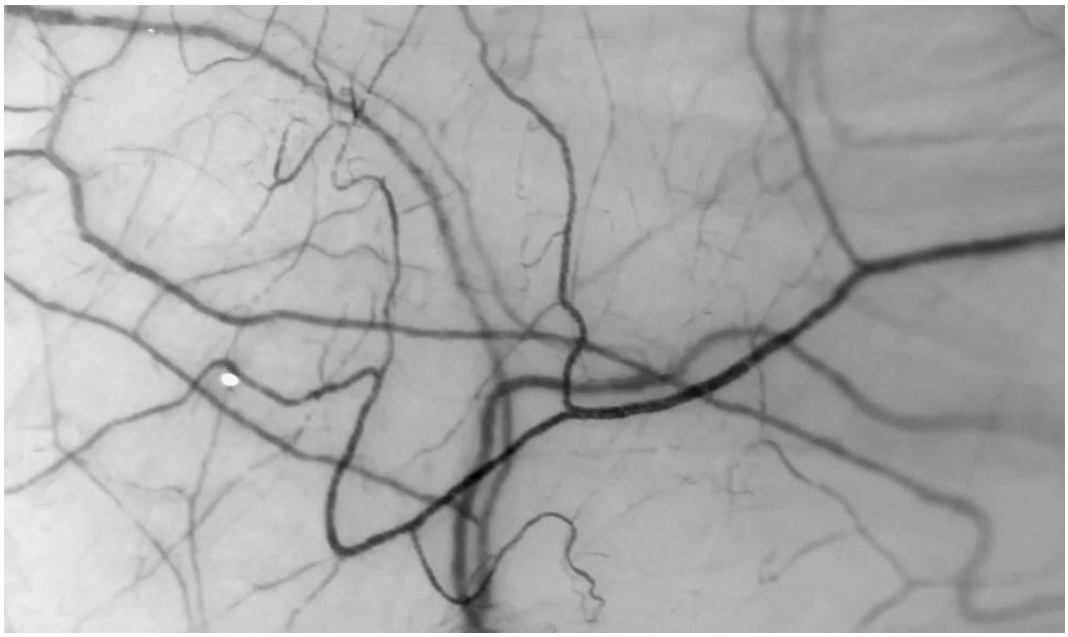

All subjects underwent conjunctival imaging at least 4 hours after coronary angiography. Given the short half-lives of the administered intravenous and intra-arterial medications (unfractionated heparin, nitroglycerine and adenosine), this allowed time for these agents to wash out of the subjects' system and hence avoid any confounding impact on conjunctival microvascular function.

In addition to quantification of microvascular parameters, vessels were manually differentiated into arterioles and venules using the principle of blood flow direction in relation to bifurcations. This allows a more accurate comparison of microvascular function to be formed. This method of vessel

differentiation has been described previously (Khansari et al, 2016 & 2017). Vessels were defined as arterioles if blood flow was towards a diverging bifurcation; venules if blood flow was towards a converging bifurcation; and undifferentiated if no bifurcation was present in the imaging field to allow vessel differentiation. Undifferentiated vessels were excluded from subsequent sub-group analyses.

Conjunctival vessel diameter, axial velocity (V_a), cross-sectional velocity (V_{cs}), blood flow rate (Q), wall shear rate (WSR) and wall shear stress (WSS) were quantified in vessels with observable blood flow. The methods by which these haemodynamic parameters were measured and derived using specifically designed software has been fully described in two previous publications (Brennan et al 2019 & 2021). A comprehensive description of these methods can be found in the supplementary appendix. Given the significant impact of diameter on Q, WSR and WSS; parameters were further analysed in two distinct diameter groupings (10 – 25 μm and 25 – 40 μm). These diameter groups were chosen by including only conjunctival vessels with a diameter that fell within 2 standard deviations of the total mean of all conjunctival vessels analysed. The range of these vessels was 10 to 40 μm, which was then divided evenly into the two groups.

Statistical Analysis

The results of a pilot study published by our research group (Brennan et al, 2021) were used for a formal power calculation. We estimated that a sample size of 100 patients (3600 conjunctival vessels) would provide the study with a power of at least 80% to reject the null hypothesis of no between-group differences in conjunctival microvascular function.

Statistical analysis was performed using Statistical Package for the Social Sciences (SPSS) for Apple iOS version 27 (property of IBM). Continuous variables were described using the mean and standard deviation of the mean. Kolmogorov–Smirnov testing was used to assess normality of the continuous variables. Categorical variables were expressed as a number and percentage of the total category number to which the variable belonged.

Normally distributed variables were compared between the two populations using the independent-samples t-test. Non-normally distributed continuous variables were compared using non-parametric tests e.g. Mann–Whitney U test. Categorical comparisons were made between the two groups using Pearson Chi-Square or Fisher's exact test as appropriate. Repeatability was assessed using Intraclass Correlation Coefficient for continuous variables and Fleiss Kappa for categorical variables.

RESULTS

Baseline Characteristics

Between November 2020 and February 2022, a total of 119 patients were recruited to this study. There were two patients excluded due to symptoms that did not fulfil the above specified inclusion criteria and six patients due to non-reproducibility of the measured coronary microvascular indices (>20% variation in the measurements of coronary mean transit time obtained during microvascular function testing). The remaining 111 patients had a mean age of 64.2 ± 9.5 years (range 38 – 81 years). A small majority of patients were male (56.8%).

A total of 43 patients were included in the CMD cohort and 68 patients in the control cohort. There were no significant differences in baseline characteristics between the groups (**Table 4.1**). The majority of patients had the physiological assessment of microvascular function performed in the left anterior descending artery (LAD) (91.0%). In the remainder of cases, this was performed in the left circumflex artery (LCX) (5.4%) and right coronary artery (RCA) (3.6%).

The mean qualitative % coronary stenosis did not differ between the CMD and control cohorts (LMS 3.7 ± 8.7% vs 4.7 ± 12.4%, p= 0.93; LAD 37.7 ± 22.9% vs 33.7 ± 18.5%, p= 0.17; LCX 13.0 ± 15.8% vs 13.8 ± 15.8%, p=0.89; RCA 17.4 ± 22.2% vs 13.1 ± 15.2%, p=0.57). The measurements of resting full-cycle ratio (RFR) and FFR did not differ between the CMD

and control cohorts (0.92 ± 0.03 vs 0.93 ± 0.03, p=0.08 and 0.88 ± 0.05 vs 0.89 ± 0.05, p=0.83 respectively). Indices of microvascular coronary function were significantly different between the groups, as expected given the nature of the study design. The CMD cohort had mean reductions in CFR (2.5 ± 1.3 vs 5.2 ± 2.5, p<0.001) and elevations in IMR (28.4 ± 11.8 vs 13.7 ± 5.0, p<0.001).

Table 4.1. Baseline Characteristics

Characteristic	**CMD (n=43)**	**Control (n=68)**	**p-value**
Age- *yrs ± SD*	66.0 ± 9.8	63.1 ± 9.2	0.08
Male sex- *n (%)*	21 (48.8)	42 (61.8)	0.18
Body mass index- *kg/m^2 ± SD*	29.4 ± 5.7	30.9 ± 6.8	0.13
Systolic BP- *mmHg ± SD*	124.6 ± 17.0	125.2 ± 15.8	0.58
Diastolic BP- *mmHg ± SD*	70.5 ± 9.6	72.4 ± 10.7	0.64
Smoking history- *n (%)*	23 (53.5)	35 (51.5)	0.84
Hypertension- *n (%)*	22 (51.2)	36 (52.9)	0.86
Diabetes mellitus- *n (%)*	13 (30.2)	21 (30.9)	0.94
Hypercholesterolaemia- *n (%)*	37 (86.0)	51 (75.0)	0.16
Ischaemic heart disease- *n (%)* • Previous MI • Previous PCI	13 (30.2) 10 (23.3) 13 (30.2)	26 (38.2) 16 (23.5) 25 (36.8)	0.39 0.97 0.48
Stroke- *n (%)*	4 (9.3)	6 (8.8)	1.0
Peripheral vascular disease- *n (%)*	3 (7.0)	1 (1.5)	0.30
Chronic kidney disease- *n (%)* • eGFR >60 • eGFR 45-59 • eGFR 30-44	7 (16.3) 36 (83.7) 6 (14.0) 1 (2.3)	9 (13.2) 59 (86.8) 8 (11.8) 1 (1.5)	0.66
Chronic lung disease- *n (%)*	8 (18.6)	4 (5.9)	0.06

Baseline blood results demonstrated significant differences between the CMD and control cohorts in NT-proBNP (910 ± 3001 ng/L vs 199 ± 291 ng/L, respectively; p=0.01), triglycerides (1.65 ± 1.51 mmol/L vs 1.79 ± 0.88 mmol/L, respectively; p=0.046) and high-density lipoprotein (1.32 ± 0.34 mmol/L vs 1.19 ± 0.31 mmol/L, respectively; 0.04) (see supplementary appendix for full comparison of blood results).

Conjunctival microvascular parameters

Indices of microvascular function were obtained from a total of 2295 conjunctival vessels across all 111 subjects. A mean of 22.6 ± 13.2 vessels (3.1 ± 2.7 arterioles, 16.5 ± 10.9 venules and 3.1 ± 3.6 undifferentiated vessels) were analysed in the CMD cohort and 20.0 ± 12.5 (3.2 ± 3.9 arterioles, 13.8 ± 10.7 venules and 3.0 ± 3.2 venules) in the control cohort (p=0.18).

Table 4.2 demonstrates a comparison of measured conjunctival microcirculatory parameters in CMD and control cohorts across all analysed vessels. Mean diameter did not differ between the groups. V_a, V_{cs}, WSR and WSS were all significantly lower in the CMD cohort. Q was numerically lower in the CMD cohort and the difference approached statistical significance (p=0.06).

Table 4.2. Comparison of conjunctival microcirculatory parameters in all vessels

Parameter	**CMD (n=975)**	**Control (n=1320)**	**p-value**
Diameter- *μm ± SD*	24.9 ± 8.4	24.8 ± 7.9	0.88
Axial velocity- *mm/s ± SD*	0.52 ± 0.15	0.55 ± 0.14	**<0.001**
Cross-sectional velocity- *mm/s ± SD*	0.36 ± 0.10	0.38 ± 0.10	**<0.001**
Blood flow rate- *pl/s ± SD*	193.6 ± 132.8	200.5 ± 131.4	0.06
Wall shear rate- s^{-1} ± *SD*	136.4 ± 75.5	142.3 ± 74.6	**0.03**
Wall shear stress- *dynes/cm²* ± *SD*	8.8 ± 4.5	9.6 ± 5.0	**<0.001**

Significant reductions in V_a (0.53 ± 0.15 mm/s vs 0.55 ± 0.14 mm/s, p= 0.01), V_{cs} (0.37 ± 0.10 vs 0.38 ± 0.10 mm/s, p= 0.009) and WSS (8.6 ± 4.4 dynes/cm^2 vs 9.2 ± 4.9 dynes/cm^2, p= 0.01), but not Q or WSR were observed in venules in the CMD cohort. A full list of results can be found in **Table S2** in the supplementary appendix.

The number of arterioles per patient in which results were obtained was lower than venules (354 vs 1605), but the most marked haemodynamic differences were observed in this vessel type. In the CMD cohort reductions were observed in V_a (0.50 ± 0.14 mm/s vs 0.56 ± 0.13 mm/s, p <0.001), V_{cs} (0.36 ± 0.10 mm/s vs 0.39 ± 0.09 mm/s, p <0.001) and Q

(137.7 ± 96.9 pl/s vs 180.3 ± 116.9 pl/s, p <0.001). WSR (155.4 ± 89.8 s^{-1} vs 160.4 ± 85.5 s^{-1}, p= 0.40) and WSS (9.8 ± 5.2 dynes/cm^2 vs 10.5 ± 5.8 dynes/cm^2, p= 0.30) did not differ, however WSR and WSS are inversely related to vessel diameter. Vessel diameter in isolation is not a marker of microvascular function; instead, being predominantly influenced by the field of imaging, vessel selection and the height and weight of the subject. To overcome this difference and measure differences in comparable vessels, arterioles were further analysed in two distinct diameter groups. These groups were selected as described in the methods. In both 10 - 25 µm and 25 – 40 µm arterioles, reductions were observed in all measured microcirculatory parameters in the CMD cohort (**Figure 4.3**).

Figure 4.3. Comparison of conjunctival arteriolar microcirculatory parameters divided by diameter

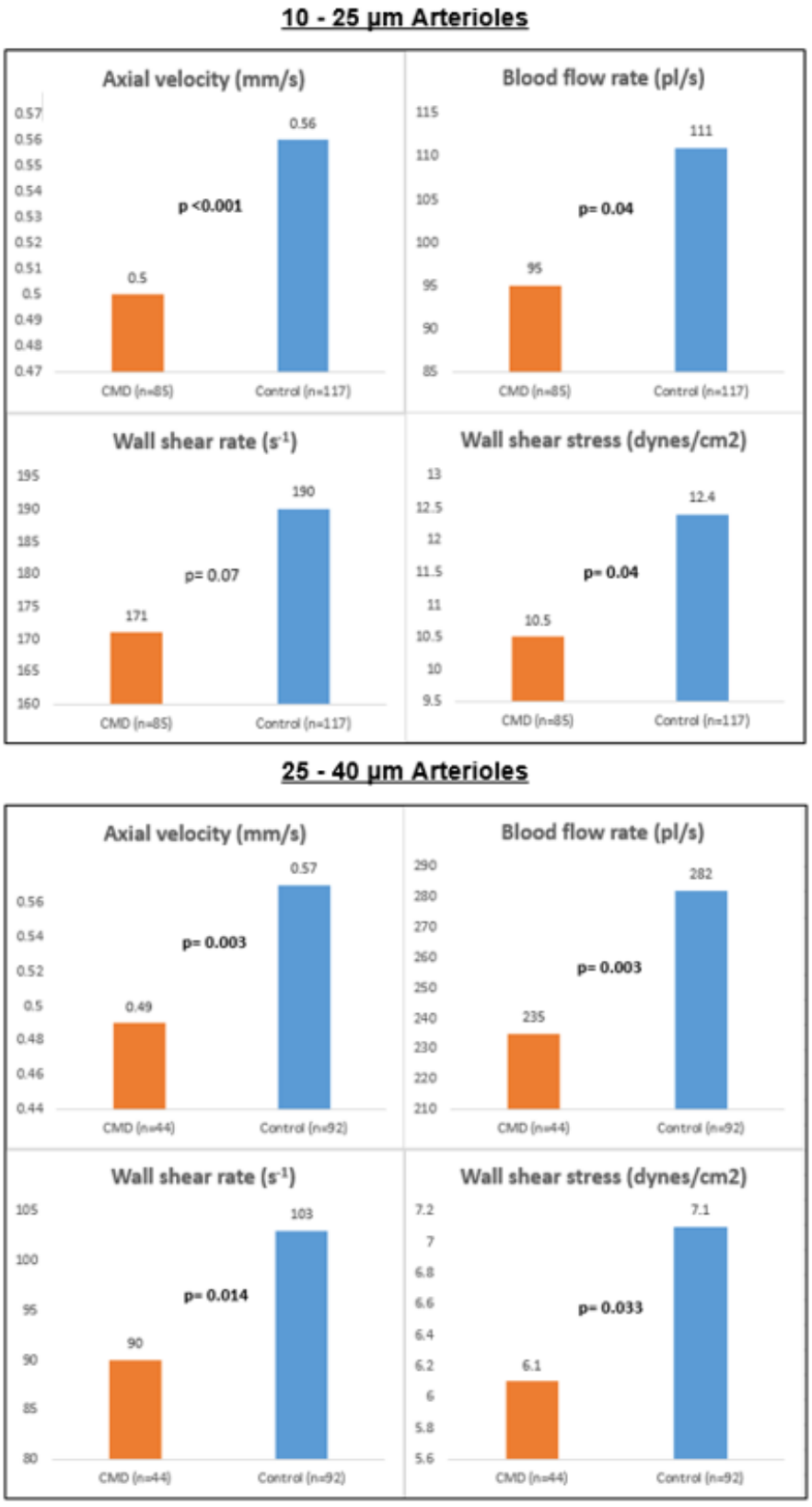

Baseline co-morbidities and pharmacological therapies

To evaluate the impact of potentially confounding medical conditions on microvascular parameters, we performed a comparative analysis of the CMD and control cohorts, excluding subjects with a past medical history of percutaneous coronary intervention, myocardial infarction, diabetes mellitus or systemic hypertension. This enabled subjects with isolated CMD to be compared to healthy controls with no significant co-morbidities associated with conventional cardiovascular (CV) risk and the development of atherosclerosis. A total of 13/43 subjects in the CMD cohort and 16/68 subjects in the control cohort fulfilled this inclusion criteria for analysis. In the CMD cohort there were 310 analysable conjunctival vessels (50 arterioles, 221 venules and 39 undifferentiated vessels). In the Control cohort there were 241 analysable conjunctival vessels (37 arterioles, 163 venules and 41 undifferentiated vessels).

A comparison of all vessels demonstrated significant reductions in the CMD cohort in V_a (0.50 ± 0.15 mm/s vs 0.57 ± 0.13 mm/s, p <0.001), V_{cs} (0.35 ± 0.10 mm/s vs 0.40 ± 0.10 mm/s, p <0.001), WSR (125.0 ± 62.5 s^{-1} vs 149.6 ± 74.6 s^{-1}, p <0.001) or WSS (7.6 ± 3.4 dynes/cm^2 vs 9.7 ± 4.8 dynes/cm^2, p <0.001). Q was numerically lower in the CMD cohort, but this did not reach statistical significance (184.7 ± 117.9 pl/s vs 197.0 ± 121.2 pl/s, p=0.19) (**Figure 4.4**).

Figure 4.4. Boxplots comparing conjunctival microvascular parameters in all vessels in subjects without established coronary artery disease, diabetes mellitus, systemic hypertension and hypercholesterolaemia

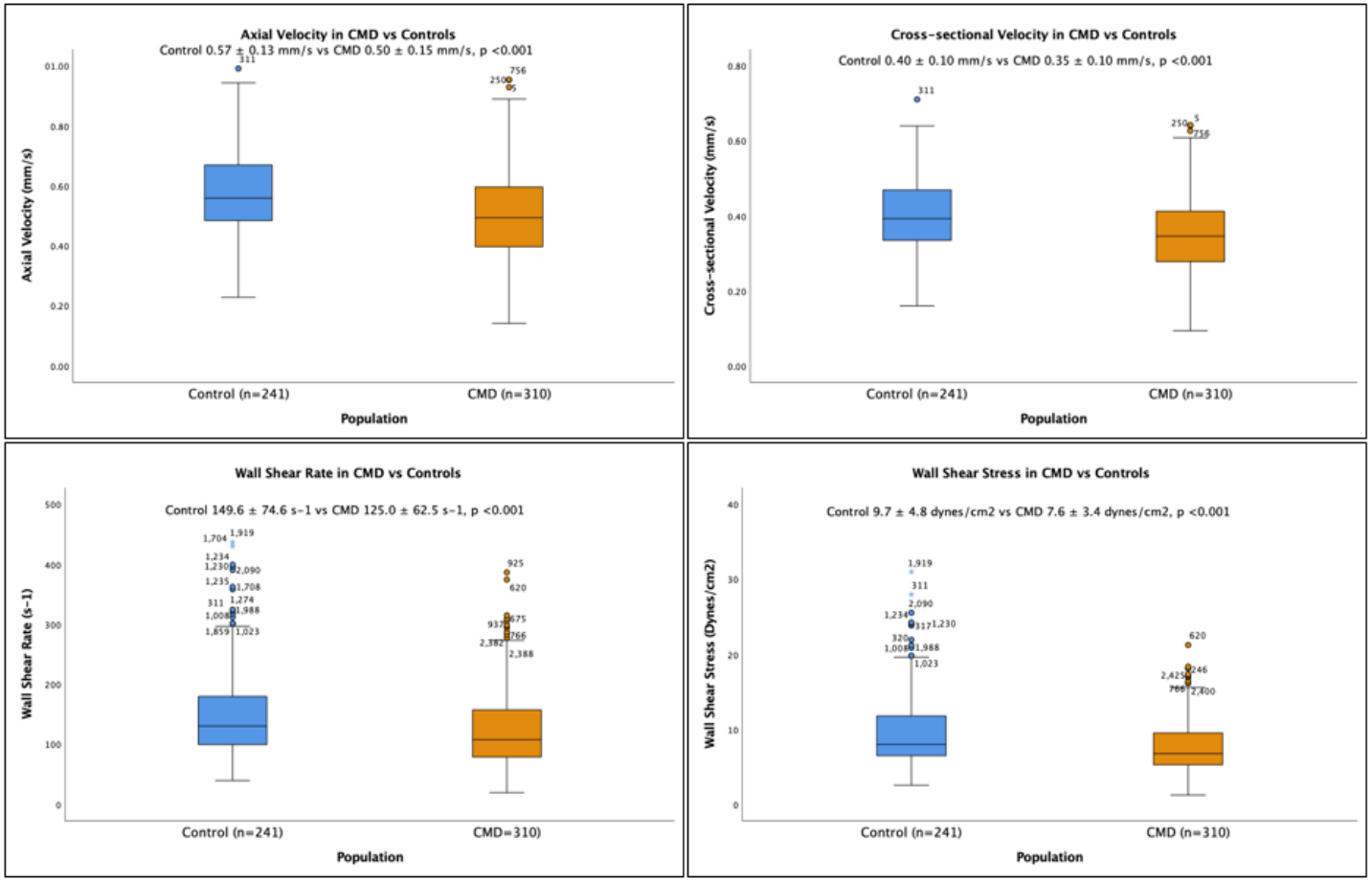

In this sub-population of patients with no confounding co-morbidities, similar differences were observed in both arteriole and venule sub-groups. In the CMD cohort reductions in arteriole V_a, V_{cs}, and Q; and venule V_a, V_{cs}, WSR and WSS were demonstrated (**Table 4.3**).

Table 4.3. Comparison of conjunctival microvascular parameters in arterioles and venules (excluding subjects with a previous history of PCI, MI, diabetes mellitus or systemic hypertension)

Arterioles			
Parameter	**CMD (n=50)**	**Control (n=37)**	**p-value**
Diameter- *µm ± SD*	21.4 ± 6.8	22.8 ± 7.4	0.36
Axial velocity- *mm/s ± SD*	0.48 ± 0.12	0.56 ± 0.14	**0.002**
Cross-sectional velocity- *mm/s ± SD*	0.34 ± 0.09	0.40 ± 0.10	**0.004**
Blood flow rate- *pl/s ± SD*	129.9 ± 94.8	169.5 ± 100.9	**0.03**
Wall shear rate- s^{-1} *± SD*	144.6 ± 78.4	161.7 ± 88.5	0.25
Wall shear stress- *dynes/cm^2 ± SD*	8.2 ± 3.8	10.4 ± 5.5	0.06
Venules			
Parameter	**CMD (n=221)**	**Control (n=163)**	**p-value**
Diameter- *µm ± SD*	26.2 ± 7.6	24.4 ± 7.4	**0.02**
Axial velocity- *mm/s ± SD*	0.51 ± 0.15	0.57 ± 0.13	**<0.001**

Cross-sectional velocity- *mm/s ± SD*	0.35 ± 0.11	0.40 ± 0.10	**<0.001**
Blood flow rate- *pl/s ± SD*	201.7 ± 121.1	200.2 ± 124.6	0.88
Wall shear rate- s^{-1} ± *SD*	120.8 ± 59.8	148.4 ± 74.3	**<0.001**
Wall shear stress- *dynes/cm^2 ± SD*	7.4 ± 3.3	9.6 ± 4.6	**<0.001**

These findings coupled with the lack of significant differences in baseline co-morbidities between CMD and control groups suggests that the differences observed in conjunctival parameters in the CMD cohort are independent of these conventional CV risk factors for the development of atherosclerosis.

A comparison of baseline pharmacological therapies at the time of conjunctival vascular imaging is shown in **Table 4.4**. The only difference observed was a more prevalent use of angiotensin-2 receptor blockers (ARBs) in the CMD cohort. A comparison of microvascular parameters in patients taking ARBs vs ARB naïve participants revealed no differences in the conjunctival parameters of diameter (23.7 ± 2.4 vs 24.6 ± 3.3, p=0.22), V_a (0.54 ± 0.05 mm/s vs 0.54 ± 0.06 mm/s, p=0.93), V_{cs} (0.38 ± 0.03 mm/s vs 0.38 ± 0.04 mm/s, p=0.96), Q (181.3 ± 37.9 pl/s vs 193.6 ± 49.2 pl/s, p=0.36), WSR (141.9 ± 16.6 s^{-1} vs 141.9 ± 30.2 s^{-1}, p =0.78) or WSS (8.6 ± 1.8 dynes/cm^2 vs 9.3 ± 2.5 dynes/cm^2, p=0.28). Only 13.5% of the total number of patients in this study were on regular ARBs. This difference is

therefore unlikely to impact or confound the results or conclusions that can be drawn from this study.

Haemodynamics were not influenced by the field of imaging (nasal vs temporal) or the eye that was imaged (right vs left). This was evaluated by comparing mean V_{cs} in the control cohort separated by the field of conjunctiva that was imaged (Left nasal 0.40 ± 0.10 mm/s; left temporal 0.38 ± 0.10 mm/s; right nasal 0.38 ± 0.09 mm/s; right temporal 0.38 ± 0.09 mm/s; p= 0.10). The hand dominance of the subject did not significantly impact mean V_{cs} in either the right (right dominant 0.38 ± 0.09 mm/s vs left dominant 0.38 ± 0.09 mm/s; p= 0.98) or left (right dominant 0.39 ± 0.10 mm/s vs left dominant 0.40 ± 0.12 mm/s; p=0.47) eyes.

Table 4.4. Comparison of baseline pharmacological therapies between groups

Medication	**CMD (n=43)**	**Control (n=68)**	**p-value**
Antiplatelet- *n (%)*			
• Aspirin	29 (67.4)	41 (60.3)	0.45
• P2Y12 inhibitor	11 (25.6)	20 (29.4)	0.66
Anti-hypertensive- *n (%)*			
• ACE inhibitor	20 (46.5)	29 (42.6)	0.69
• Angiotensin-2 receptor blocker	10 (23.3)	5 (7.4)	**0.02**
• Mineralocorticoid receptor antagonist	1 (2.3)	1 (1.5)	1.0
• Calcium channel blocker	14 (32.6)	15 (22.1)	0.22
• Thiazide diuretic	5 (11.6)	5 (7.4)	0.51
SGLT-2 inhibitor- *n (%)*	7 (16.3)	4 (5.9)	0.10
Anti-anginal- *n (%)*			
• Beta blocker	31 (72.1)	41 (60.3)	0.21
• Ranolazine	8 (18.6)	5 (7.4)	0.07
• Nicorandil	4 (9.3)	3 (4.4)	0.43
• Long-acting nitrate	18 (41.9)	25 (36.8)	0.59
Statin- *n (%)*	37 (86.0)	55 (80.9)	0.48

DISCUSSION

This study demonstrates significant differences in parameters of conjunctival microcirculatory function in patients with CMD in comparison to an age and sex-matched group of controls. The findings suggest that the physiological changes involved in this sub-type of INOCA are associated with systemic microvascular dysfunction. To the best of our knowledge this is the first study to demonstrate a correlation with CMD and systemic microvascular dysfunction detected non-invasively in an alternative vascular network.

The elevations in IMR and reductions in CFR that are observed in CMD occur due to reductions in coronary blood flow velocity and rate. This is the result of structural and/or functional obstruction at a microvascular level. The findings of this study highlight that similar reductions in V_a, V_{cs} and Q can be observed in the conjunctival microcirculation in patients with CMD. The physiological differences were most pronounced in conjunctival arterioles, mirroring the site of pathophysiological changes observed in CMD.

Previous studies suggest that both low and high WSS are associated with atherosclerotic coronary artery disease. High WSS is associated with apoptosis of smooth muscle cells that might develop necrotic core progression and enhance plaque vulnerability (Samady et al, 2011).

Endothelial cells exposed to low WSS are activated, displaying a pro-inflammatory state (Kwak et al, 2014). Low WSS has therefore been associated with atherosclerotic plaque development and hence both early and advanced coronary atherosclerosis (Gijsen et al, 2019). This study found reductions in conjunctival vessel WSS in a CMD cohort. These changes were demonstrated in all conjunctival vessels, but similar to V_a, V_{cs} and Q were most evident in arterioles.

The potential clinical utility for non-invasive vascular imaging to diagnose microvascular disease is two-fold. Firstly, the gold standard for the diagnosis of CMD involves invasive coronary angiography, thereby exposing the patient to a variety of potentially serious procedural risks. A diagnostic algorithm for CMD that incorporates the non-invasive demonstration of systemic microvascular dysfunction could, theoretically in combination with typical symptoms and non-obstructive epicardial CAD detected on CTCA, replace the need for invasive angiography and coronary function testing. This hypothesis would need to be validated in future prospective studies evaluating the technique as a diagnostic tool for CMD.

Secondly, the demonstration of microvascular dysfunction may have a role in CV risk stratification and primary prevention. The underlying mechanisms involved in the development of atherosclerotic vascular disease can be observed earliest in the microcirculation of affected

vascular beds (Stokes et al, 2005). The presence of CMD has been shown to confer an adverse long-term CV prognosis (Kelshiker et al, 2022, Bairey Merz et al, 2017, Ford et al, 2018 & Kaski et al, 2018). This was highlighted in a recent large meta-analysis of 79 studies involving 59,740 patients. This study demonstrated that the presence of CMD, as evidenced by a reduction in CFR (multiple modalities of measurement across the included studies) was strongly associated with an increased risk of all-cause mortality (HR: 3.78, 95% CI: 2.39 – 5.97) and MACE (HR 3.42, 95% CI: 2.92 – 3.99) (Kelshiker et al, 2022). In this meta-analysis each 0.1 unit reduction in CFR was associated with a proportional increase in both mortality and MACE. The adverse prognosis was observed in patients with isolated CMD in addition to those with co-existent and potentially contributory pathologies such as acute coronary syndrome, previous cardiac transplant and diabetes mellitus. These findings highlight the potential value in utilising indices of microvascular function to identify individuals at an elevated CV risk and hence target vascular risk factor modification more aggressively.

Conventional CV risk stratification tools typically identify the majority of individuals as low-intermediate risk. The ability to detect systemic microvascular dysfunction therefore has potential clinical utility in enhancing CV risk assessment. Similar to CT coronary calcium scoring, this may allow appropriate CV risk re-categorisation and hence targeted primary preventative lifestyle and pharmacological recommendations. Conjunctival vascular imaging is advantageous as it is easy to perform,

with limited expertise required for image acquisition and does not involve exposure of the patient to ionising radiation. Future research would be required to establish the prognostic benefit of conjunctival vascular screening and the ability to correlate to intermediate and long-term CV risk.

LIMITATIONS

In this study coronary microvascular function testing did not incorporate coronary vasoreactivity testing to diagnose vasospastic angina. Therefore, a small number of patients in both the CMD and control cohorts may in fact have had this INOCA sub-type. A small minority of subjects had physiological evaluation of either the RCA or LCX, vessels in which, evaluation of microvascular function is less well validated.

Patients in the CMD cohort had evidence of coronary microvascular dysfunction during pharmacological stress, however conjunctival microvascular measurements were made at rest. Therefore, whilst differences between groups were observed the coronary and conjunctival microvasculature were assessed during different physiological conditions. However, one would hypothesis that similar to the coronary circulation, patients with systemic microvascular dysfunction will have a more pronounced reduction in blood flow velocity and rate during stress than at rest.

Given the nature of this study, a proportion of subjects had potentially confounding medical co-morbidities in addition to regular pharmacological therapies known to impact systemic microvascular function. Whilst we acknowledge this as a limitation, analysis of the impact of both co-morbidities (established coronary artery disease, diabetes mellitus, hypertension and hypercholesterolaemia) and medication use revealed no significant association with conjunctival microvascular parameters. There was also no difference in the prevalence of baseline co-morbidities between CMD and control cohorts.

CONCLUSION

This study demonstrates the presence of physiological changes in the conjunctival microcirculation of patients with CMD that are consistent with systemic microvascular dysfunction in this population. The findings support the hypothesis that the microvascular changes in CMD are not limited to the coronary circulation. The potential clinical utilities of conjunctival vascular imaging lie both in the diagnosis of CMD and in the augmentation of conventional CV risk assessment. Future research is required to both validate this observation and importantly establish a threshold of abnormality for the various measured conjunctival parameters.

CHAPTER 4 SUPPLEMENTARY APPENDIX

Table of Contents

Equipment for Image Acquisition

In order to obtain video imaging of the conjunctiva of sufficient quality to allow quantification of microvascular parameters, a combination of hardware that provides sufficient illumination and magnification of the vessels is required. The equipment used for conjunctival vascular imaging included:

1. Topcon SL-D4 Slit-lamp Biomicroscope (Topcon Medical Systems Inc., Oakland, NJ, USA)
2. Apple iPhone 11 Pro Smartphone (Apple Inc., Cupertino, CA, USA)
3. Digital Photomicrography Slit-lamp Lens Adapter (Zarf Enterprises Inc., Spokane, WA, USA)

The Topcon SL-D4 (Topcon Medical Systems Inc., Oakland, NJ, USA) slit-lamp biomicroscope was used for both illumination and magnification of the bulbar conjunctival microvasculature. This provided a 40x magnification of the micro-vessels being imaged. Images were then also magnified by the smartphone camera by a further 2x factor of magnification. This allowed sufficient image quality, whilst not compromising the size of the field of view and hence number of blood vessels visualised. The slit-lamp and iPhone were coupled using a bespoke adapter.

A smartphone gives little control over relevant camera properties (focus, ISO, shutter speed, aperture and compression). In this study we overcame this by using a commercially available third-party application “ProMovie Recorder” (www.promovieapp.com). This enabled conjunctival imaging to be performed in line with a set imaging protocol (as described below), providing consistent imaging settings with respect to zoom, ISO, focus, shutter speed and exposure. This allowed calculation of a pixel to millimetre conversion factor for the video settings applied. This conversion factor was used for the downstream measurement of vessel diameter and blood flow velocity, in addition to the calculation of other parameters of microcirculatory function.

Protocol for Image Acquisition

1. All imaging was performed with surrounding external lighting dimmed and the primary source of ocular illumination provided by the slit-lamp biomicroscope.
2. The 12 megapixel rear facing wide lens on the iPhone 11 pro was used to acquire videos.
3. Magnification on the slit-lamp biomicroscope was set at a factor of 40x.
4. An external fixation target was used to minimise blinking and eye movement.
5. Videos were captured using the camera application “Promovie Recorder”. The fixed camera settings used were as follows:

a. Aspect ratio 16 : 9
b. Resolution 3840 x 2160 pixels
c. Frame rate 60 frames per second
d. Maximal available compression bitrate (120Mbps)
e. Camera zoom 2x magnification
f. Focus 0.5
g. ISO set to the minimum level (30)
h. Shutter speed set to minimum level (61)

6. For each subject 5 to 10 second videos were obtained from both the nasal and temporal fields of each eye (a total of 4 videos per subject)

7. Videos were saved under a unique anonymised study number prior to being electronically transferred to a University laptop for image processing

Image Processing and Microvascular Parameter Quantification

A summary of the image processing steps used to estimate haemodynamics and analyse conjunctival microvascular function is provided in **Figure 4.S1**.

Figure 4.S1. Stepwise schematic of image processing

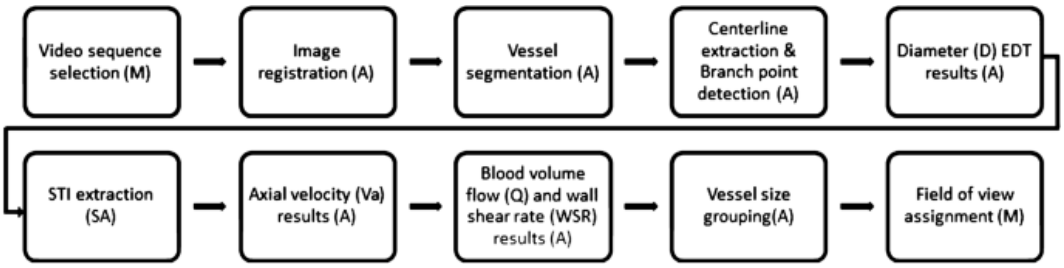

Following image acquisition, an initial manual visual inspection of the videos was performed (see **Figure 4.S2** for example of initial conjunctival image). This allowed for consecutive frames of the highest quality to be selected for subsequent image processing and analysis by researchers. The criteria applied to select these frames included:

- Conjunctival microvasculature in focus
- No eye blinking
- Minimal eye movement
- Field of view did not drift by more than 25% of the width of the frame

Figure 4.S2. Conjunctival imaging prior to the sequence selection and video stabilisation process

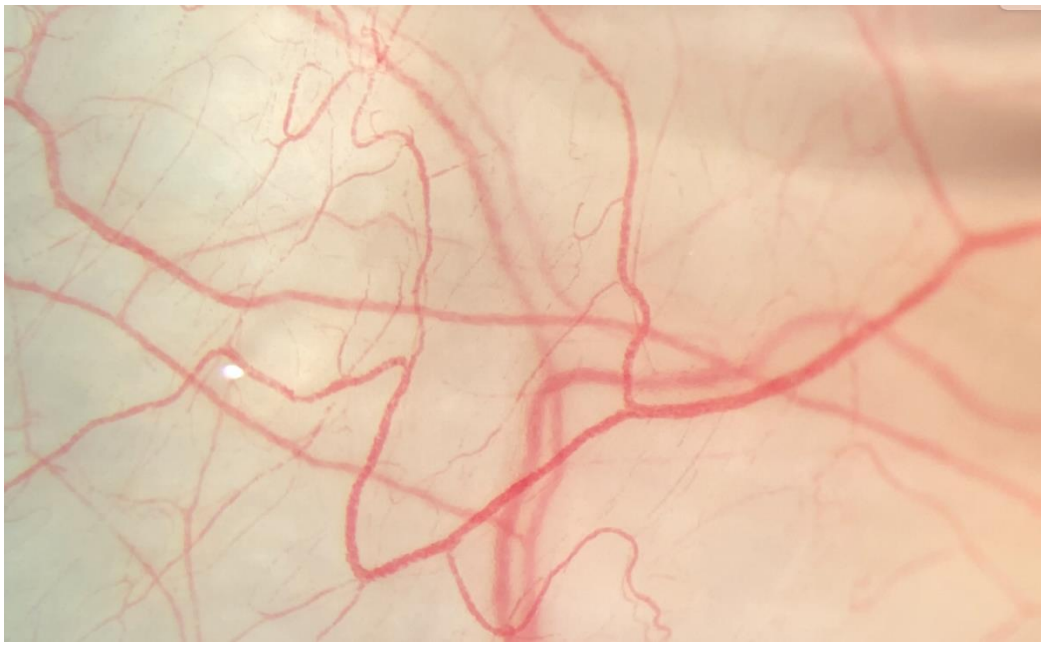

Colour videos were converted into grey scale and any underexposed or out of focus regions were excluded. The sharpest frame in the selected sequence was then chosen as a reference frame and all other frames registered to it through an affine registration procedure (Forsberg, 2007). A vessel enhancement filter was then applied to the mean registered images (Jerman et al, 2016) to enhance the performance of the Frangi filter (Frangi et al, 1998). A binary map of the conjunctival vasculature and corresponding centrelines was extracted via standard skeletisation techniques. This allowed small spurious branches to be removed and for the detection of the end and branch points of the vessels connected vessel network was broken into individual vessel segments by setting the

branch points' neighbouring pixels to zero. Any vessel segments longer than 30 pixels were selected for further assessment.

Estimation of vessel diameter

The Euclidean Distance Transform (EDT) was used for vessel diameter estimation. This method can be applied to binary images to measure the straight-line distance in pixels between two points on the image. The value at each pixel of EDT map was calculated based on the Euclidean distance between the pixel and its' nearest nonzero pixel in the binary vessel image. The centreline of the vessel was used to obtain the central EDT values and thus the radius along the vessel axis. This measurement in pixels is then converted to millimetres using the previously calibrated pixel to mm conversion factor. Using this method, the vessel centreline is used to obtain the central EDT values and thus the radius along the vessel axis. The average of the diameters along the analysed vessel length was used to provide the final vessel diameter estimation.

Estimation of axial velocity

The axial velocity (V_a) of blood flow within the vessel was estimated via 1D+T continuous wavelet transform (1DTCWT) based on spatial-temporal image (STI) generated for each vessel segment (**Figure 4.S3**). In these STI graphs a change in signal intensity is reflective of erythrocyte movement through the blood vessel. The graphs provide a plot of signal

intensity against vessel segment length on the y-axis and the frame number on the x-axis. All imaging was recorded at a consistent setting of 60 frames per second, meaning 1 frame= 0.01667 seconds. Since the change of intensity in STI represents the erythrocyte flowing through the vessel within the given time (video frames), V_a can also be obtained by finding the slope of the prominent intensity bands in STI. The process of generating STI graphs is automated using specially designed software. However, the flow analysis methods described in this study required human input to differentiate and select the graphs of sufficient quality (without artefact) to enable erythrocyte tracking and hence estimate V_a .

Figure 4.S3. Sample of spatial-temporal image graphs used for axial velocity estimation

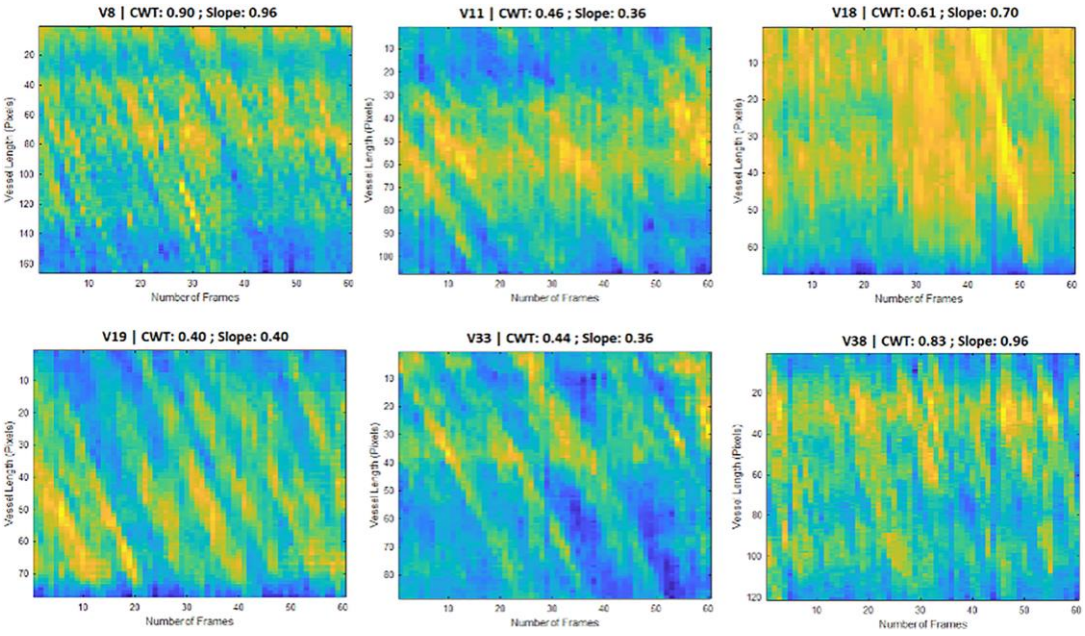

Additional conjunctival microvascular parameters

Cross-sectional velocity, blood flow rate, wall shear rate and wall shear stress were estimated using the formulae described below. These calculations are performed using the results for diameter and axial velocity described in previous publications (Khansari et al, 2016 & Koutsiaris et al, 2007).

Cross-sectional velocity (V_{cs})

V_{cs} is impacted by the diameter of the vessel in which blood is travelling. In this study it was estimated according to these formulae:

Diameter / human erythrocyte diameter (D_c) ≤ 0.6:

$$V_{cs} = V_a$$

Diameter / human erythrocyte diameter (D_c) > 0.6:*

$$V_{cs} = V_a / 1.58 \times (1 - e^{-\sqrt{2}D_c})$$

* In these equations D_c was taken to be a constant, equal to 7.65 μm.

Blood flow rate (Q)

Q has a linear relationship to V_{cs} and is exponentially related to diameter according to this formula:

$$Q = V_{cs} (\pi D^2 / 4)$$

Wall shear rate (WSR)

WSR has a linear relationship to V_{cs} and an inverse relationship to diameter according to this formula:

$$WSR = (8V_{cs}) / D$$

Wall shear stress

Wall shear stress (WSS) is calculated as the product of wall shear rate (WSR) and whole blood viscosity (η):

$$WSS = WSR \times \eta$$

Newton's law defines the relationship between shear stress and the shear rate of a fluid subjected to mechanical stress. The ratio of shear stress to shear rate is a constant for a given temperature and pressure, and hence in Newtonian fluids the viscosity is independent of the shear rate (George et al, 2013). Blood does not follow Newton's law of viscosity, and hence is described as a non-Newtonian fluid. The primary determinants of η are

plasma viscosity (η_p) (in turn primarily influenced by total protein concentration), haematocrit (HCT) and the mechanical properties of red blood cells (Baskurt et al, 2003).

In this study it was not possible to measure η directly on participants due to the lack of the specialised equipment required. The Quemada model for estimation of η was therefore chosen to obtain results and in turn estimate WSS (Quemada et al, 1981). This model takes into consideration HCT, η_p and WSR as defined in the equation below:

$$\eta = \eta_p \left(1 - \frac{1}{2} \frac{k_0 + k_\infty \sqrt{\dot{\gamma} / \gamma_c}}{1 + \sqrt{\dot{\gamma} / \gamma_c}} H_t \right)^{-2}$$

In this equation k_0, k_∞ and γ_c are constants (4.33, 2.07 and 1.88 respectively). HCT and η_p were obtained from blood sampling during the recruitment process and WSR estimated for the individual vessels as described previously.

Assessing repeatability of conjunctival microvascular parameter quantification

The aforementioned process to quantify physiological parameters of microcirculatory function needs to consider several possible areas that may impact the reproducibility of results:

1. Time of day conjunctival imaging performed
2. Procedural administration of vasoactive medications
3. Conjunctival video stabilisation and sequence selection
4. Downstream image processing and microvascular parameter quantification

1. Time of day conjunctival imaging performed

A previous study evaluated the impact that time of day had on conjunctival haemodynamics. In this study the conjunctiva of 20 healthy subjects were imaged by two independent operators and then measurements were repeated every 2 hours to evaluate the variations that occurred over the course of a single day. No significant differences were observed in the microvascular parameters obtained between the various time intervals of imaging, suggesting that slit-lamp imaging of the conjunctiva can be performed at any time throughout the day, without the time itself impacting the results obtained (Xu et al, 2015).

On the basis of the results from this study, imaging of the conjunctiva was not performed at a pre-specified time of day, instead this was dictated by timing in relation to the administration of peri-procedural medications.

2. Procedural administration of vasoactive medications

All participants in the microvascular disease cohort of this study were recruited following the performance of a coronary angiogram and pressure wire evaluation of coronary physiology. This involves the administration of intra-arterial nitroglycerine and unfractionated heparin in addition to intravenous adenosine. Adenosine and nitroglycerine have very short half-lives (10-30 seconds and 1.5-7.5 minutes respectively) (Pantely et al, 1990 & Kim et al, 2022). Unfractionated heparin has a longer half-life (30 minutes) (Blann et al, 2002). In order to mitigate the impact of these medications on the conjunctival microcirculation and avoid any potentially confounding effect, participants were recruited a minimum of 4 hours following their procedure, to ensure these medications would not impact results.

3. Conjunctival video stabilisation and sequence selection

The process of video stabilisation and conversion of images to a binary format for analysis is semi-automated. Researchers review the 5-10 second conjunctival videos and select 1 second (60 frames) for subsequent analysis as described previously. This process may be subject to operator variation. Whilst this may influence results, it is performed to select the sequence with the best image quality and hence we believe provide the most accurate assessment of blood flow. Following sequence selection, the process of video stabilisation is entirely automated and provided the same sequence is selected introduces no variability.

4. Downstream image processing and parameter quantification

The repeatability of the methodology to obtain haemodynamic results following video stabilisation was assessed. A total of 16 videos recorded from 4 participants were analysed twice by the same operator independent of clinical details or the participant cohort. A total of 221 vessels were analysed. Differences in the four main measured parameters (D, V_a, Q, WSR) were compared. Stabilised vessel maps were then reviewed by another independent operator to ensure the same vessels were compared. For each vessel the mean difference in 5 measured parameters (D, V_a, V_{cs}, Q and WSR) was calculated. The mean difference for D was 0.02 ± 0.31 µm, V_a was 0.002 ± 0.02 mm/s, V_{cs} was 0.001 ± 0.02 mm/s, Q was 0.08 ± 11.31 pl/s and WSR was 0.98 ± 8.39 s^{-1}. Intraclass correlation coefficient suggested excellent repeatability across all parameters (D 0.999, 95% CI 0.999 – 0.999; V_a 0.986, 95% CI 0.981 – 0.989; V_{cs} 0.985, 95% CI 0.980 – 0.988; Q 0.997, 95% CI 0.996 – 0.998; and WSR 0.988, 95% CI 0.985 – 0.991).

Table 4.S1. Comparison of baseline blood results between CMD and control cohorts

Blood test	**CMD (n=43)**	**Control (n=68)**	**p-value**
HbA1c- *mmol/mol ± SD*	43.7 ± 15.8	44.2 ± 12.8	0.38
Creatinine- *µmol/L ± SD*	79.9 ± 23.7	84.3 ± 15.5	0.057
Creatinine Clearance- *ml/min ± SD*	99.1 ± 30.6	104.6 ± 39.7	0.73
Haemoglobin- *g/L ± SD*	137.1 ± 12.6	138.9 ± 13.6	0.47
Haematocrit- *l/l ± SD*	0.41 ± 0.03	0.41 ± 0.04	0.57
Platelets- *10^9/L ± SD*	258.9 ± 65.5	244.9 ± 59.4	0.36
NT-proBNP- *ng/L ± SD*	910.0 ± 3000.5	199.4 ± 290.6	**0.01**
Cholesterol- *mmol/L ± SD*	3.7 ± 0.9	3.8 ± 1.1	0.75
Triglycerides- *mmol/L ± SD*	1.65 ± 1.51	1.79 ± 0.88	**0.046**
High Density Lipoprotein- *mmol/L ± SD*	1.32 ± 0.34	1.19 ± 0.31	**0.042**
Low Density Lipoprotein- *mmol/L ± SD*	1.71 ± 0.76	1.86 ± 0.96	0.95
Urate- *mmol/L ± SD*	0.33 ± 0.08	0.33 ± 0.07	0.78
C-reactive protein- *mg/L ± SD*	3.6 ± 5.0	2.8 ± 3.3	0.60
Plasma viscosity- *mPa.s ± SD*	1.68 ± 0.09	1.67 ± 0.11	0.65

Table 4.S2. Comparison of conjunctival microcirculatory parameters by vessel sub-type (arterioles and venules)

Arterioles			
Parameter	**CMD (n=135)**	**Control (n=219)**	**p-value**
Diameter- *μm ± SD*	21.4 ± 7.1	23.1 ± 7.9	**0.04**
Axial velocity- *mm/s ± SD*	0.50 ± 0.14	0.56 ± 0.13	**<0.001**
Cross-sectional velocity- *mm/s ± SD*	0.36 ± 0.10	0.39 ± 0.09	**<0.001**
Blood flow rate- *pl/s ± SD*	137.7 ± 96.9	180.3 ± 116.9	**<0.001**
Wall shear rate- s^{-1} *± SD*	155.4 ± 89.8	160.4 ± 85.5	0.40
Wall shear stress- *dynes/cm*^{2} *± SD*	9.8 ± 5.2	10.5 ± 5.8	0.30
Venules			
Parameter	**CMD (n=707)**	**Control (n=898)**	**p-value**
Diameter- *μm ± SD*	25.9 ± 8.6	25.5 ± 7.8	0.54
Axial velocity- *mm/s ± SD*	0.53 ± 0.15	0.55 ± 0.14	**0.01**
Cross-sectional velocity- *mm/s ± SD*	0.37 ± 0.10	0.38 ± 0.10	**0.009**
Blood flow rate- *pl/s ± SD*	207.1 ± 136.7	207.5 ± 133.8	0.67
Wall shear rate- s^{-1} *± SD*	132.4 ± 74.4	135.9 ± 71.6	0.16
Wall shear stress- *dynes/cm*^{2} *± SD*	8.6 ± 4.4	9.2 ± 4.9	**0.01**

Table 4.S3. Comparison of conjunctival arteriolar microcirculatory parameters divided by diameter groupings (10 - 25 and 25 - 40μm)

10 - 25 μm arterioles			
Parameter	**CMD (n=85)**	**Control (n=117)**	**p-value**
Diameter- *μm ± SD*	17.9 ± 3.8	18.2 ± 4.3	0.47
Axial velocity- *mm/s ± SD*	0.50 ± 0.14	0.56 ± 0.13	**<0.001**
Cross-sectional velocity- *mm/s ± SD*	0.36 ± 0.10	0.40 ± 0.09	**<0.001**
Blood flow rate- *pl/s ± SD*	95.2 ± 50.9	111.1 ± 57.2	**0.04**
Wall shear rate- s^{-1} ± *SD*	170.6 ± 64.9	190.1 ± 72.2	0.07
Wall shear stress- *dynes/cm*^{2} ± *SD*	10.5 ± 3.6	12.4 ± 5.8	**0.04**
25 - 40 μm arterioles			
Parameter	**CMD (n=44)**	**Control (n=92)**	**p-value**
Diameter- *μm ± SD*	29.8 ± 3.4	30.5 ± 4.0	0.39
Axial velocity- *mm/s ± SD*	0.49 ± 0.14	0.57 ± 0.14	**0.003**
Cross-sectional velocity- *mm/s ± SD*	0.33 ± 0.10	0.38 ± 1.0	**0.003**
Blood flow rate- *pl/s ± SD*	235.2 ± 95.4	281.7 ± 95.8	**0.003**
Wall shear rate- s^{-1} ± *SD*	89.6 ± 26.3	103.1 ± 30.9	**0.014**
Wall shear stress- *dynes/cm*^{2} ± *SD*	6.1 ± 1.7	7.1 ± 2.4	**0.033**

Chapter 5

Assessment of indices of conjunctival microvascular function in patients with severe aortic stenosis pre- and post-transcatheter aortic valve intervention

ABSTRACT

Background

Aortic stenosis (AS) is associated with pathophysiological changes in both left ventricular and coronary microvascular structure and function. The treatment of AS with transcatheter aortic valve implantation (TAVI) has been associated with improvements in invasive indices of coronary microvascular function. This study sought to address whether systemic microvascular dysfunction was present in patients with AS and if microvascular function was altered by treatment of AS with TAVI. The conjunctival microcirculation was used as the site for the non-invasive assessment of systemic microvascular function.

Methods

Patients undergoing TAVI for the treatment of severe AS were compared to a cohort of age- and sex-matched controls without valvular heart disease. Conjunctival vascular imaging was performed in all subjects using a previously validated combination of a smartphone and slit-lamp biomicroscope. This technique allowed measurement of vessel diameter and other indices of microvascular function by tracking erythrocyte motion. Conjunctival haemodynamics were compared pre- and post-TAVI, in addition to between the severe AS and control cohorts.

Results

A total of 165 patients were included (90 severe AS and 75 controls). Baseline characteristics were largely well matched between groups. In

comparison to the control cohort, arteriole axial (V_a) and cross-sectional velocity (V_{cs}) were significantly lower in females with AS (V_a severe AS 0.53 ± 0.11 vs control 0.59 ± 0.12, **p=0.047**; V_{cs} severe AS 0.38 ± 0.07 vs control 0.41 ± 0.08, **p=0.043**), but not in males (V_a severe AS 0.61 ± 0.11 vs control 0.58 ± 0.10, p=0.19; V_{cs} severe AS 0.43 ± 0.08 vs control 0.41 ± 0.07, p=0.20). Arteriole V_a and V_{cs} significantly increased following TAVI in females (V_a Pre-TAVI 0.52 ± 0.16 vs post-TAVI 0.59 ± 0.15, **p<0.001;** V_{cs} Pre-TAVI 0.37 ± 0.11 vs post-TAVI 0.42 ± 0.11, **p<0.001**).

Conclusion

This study highlights sex-specific differences in conjunctival microvascular function in patients with severe aortic stenosis. In this study TAVI resulted in significant improvement in conjunctival arteriolar V_a and V_{cs}. These conjunctival findings are consistent with severe AS being a cause of systemic microvascular dysfunction.

INTRODUCTION

Epidemiology of aortic stenosis

Aortic stenosis (AS) represents the most prevalent form of valvular heart disease (VHD) in Europe (Iung et al, 2019). A previous meta-analysis demonstrated a population prevalence of AS of any severity of 12.4%, and a prevalence of severe AS of 3.4% in those aged 75 years and older (Osnabrugge et al, 2013). In developed countries, the prevalence of AS has been steadily increasing due to a combination of the ageing population, ease of access to echocardiography and the availability of less invasive treatment options prompting clinicians to organise screening investigations more readily (Yadgir et al, 2020). Severe AS therefore remains the most common indication for either surgical or transcatheter valvular intervention in both Europe and North America (Bevan et al, 2019).

Severe AS carries a highly adverse intermediate to long-term prognosis with early studies identifying high rates of sudden cardiac death in the absence of aortic valve replacement (Schwarz et al, 1982 & Ross et al, 1968). In the landmark PARTNER study, all-cause mortality at two years was over 50% in patients with symptomatic severe AS that did not undergo intervention (Leon et al, 2010).

Severe AS is associated with a significant symptom burdon to affected patients. In the early stages of the disease patients' typically experience dyspnoea, fatigue and exertional limitation. As the severity of the valvular stenosis worsens, these symptoms often progress to chest pain, pre-syncope and syncope. Overall these symptoms can be highly disabling and significantly impact an individual's quality of life.

Impacts of aortic stenosis on cardiac remodelling and coronary microvascular function

The haemodynamic effects of AS have significant implications for the left ventricle (LV). Initially LV remodelling is a beneficial compensatory mechanism, but quickly transitions to a maladaptive and potentially irreversible process with prognostic implications for the patient (Rassi et al, 2014). In order to overcome the outlet obstruction created by severe AS, left ventricular pressure increases, which in turn leads to progressive left ventricular hypertrophy (LVH). As the degree of LVH progresses, there is development of myocardial fibrosis, reduced ventricular compliance, LV diastolic dysfunction and eventually LV systolic dysfunction at an advanced stage of the disease process (Yarbrough et al, 2011).

The compensatory increase in LV mass associated with haemodynamically significant AS leads to physiological and pathological alterations in coronary and LV haemodynamics (Wiegerinck et al, 2015, Cramariuc et al, 2009 & Koide et al, 1997). These alterations are

associated with coronary microvascular dysfunction (CMD), which has in turn been associated with an adverse intermediate to long-term CV prognosis. CMD in combination with LV remodelling in AS are thought to be responsible for the development of angina in the absence of epicardial coronary disease. In this setting angina occurs due to both the increase in myocardial oxygen demand and inability for supply to be met in the setting of microvascular dysfunction (Ahn et al, 2016 & Davies et al, 2011) and/or a reduced cardiac output. Angina is known to be prognostically adverse in AS, which may correlate with the known prognostic significance of CMD.

Relief of the LV outflow tract (LVOT) obstruction created by AS immediately changes ventricular haemodynamics and studies have demonstrated immediate and long-term improvements in LV systolic (Schattke et al, 2012) and diastolic function (Gonçalves et al, 2011) in addition to reductions in LV mass (Rajappan et al, 2003) following aortic valve intervention.

Impact of aortic valve intervention on coronary microvascular function

Changes in coronary microcirculatory function in patients with AS after valvular intervention are not solely dependent on the regression of LVH and it has been suggested that a reduction in the extrinsic compression of coronary arterioles and an increased diastolic perfusion time are the main mechanisms for an improvement in myocardial blood flow and coronary flow reserve (CFR) (Rajappan et al, 2003).

In 2015 Wiegerinck et al published a study evaluating invasive coronary haemodynamics in 27 patients with severe AS compared to 28 patients without AS. Coronary microvascular function was assessed both before and immediately after transcatheter aortic valve intervention (TAVI). All patients had non-obstructive epicardial coronary arteries. Hyperaemic microvascular resistance was higher in patients with AS (2.10 ± 0.69 mmHg/cm/s^{-1} vs 1.80 ± 0.60 mmHg/cm/s^{-1}, p=0.096) and CFR was lower (1.9 ± 0.5 vs 2.7 ± 0.7, **p<0.001**). In patients with AS undergoing TAVI (in the absence of significant post TAVI aortic regurgitation), immediate improvements in hyperaemic microvascular resistance (2.03 ± 0.71 mmHg/cm/s^{-1} to 1.66 ± 0.45 mmHg/cm/s^{-1}, **p=0.05**) and CFR (1.9 ± 0.4 to 2.2 ± 0.6, **p=0.009**) were observed (10). Improvements in CFR following AVR have also been observed non-invasively using adenosine stress echocardiography to measure CFR (Pre-AVR CFR 1.76 ± 0.5 vs post-AVR CFR 2.61 ± 0.7, **p<0.001**) (Hildick-Smith et al, 2000).

Aortic stenosis is a heterogenous disorder with a patient group that often have overlapping co-morbid cardiovascular conditions that may produce co-existent impacts on coronary physiology (e.g. heart failure with preserved ejection fraction, atrial fibrillation, hypertension, coronary artery disease). In AS variations in pathological and physiological responses to pressure overload are incompletely understood and generate a range of flow and pressure gradient patterns, which ultimately cause varying microvascular effects (McConkey et al, 2019). Current literature highlights both an association between AS and CMD; and improvements in coronary

microvascular function following aortic valve intervention (Wiegerinck et al, 2015). However, the exact pathophysiological mechanism for this remains unclear and a topic for further evaluation. The effect of severe AS on both epicardial and microvascular coronary physiology is currently under investigation in the COMIC-AS study, that will evaluate coronary physiology in 100 patients with severe AS at baseline, immediately post-intervention and then 6 months post-intervention (Minten et al, 2021).

Study design and hypothesis

We hypothesised that microvascular dysfunction in severe AS was not limited to the coronary circulation and could be demonstrated at a systemic level in an alternative microvascular network. Microvascular abnormalities have previously been observed in the conjunctival microcirculation of patients with coronary artery disease (CAD) (Brennan et al, 2021), diabetes mellitus (Cheung et al, 1999), cyanotic congenital heart disease (Brennan et al, 2021), cerebrovascular disease (Kord Valeshabad et al, 2015) and sickle cell disease (Kord Valeshabad et al, 2014). The conjunctiva provides a vascular network in which blood flow can be directly observed and indices of microvascular function assessed non-invasively. We conducted a study, evaluating systemic microvascular function in patients with severe AS compared to a group of controls without haemodynamically significant valvular heart disease (VHD). The patients in this study with severe AS all underwent TAVI and conjunctival microvascular indices were re-assessed following this intervention.

METHODS

We conducted a prospective study (Integrated Research Application System study number 166742) evaluating conjunctival microcirculatory function in a group of patients with severe AS (SAS cohort) (n=90), in comparison to a group of controls with no haemodynamically significant VHD (control cohort) (n=75). All patients in the SAS cohort subsequently underwent TAVI. Indices of conjunctival microvascular function were re-assessed after TAVI to allow assessment of the impact of relief from severe aortic stenosis on the conjunctival microcirculation.

All subjects provided written informed consent for participation in this study. The experimental protocol was approved by the Research Governance department in the Belfast Health and Social Care Trust (BHSCT) and Ulster University (UU). The study was carried out in accordance with the Declaration of Helsinki.

Baseline clinical data and characteristics were obtained using a recruitment questionnaire, subject's clinical notes, hospital cardiology database (Cardiovascular Information System Tomcat, Phillips, Eindhoven, Netherlands) and each subject's electronic healthcare record.

Inclusion criteria

Severe AS cohort

Patients that fulfilled the European Society of Cardiology (ESC) valvular heart disease criteria for valve intervention for the treatment of severe AS were included in this cohort (Vahanian et al, 2022). All patients had been discussed by a Heart Team at our institution's multidisciplinary meeting and were deemed suitable for aortic valve intervention. This cohort was divided into two groups defined by echocardiographic measurements:

1. High gradient severe AS
    a. Aortic mean gradient ≥40mmHg and/or peak gradient ≥64mmHg
    b. Valve area <1.0cm^2
2. Low gradient severe AS (low flow low gradient AS)
    a. Aortic mean gradient <40mmHg and peak gradient <64mmHg, but
    b. Valve area <1.0cm^2
    c. Indexed left ventricular stroke volume ≤35ml/m^2 secondary to either:
        i. left ventricular ejection fraction ≤50%*; or
        ii. low cardiac output with preserved left ventricular systolic function^

*Severe AS confirmed with low dose dobutamine stress echocardiogram

^Severe AS confirmed with aortic valve calcium score that met threshold for valve severity

Patients with previous surgical aortic valve replacement (SAVR) that fulfilled these criteria due to structural valve degeneration (SVD) were also included in this cohort as this was deemed to produce the same haemodynamic impact on the LV and coronary/systemic circulation.

Control cohort

All subjects were identified when attending the Royal Victoria Hospital for an alternative purpose (e.g. echocardiography, electrocardiography, blood pressure monitoring, pacemaker device checks). All subjects had undergone echocardiography within two years of recruitment. Subjects were included in the control cohort if they fulfilled the following inclusion criteria:

1. No haemodynamically significant stenotic or regurgitant valvular lesion on echocardiogram
2. No history of surgical or transcatheter valve repair or replacement
3. Left ventricular ejection fraction ≥50%

Exclusion criteria in both cohorts

1. Inability to consent
2. Age less than 18 years of age
3. Pregnancy at time of recruitment
4. History of conjunctival inflammation or contact lens use in the 24 hours prior to recruitment

Conjunctival Microvascular Assessment

Conjunctival imaging was performed using a Topcon SL-D4 slit-lamp biomicroscope (Topcon Medical Systems Inc., USA), iPhone 11pro smartphone (Apple, Inc, USA) and an adapter (Zarf Enterprises Inc., USA) to allow coupling of these devices. This technique has previously been validated and published by our research group (Brennan et al, 2021) and is described in more detail in Chapter 2 of this thesis.

In summary, we acquired 5–10 s digital video recordings of the microcirculation in both nasal and temporal fields of the bulbar conjunctiva, thus generating four video recordings per subject. All video recordings were converted to grayscale and underwent a process of sequence selection and stabilisation. The stabilised sequences were then analysed to obtain measurements of vessel diameter and other physiological parameters of microvascular function using the principle of erythrocyte tracking, to quantify blood flow velocity. All other parameters of microcirculatory function were derived from the measurements of vessel diameter and blood flow velocity.

Conjunctival imaging was performed in the SAS cohort either immediately prior to TAVI or during attendance at a pre-assessment clinic in the 2 weeks before TAVI. Imaging was then repeated prior to hospital discharge following TAVI, but at least 6 hours post procedure. All subjects in the SAS

cohort had blood tests performed both at the time of pre-TAVI conjunctival imaging and again at post-TAVI imaging. In the control cohort, bloods were only performed on one occasion, as no intervention was performed.

In addition to quantification of microvascular indices, vessels were manually differentiated into arterioles and venules using the principle of blood flow direction in relation to bifurcations. This allows a more accurate comparison of microvascular function to be performed. This method of vessel differentiation has been described previously (Khansari et al, 2016 & 2017). Vessels were defined as arterioles if blood flow was towards a diverging bifurcation; venules if blood flow was towards a converging bifurcation; and undifferentiated if no bifurcation was present in the imaging field to allow vessel differentiation. Undifferentiated vessels were excluded from subsequent sub-group analyses, but included when presenting results for all vessels not sub-categorised into vessel type.

Conjunctival vessel diameter, axial velocity (V_a), cross-sectional velocity (V_{cs}), blood flow rate (Q), wall shear rate (WSR) and wall shear stress (WSS) were quantified in vessels with observable blood flow

Statistical Analysis

The results of a pilot study published by our research group (Brennan et al, 2021) were used for a formal power calculation. We estimated that a

sample size of 100 patients (3600 conjunctival vessels) would provide the study with a power of at least 80% to reject the null hypothesis of no between-group differences in conjunctival haemodynamics.

Statistical analysis was performed using Statistical Package for the Social Sciences (SPSS) for Apple iOS version 27 (property of IBM). Continuous variables were described using the mean and standard deviation of the mean. Kolmogorov–Smirnov testing was used to assess normality of the continuous variables. Categorical variables were expressed as a number and percentage of the total category number to which the variable belonged.

Normally distributed variables were compared between the two populations using the independent-samples t-test. Non-normally distributed continuous variables were compared using non-parametric tests e.g. Mann–Whitney U test. Categorical comparisons were made between the two groups using Pearson Chi-Square or Fisher's exact test as appropriate.

Correlation between two continuous variables was assessed using Spearman's correlation and between one continuous variable and one dichotomous variable using point biserial correlation.

RESULTS

Between October 2020 and December 2021, a total of 169 patients were recruited to this study. There were 94 patients in the SAS cohort, but a total of 4 patients from this cohort were excluded as it was not possible for researchers to obtain post-TAVI conjunctival vascular imaging (predominantly due to TAVI related procedural complications). There were a total of 75 patients included in the age- and sex-matched control cohort.

Table 5.1 compares the baseline demographics of the SAS and control cohorts. The mean age was 82.1 ± 5.7 yrs in the SAS cohort and 80.6 ± 5.8 yrs in the control cohort (p=0.07). There was broadly an even distribution of males and females in both cohorts (see **Table 5.1**). At the time of recruitment both groups had a high-normal systolic blood pressure (SBP), but no difference was observed between the groups in mean SBP immediately prior to conjunctival vascular imaging (SAS 135.9 ± 21.0 mmHg vs control 135.3 ± 20.5 mmHg, p=0.99). These were largely well balanced between the groups, other than a higher prevalence of chronic kidney disease (CKD) in the SAS cohort. New York Heart Association Dyspnoea (NYHA) grade was higher in the SAS cohort, as they had symptomatic haemodynamically significant VHD.

In the SAS cohort echocardiographic and invasive parameters of AS severity were recorded for all patients prior to intervention. Mean aortic valve peak velocity was 4.4 ± 0.6 m/s, velocity-time integral (VTI) ratio was 0.22 ± 0.06, peak gradient was 78.0 ± 22.8 mmHg, mean gradient was

45.7 ± 14.4 mmHg, valve area was 0.7 ± 0.2 cm^2, invasive peak gradient was 43.6 ± 19.1 mmHg, invasive mean gradient was 43.4 ± 14.4 mmHg and left ventricular end diastolic pressure (LVEDP) was 19.9 ± 8.5 mmHg.

Table 5.2 is a comparison of salient baseline blood results between the groups. Given the higher prevalence of CKD in the SAS cohort, mean creatinine clearance was lower in this group (57.0 ± 20.3 ml/min vs 67.1 ± 21.5 ml/min, **p<0.001**). NT-proBNP was unsurprisingly higher in the SAS cohort (2545 ± 3564 ng/L vs 1145 ± 2714 ng/L, **p<0.001**), however the mean NT-proBNP was not normal in the control cohort suggesting that in the setting of normal LV systolic function, a proportion of this population may have undiagnosed heart failure with preserved ejection fraction (HFpEF). This is discussed in more detail in a subsequent section of this chapter when analysing conjunctival haemodynamics. This may also have been influenced by the prevalence of atrial fibrillation in the control cohort (38.7%), a co-morbid condition known to be associated with elevations in NT-proBNP.

Table 5.1. Baseline demographics in the SAS vs control cohorts

Characteristic	**Severe AS (n=90)**	**Control (n=75)**	**p-value**
Male sex- *n (%)*	42 (46.7)	38 (50.7)	0.61
Age- *yrs ± SD*	82.1 ± 5.7	80.6 ± 5.8	0.07
BMI*- *kg/m^2 ± SD*	27.9 ± 5.1	28.2 ± 5.3	0.55
Systolic BP*- *mmHg ± SD*	135.9 ± 21.0	135.3 ± 20.5	0.99
Right hand dominance- *n (%)*	87 (96.7)	70 (93.3)	0.47
Smoking history- *n (%)*	33 (36.7)	25 (33.3)	0.66
Hypertension- *n (%)*	58 (64.4)	53 (70.7)	0.40
Diabetes mellitus- *n (%)*	27 (30.0)	24 (32.0)	0.61
Hypercholesterolaemia- *n (%)*	61 (67.8)	53 (70.7)	0.68
Previous MI*- *n (%)*	12 (13.3)	12 (16.0)	0.63
Previous PCI*- *n (%)*	24 (26.7)	18 (24.0)	0.99
Previous CABG*- *n (%)*	11 (12.2)	2 (2.7)	0.10
NYHA* grade- *n (%)* • 1 • 2 • 3 • 4	 0 (0.0) 65 (72.2) 25 (27.8) 0 (0.0)	 74 (98.7) 1 (1.3) 0 (0.0) 0 (0.0)	**<0.001**
Previous stroke- *n (%)*	5 (5.6)	9 (12.0)	0.14
Atrial fibrillation- *n (%)*	26 (28.9)	29 (38.7)	0.19
CKD*- *n (%)*	53 (58.9)	30 (40.0)	**0.02**
COPD*- *n (%)*	8 (8.9)	6 (8.0)	0.84

LV* function- *n (%)* • Normal • Mild • Moderate • Severe	 69 (76.7) 6 (6.7) 8 (8.9) 7 (7.8)	 - - - -	-

**BMI=body mass index, BP=blood pressure, MI=myocardial infarction, PCI=percutaneous coronary intervention, CABG=coronary artery bypass grafting, NYHA=New York heart association, CKD=chronic kidney disease, COPD=chronic obstructive pulmonary disease, LV=left ventricular*

Table 5.2. Baseline blood results in the SAS vs control cohorts

Characteristic	**Severe AS (n=90)**	**Control (n=75)**	**p-value**
HbA1c- *mmol/mol ± SD*	44.6 ± 13.1	44.1 ± 10.4	0.48
Creatinine- *µmol/L ± SD*	102.5 ± 40.5	96.5 ± 49.0	0.08
Creatinine Clearance- *ml/min ± SD*	57.0 ± 20.3	67.1 ± 21.5	**<0.001**
Haemoglobin- *g/L ± SD*	125.6 ± 16.7	128.7 ± 15.0	0.33
NT-proBNP- *ng/L ± SD*	2545 ± 3564	1145 ± 2714	**<0.001**
Cholesterol- *mmol/L ± SD*	4.1 ± 1.1	3.5 ± 0.8	**<0.001**
Low Density Lipoprotein- *mmol/L ± SD*	2.1 ± 0.9	1.6 ± 0.7	**<0.001**
Plasma viscosity- *mPa.s ± SD*	1.75 ± 0.16	1.69 ± 0.07	**0.04**

There were differences in the baseline pharmacological therapies between both cohorts (see **Table 5.3**). Given the relative contraindications in the setting of severe AS, the use of both ACE inhibitors and calcium channel blockers was lower in the SAS cohort (16.7% vs 38.7%, **p=0.001** and 23.3% vs 38.7%, **p=0.03**; respectively). Both loop diuretic and P2Y12 inhibitor use was higher in the SAS cohort (48.9% vs 26.7%, **p=0.004** and 28.9% vs 10.7%, **p=0.004**; respectively). The impact of pharmacological therapies on conjunctival microvascular function will be discussed later in this chapter.

Table 5.3. Baseline pharmacological therapies in the SAS vs control cohorts

Medication	**Severe AS (n=90)**	**Control (n=75)**	**p-value**
Aspirin- *n (%)*	35 (38.9)	34 (45.3)	0.40
P2Y12 inhibitor- *n (%)*	26 (28.9)	8 (10.7)	**0.004**
Warfarin- *n (%)*	2 (2.2)	0 (0.0)	0.50
NOAC- *n (%)*	32 (35.6)	31 (41.3)	0.45
ACE inhibitor- *n (%)*	15 (16.7)	29 (38.7)	**0.001**
Angiotensin-2 receptor blocker- *n (%)*	14 (15.6)	15 (20.0)	0.46
Mineralocorticoid receptor antagonist- *n (%)*	3 (3.3)	1 (1.3)	0.63
SGLT2 inhibitor- *n (%)*	5 (5.6)	4 (5.3)	1.0
Beta blocker- *n (%)*	52 (57.8)	42 (56.0)	0.82
Calcium channel blocker- *n (%)*	21 (23.3)	29 (38.7)	**0.03**
Thiazide diuretic- *n (%)*	7 (7.8)	7 (9.3)	0.72
Loop diuretic- *n (%)*	44 (48.9)	20 (26.7)	**0.004**
Statin- *n (%)*	55 (61.1)	56 (74.7)	0.07

Conjunctival microvascular indices: Aortic stenosis vs controls

Videos of the temporal and nasal fields of each patient's bulbar conjunctiva were recorded. This generated a total of 4 videos per patient for subsequent conjunctival microvascular function analysis.

Quantitative analysis was possible in a total of 3387 conjunctival vessels across all patients (1853 SAS cohort vs 1534 control cohort). There were no differences between the SAS and control cohorts.in the mean number of vessels analysed (SAS 20.6 ± 15.6 vs control 20.5 ± 13.4, p=0.77), the number of arterioles analysed (SAS 3.9 ± 4.8 vs control 3.3 ± 3.0, p=0.78) or the number of venules analysed (SAS 14.9 ± 11.9 vs control 14.6 ± 11.0, p=0.99). Arterioles were not detected in the conjunctiva of all subjects (78/90 of the SAS cohort and 68/75 of the control cohort). Venules were detected in all subjects in the SAS cohort and 74/75 of subjects in the control cohort.

Conjunctival microvascular indices were obtained for all vessels and then results averaged in each patient in all vessels combined, in addition to the individual vessel sub-type (arterioles vs venules). **Table 5.4** demonstrates a comparison of conjunctival parameters between the SAS and control cohorts.

Table 5.4. Conjunctival microvascular indices in the SAS vs control cohorts

All vessels			
Parameter	**Severe AS (n=90)**	**Control (n=75)**	**p-value**
Diameter- *µm ± SD*	25.5 ± 3.6	25.3 ± 2.6	0.84
Axial velocity- *mm/s ± SD*	0.56 ± 0.06	0.56 ± 0.05	0.82
Cross-sectional velocity- *mm/s ± SD*	0.39 ± 0.04	0.39 ± 0.03	0.81
Blood flow rate- *pl/s ± SD*	218.9 ± 64.5	215.4 ± 48.9	0.70
Wall shear rate- s^{-1} *± SD*	139.0 ± 27.1	139.3 ± 24.7	0.97
Wall shear stress- *dynes/cm*^{2} *± SD*	6.7 ± 1.8	6.8 ± 1.8	0.92
Arterioles			
Parameter	**Severe AS (n=78)**	**Control (n=68)**	**p-value**
Diameter- *µm ± SD*	23.2 ± 6.2	23.2 ± 5.9	1.0
Axial velocity- *mm/s ± SD*	0.57 ± 0.11	0.58 ± 0.11	0.50
Cross-sectional velocity- *mm/s ± SD*	0.40 ± 0.08	0.41 ± 0.08	0.53
Blood flow rate- *pl/s ± SD*	186.3 ± 99.4	187.6 ± 98.3	0.95
Wall shear rate- s^{-1} *± SD*	160.8 ± 70.5	162.5 ± 62.7	0.55
Wall shear stress- *dynes/cm*^{2} *± SD*	7.9 ± 3.8	8.0 ± 3.7	0.56

Venules			
Parameter	**Severe AS (n=90)**	**Control (n=74)**	**p-value**
Diameter- *μm ± SD*	25.8 ± 3.9	26.0 ± 3.3	0.77
Axial velocity- *mm/s ± SD*	0.56 ± 0.07	0.56 ± 0.06	0.73
Cross-sectional velocity- *mm/s ± SD*	0.39 ± 0.05	0.39 ± 0.05	0.72
Blood flow rate- *pl/s ± SD*	225.1 ± 74.6	222.6 ± 55.3	0.79
Wall shear rate- s^{-1} ± *SD*	137.0 ± 30.3	135.6 ± 31.2	0.81
Wall shear stress- $dynes/cm^2$ ± *SD*	6.7 ± 1.9	6.7 ± 2.0	1.0

There was no difference in any measured parameter of conjunctival microvascular function between the SAS and control cohorts. This finding generated the following hypotheses:

1. There is no association between aortic stenosis and conjunctival microvascular dysfunction
2. Conjunctival microvascular dysfunction exists in a sub-group of patients with severe AS, but is not present in all patients
3. Conjunctival microvascular dysfunction exists in a proportion of the control patients due to their intrinsic characteristics or co-morbid conditions confounding the results (e.g. HFpEF which has been associated with both coronary and systemic microvascular dysfunction, thus confounding results)

4. Differences in baseline pharmacological therapies have influenced conjunctival microcirculatory function

Prior to accepting the 1st hypothesis that no between group difference existed. Statistical analysis was performed to address the other 3 hypotheses in an effort to examine the initial findings in more depth.

Correlation of conjunctival microvascular function parameters to demographics, co-existing medical conditions and pharmacological therapies

In the above analysis, vessel diameter was not correlated to V_a ($r_s(98)$= 0.049, p= 0.54) or V_{cs} ($r_s(98)$= -0.091, p= 0.25), but was strongly correlated to Q ($r_s(98)$= 0.872, **p<0.001**), WSR ($r_s(98)$= -0.771, **p<0.001**) and WSS ($r_s(98)$= -0.527, **p<0.001**).

Vessel diameter is largely influenced by the selected field of imaging and automated selection of vessels for analysis rather than reflecting microvascular function. Given the absence of an associated relationship between vessel diameter and velocity measurements, V_a or V_{cs} represent the best parameters to use to assess possible confounders.

Sex

There was a statistically significant correlation between sex and mean V_{cs} in aortic stenosis patient's arterioles ($r_{pb}(38)$= -0.341, **p= 0.002**), but not

venules ($r_{pb}(38)$= -0.130, p= 0.222). This correlation was not observed in the control cohort arterioles ($r_{pb}(38)$= 0.034, p= 0.78), or venules ($r_{pb}(38)$ = 0.056, p= 0.63). A comparison of arterioles in females to males with severe AS revealed significant reductions in D, V_a, V_{cs} and Q (see **Table 5.5**).

Table 5.5. Comparison of arteriole microvascular parameters (males vs females)

Parameter	**Male (no. of vessels=127)**	**Female (no. of vessels=219)**	**p-value**
Diameter- *μm ± SD*	25.7 ± 8.0	23.6 ± 9.0	**0.01**
Axial velocity- *mm/s ± SD*	0.61 ± 0.16	0.52 ± 0.16	**<0.001**
Cross-sectional velocity- *mm/s ± SD*	0.42 ± 0.11	0.37 ± 0.11	**<0.001**
Blood flow rate- *pl/s ± SD*	227.8 ± 132.9	176.1 ± 132.9	**<0.001**
Wall shear rate- s^{-1} *± SD*	153.4 ± 87.5	147.1 ± 85.6	0.31
Wall shear stress- *dynes/cm^2 ± SD*	7.1 ± 4.1	7.1 ± 4.6	0.45

A comparison of females in the SAS cohort to controls revealed significant reductions in both arteriole V_a and V_{cs} (see **Table 5.6**). This was driven by numerical reductions in V_a and V_{cs} in arterioles across all vessel diameter sub-groups (see **Table 5.7**). V_a and V_{cs} did not differ significantly in the individual diameter sub-groupings. However, this is reflective of the small

number of vessels in each sub-group, thereby rendering the analysis underpowered to detect a between group difference. There was no difference in any parameter in any vessel sub-group in males in the SAS cohort vs controls (see **Table 5.8**).

Table 5.6. Comparison of microvascular indices in the arterioles of females with severe aortic stenosis vs controls

All vessels			
Parameter	**Severe AS (n=48)**	**Control (n=36)**	**p-value**
Diameter- *µm ± SD*	24.9 ± 2.8	25.2 ± 2.5	0.59
Axial velocity- *mm/s ± SD*	0.55 ± 0.05	0.56 ± 0.04	0.29
Cross-sectional velocity- *mm/s ± SD*	0.38 ± 0.04	0.39 ± 0.03	0.34
Blood flow rate- *pl/s ± SD*	203.2 ± 46.0	208.2 ± 40.1	0.60
Wall shear rate- s^{-1} *± SD*	139.8 ± 24.4	139.7 ± 19.2	0.98
Wall shear stress- *dynes/cm²* ± *SD*	6.8 ± 2.0	6.5 ± 1.2	0.61
Arterioles			
Parameter	**Severe AS (n=41)**	**Control (n=33)**	**p-value**
Diameter- *µm ± SD*	23.1 ± 6.0	22.4 ± 4.9	0.59
Axial velocity- *mm/s ± SD*	0.53 ± 0.11	0.59 ± 0.12	**0.047**
Cross-sectional velocity- *mm/s ± SD*	0.38 ± 0.07	0.41 ± 0.08	**0.043**
Blood flow rate- *pl/s ± SD*	177.6 ± 93.1	176.2 ± 89.0	0.85
Wall shear rate- s^{-1} *± SD*	150.8 ± 60.5	165.1 ± 52.0	0.15
Wall shear stress- *dynes/cm²* ± *SD*	7.4 ± 3.7	7.6 ± 2.4	0.32

Venules			
Parameter	**Severe AS (n=48)**	**Control (n=37)**	**p-value**
Diameter- *μm ± SD*	25.5 ± 3.3	25.7 ± 3.8	0.76
Axial velocity- *mm/s ± SD*	0.55 ± 0.06	0.56 ± 0.06	0.50
Cross-sectional velocity- *mm/s ± SD*	0.38 ± 0.04	0.39 ± 0.04	0.52
Blood flow rate- *pl/s ± SD*	216.4 ± 63.1	218.0 ± 56.6	0.91
Wall shear rate- s^{-1} *± SD*	137.2 ± 22.9	137.7 ± 27.9	0.93
Wall shear stress- *dynes/cm*^{2} *± SD*	6.7 ± 2.0	6.4 ± 1.6	0.75

Table 5.7. Comparison of microvascular parameters in arterioles of females with severe aortic stenosis vs controls divided by vessel diameter sub-groups

Arterioles ≤ 15 µm			
Parameter	**Severe AS (no. of vessels= 45)**	**Control (no. of vessels= 20)**	**p-value**
Diameter- *µm ± SD*	12.5 ± 1.6	12.4 ± 1.9	0.86
Axial velocity- *mm/s ± SD*	0.51 ± 0.17	0.54 ± 0.17	0.48
Cross-sectional velocity- *mm/s ± SD*	0.39 ± 0.13	0.41 ± 0.12	0.49
Blood flow rate- *pl/s ± SD*	47.7 ± 17.6	51.9 ± 23.9	0.43
Wall shear rate- s^{-1} *± SD*	255.9 ± 100.1	270.5 ± 82.4	0.57
Wall shear stress- $dynes/cm^2$ *± SD*	12.1 ± 5.9	12.8 ± 3.5	0.63
Arterioles 15 – 30 µm			
Parameter	**Severe AS (no. of vessels= 120)**	**Control (no. of vessels= 103)**	**p-value**
Diameter- *µm ± SD*	22.3 ± 4.5	23.4 ± 4.2	0.06
Axial velocity- *mm/s ± SD*	0.51 ± 0.16	0.55 ± 0.15	0.11
Cross-sectional velocity- *mm/s ± SD*	0.36 ± 0.11	0.38 ± 0.10	0.16
Blood flow rate- *pl/s ± SD*	144.8 ± 72.3	168.0 ± 71.9	**0.01**

Wall shear rate- *s^{-1} ± SD*	135.3 ± 53.5	134.5 ± 47.2	0.73
Wall shear stress- *dynes/cm^2 ± SD*	6.6 ± 3.2	6.2 ± 2.2	0.97
Arterioles > 30 µm			
Parameter	**Severe AS (no. of vessels= 54)**	**Control (no. of vessels= 15)**	**p-value**
Diameter- *µm ± SD*	35.8 ± 5.4	34.1 ± 3.6	0.30
Axial velocity- *mm/s ± SD*	0.54 ± 0.16	0.58 ± 0.19	0.35
Cross-sectional velocity- *mm/s ± SD*	0.36 ± 0.11	0.39 ± 0.12	0.34
Blood flow rate- *pl/s ± SD*	352.5 ± 112.7	363.7 ± 153.7	0.76
Wall shear rate- *s^{-1} ± SD*	82.8 ± 27.7	91.7 ± 29.9	0.28
Wall shear stress- *dynes/cm^2 ± SD*	4.0 ± 1.6	4.4 ± 1.4	0.39

Table 5.8. Comparison of microvascular parameters in males with severe aortic stenosis vs controls

All vessels			
Parameter	**Severe AS (n=42)**	**Control (n=38)**	**p-value**
Diameter- *μm ± SD*	26.3 ± 4.2	25.7 ± 2.7	0.44
Axial velocity- *mm/s ± SD*	0.58 ± 0.06	0.56 ± 0.06	0.21
Cross-sectional velocity- *mm/s ± SD*	0.40 ± 0.04	0.39 ± 0.04	0.27
Blood flow rate- *pl/s ± SD*	236.9 ± 77.4	222.4 ± 55.9	0.35
Wall shear rate- s^{-1} *± SD*	138.0 ± 30.2	139.0 ± 29.4	0.95
Wall shear stress- *dynes/cm*^{2} *± SD*	6.7 ± 1.6	7.2 ± 2.2	0.50
Arterioles			
Parameter	**Severe AS (n=37)**	**Control (n=35)**	**p-value**
Diameter- *μm ± SD*	23.3 ± 6.5	23.9 ± 6.6	0.68
Axial velocity- *mm/s ± SD*	0.61 ± 0.11	0.58 ± 0.10	0.19
Cross-sectional velocity- *mm/s ± SD*	0.43 ± 0.08	0.41 ± 0.07	0.20
Blood flow rate- *pl/s ± SD*	196.1 ± 106.5	198.4 ± 106.5	0.95
Wall shear rate- s^{-1} *± SD*	171.8 ± 79.6	160.1 ± 72.0	0.63

Wall shear stress- *dynes/cm^2* ± *SD*	8.4 ± 4.0	8.3 ± 4.6	0.88
Venules			
Parameter	**Severe AS (n=42)**	**Control (n=38)**	**p-value**
Diameter- *μm* ± *SD*	26.2 ± 4.5	26.2 ± 2.8	0.97
Axial velocity- *mm/s* ± *SD*	0.57 ± 0.08	0.56 ± 0.07	0.31
Cross-sectional velocity- *mm/s* ± *SD*	0.40 ± 0.05	0.38 ± 0.05	0.33
Blood flow rate- *pl/s* ± *SD*	235.0 ± 85.6	227.0 ± 54.4	0.62
Wall shear rate- *s^{-1}* ± *SD*	136.8 ± 37.3	133.6 ± 34.3	0.76
Wall shear stress- *dynes/cm^2* ± *SD*	6.7 ± 1.8	6.9 ± 2.3	0.56

There was no statistically significant difference in baseline demographics or in the echocardiographically and invasively defined severity of AS comparing males to females that would clearly account for the significant sex-specific differences in conjunctival microvascular function (see **Table 5.9**).

Table 5.9. Comparison of baseline demographics and echocardiographic/invasive assessment of aortic stenosis severity (males vs females)

Baseline Demographics			
Characteristic	**Male (n=42)**	**Female (n=48)**	**p-value**
Age- *yrs ± SD*	82.5 ± 6.2	81.7 ± 5.3	0.41
BMI*- *kg/m^2 ± SD*	28.1 ± 4.9	27.8 ± 5.4	0.63
Systolic BP*- *mmHg ± SD*	132.2 ± 17.3	139.1 ± 23.5	0.12
Smoking history- *n (%)*	19 (45.2)	14 (29.2)	0.11
Hypertension- *n (%)*	26 (61.9)	32 (66.7)	0.64
Diabetes mellitus- *n (%)*	16 (38.1)	11 (22.9)	0.21
Hypercholesterolaemia- *n (%)*	25 (59.5)	36 (75.0)	0.12
Previous MI*- *n (%)*	10 (23.8)	2 (4.2)	**0.006**
Previous PCI*- *n (%)*	13 (31.0)	11 (22.9)	0.39
Previous CABG*- *n (%)*	7 (16.7)	4 (8.4)	0.49
NYHA* grade- *n (%)* • 1 • 2 • 3 • 4	 0 (0.0) 27 (64.3) 15 (35.7) 0 (0.0)	 0 (0.0) 38 (79.2) 10 (20.8) 0 (0.0)	0.12
Previous stroke- *n (%)*	3 (7.1)	2 (4.2)	0.66
CKD*- *n (%)*	23 (54.8)	30 (62.5)	0.46

COPD*- *n (%)*	2 (4.8)	6 (12.5)	0.28
Echocardiographic			
Peak velocity- *m/s ± SD*	4.3 ± 0.7	4.4 ± 0.5	0.17
VTI* ratio ± SD	0.21 ± 0.05	0.22 ± 0.06	0.31
Peak gradient- *mmHg ± SD*	76.2 ± 25.4	79.6 ± 20.5	0.17
Mean gradient- *mmHg ± SD*	44.8 ± 16.0	46.4 ± 13.0	0.28
LV* function- *n (%)* • Normal • Mild • Moderate • Severe	 30 (71.4) 3 (7.1) 5 (11.9) 4 (9.5)	 39 (81.3) 3 (6.3) 3 (6.3) 3 (6.3)	0.70
QRS duration- *ms ± SD*	114.5 ± 29.5	104.9 ± 24.3	0.08
Invasive			
Peak to peak gradient- *mmHg ± SD*	41.4 ± 18.6	45.6 ± 19.6	0.37
Mean gradient- *mmHg ± SD*	42.7 ± 14.9	44.0 ± 14.1	0.68
LVEDP*- *mmHg ± SD*	19.3 ± 8.7	20.5 ± 8.3	0.30

**BMI=body mass index, BP=blood pressure, MI=myocardial infarction, PCI=percutaneous coronary intervention, CABG=coronary artery bypass grafting, NYHA=New York heart association, CKD=chronic kidney disease, COPD=chronic obstructive pulmonary disease, LV=left ventricular, VTI=velocity-time integral, LVEDP=left ventricular end diastolic pressure*

Age

There was no statistically significant correlation between age and mean V_{cs} in the SAS cohort arterioles ($r_s(38)= 0.010$, $p= 0.93$) or venules ($r_s(38)= -0.064$, $p= 0.55$). There was no statistically significant correlation between age and mean V_{cs} in control patient's arterioles ($r_s(38)= -0.157$, $p= 0.20$),

but there was a weak correlation between age and mean V_{cs} in control patient's venules ($r_s(38)$= -0.295, **p= 0.01**).

Abnormalities in blood results

There was no statistically significant correlation between NT-proBNP, creatinine clearance or plasma viscosity and mean V_{cs} in control patient's arterioles (NT-proBNP $r_s(98)$= -0.057, p=0.70; creatinine clearance $r_s(98)$= 0.052, p=0.67; plasma viscosity $r_s(98)$= -0.107, p=0.39) or venules (NT-proBNP $r_s(98)$= 0.096, p=0.49; creatine clearance $r_s(98)$= -0.032, p=0.79; plasma viscosity $r_s(98)$= 0.075, p=0.53).

Co-morbidities

Established atherosclerotic cardiovascular disease was defined as any patient with a history of CAD, stroke, TIA or peripheral vascular disease. There were 44/90 patients in the SAS cohort and 27/75 patients with established CVD. The presence of CVD did not result in a significant difference in V_{cs} in arterioles or venules in either the SAS or control cohorts (SAS arterioles 0.40 ± 0.08 mm/s vs 0.40 ± 0.08 mm/s, p= 0.87; SAS venules 0.39 ± 0.05 mm/s vs 0.39 ± 0.04 mm/s, p= 0.46; control arterioles 0.42 ± 0.08 mm/s vs 0.41 ± 0.07 mm/s, p=0.48; control venules 0.39 ± 0.06 mm/s vs 0.38 ± 0.04 mm/s, p=0.49).

In the control cohort there was no statistically significant difference in either arteriole or venule V_{cs} comparing patients with and without a history of smoking, diabetes mellitus, hypertension or chronic kidney disease

(**Figure 5.1**). As discussed above creatinine clearance also did not correlate with V_{cs} in the control cohort to suggest a relationship with renal function and conjunctival microvascular function.

Figure 5.1. Comparison of the impact of potentially confounding co-morbidities on arteriole cross-sectional velocity in the control cohort

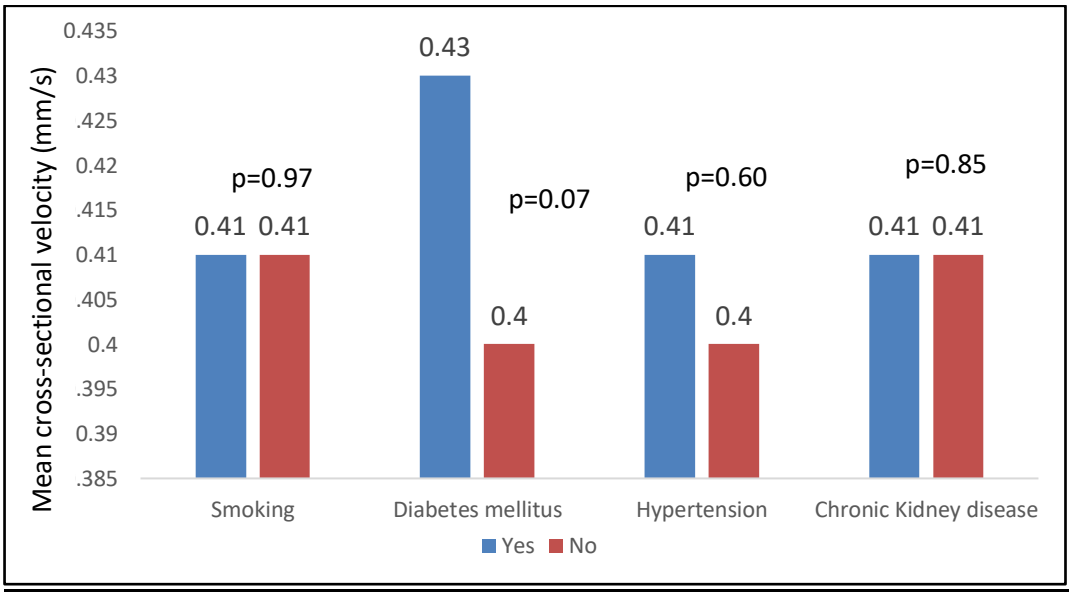

Left ventricular function and aortic valve haemodynamics

In the SAS cohort there was no correlation with mean arteriolar V_{cs} and left ventricular ejection fraction ($r_s(38)= -0.049$, $p= 0.67$), aortic valve peak gradient ($r_s(38)= 0.005$, $p= 0.97$) or left ventricular end diastolic pressure ($r_s(38)= -0.0113$, $p= 0.33$).

HFpEF

As discussed above mean NT-proBNP in the control cohort was abnormal. In the setting of normal LV systolic function, this suggested the possibility that some of the control cohort had undiagnosed HFpEF. HFpEF is

associated with both coronary and systemic microvascular dysfunction. In order to assess for confounding, arteriole haemodynamics were compared in control subjects with and without an elevation in NT-proBNP ≥500ng/L. There was no difference in vessel diameter (p=0.93), V_a (p=0.93), V_{cs} (p=0.91), Q (p=0.72), WSR (p=0.86) or WSS (p=0.67). As presented above, NT-proBNP also did not correlate with V_{cs}.

Medications

In the control cohort there was no correlation between arteriolar V_{cs} and the use of P2Y12 inhibitors ($r_{pb}(38)= 0.015$, p= 0.90), ACE inhibitors ($r_{pb}(38)= -0.060$, p= 0.63), calcium channel blockers ($r_{pb}(38)= 0.108$, p= 0.38) or loop diuretics ($r_{pb}(38)= -0.098$, p= 0.43). These medications were chosen for analysis as their use differed significantly between the SAS and control cohorts.

The influence of the eye and field of view on parameters of microvascular function

Microvascular parameters were not influenced by the eye that was imaged across the entire patient group (see **Table 5.10**). However, the field of view did significantly impact haemodynamics with a reduction in the diameter of vessels in the nasal field and a reduction in V_a, V_{cs}, WSR and WSS in the temporal field (see **Table 5.11**). A comparison of microvascular indices in the SAS vs control cohorts, revealed no between group differences when comparing the left and right temporal and nasal fields in isolation (see **Table 5.12**).

Table 5.10. Conjunctival microvascular parameters based on the eye imaged

Parameter	**Left eye (n=1521)**	**Right eye (n=1866)**	**p-value**
Diameter- *μm ± SD*	25.5 ± 8.5	25.4 ± 8.3	0.94
Axial velocity- *mm/s ± SD*	0.55 ± 0.16	0.56 ± 0.15	0.39
Cross-sectional velocity- *mm/s ± SD*	0.38 ± 0.11	0.38 ± 0.10	0.45
Blood flow rate- *pl/s ± SD*	215.0 ± 157.4	215.5 ± 161.3	0.63
Wall shear rate- s^{-1} ± *SD*	137.3 ± 70.2	137.7 ± 69.6	0.78
Wall shear stress- *dynes/cm*^{2} ± *SD*	6.6 ± 3.7	6.7 ± 3.5	0.11

Table 5.11. Conjunctival microvascular parameters based on nasal vs temporal field of view

Parameter	**Nasal (n=1466)**	**Temporal (n=1921)**	**p-value**
Diameter- *μm ± SD*	24.8 ± 8.4	26.0 ± 8.4	**<0.001**
Axial velocity- *mm/s ± SD*	0.57 ± 0.15	0.54 ± 0.15	**<0.001**
Cross-sectional velocity- *mm/s ± SD*	0.40 ± 0.11	0.37 ± 0.10	**<0.001**
Blood flow rate- *pl/s ± SD*	211.9 ± 157.8	217.8 ± 160.9	0.08
Wall shear rate- s^{-1} *± SD*	146.0 ± 72.7	131.1 ± 67.0	**<0.001**
Wall shear stress- *dynes/cm*^{2} *± SD*	7.1 ± 3.8	6.3 ± 3.4	**<0.001**

Table 5.12. Comparison of isolated field of view conjunctival microvascular parameters in the SAS vs control cohorts

Parameter	**Severe AS**	**Control**	**p-value**
Left Nasal	**No. of vessels= 408**	**No. of vessels= 297**	
Diameter- *μm ± SD*	25.0 ± 8.9	24.7 ± 8.7	0.60
Axial velocity- *mm/s ± SD*	0.58 ± 0.17	0.56 ± 0.15	0.08
Cross-sectional velocity- *mm/s ± SD*	0.40 ± 0.11	0.39 ± 0.10	0.09
Blood flow rate- *pl/s ± SD*	224.1 ± 176.0	207.1 ± 159.4	0.27
Wall shear rate- s^{-1} ± *SD*	147.3 ± 75.3	143.6 ± 70.8	0.61
Wall shear stress- $dynes/cm^2$ ± *SD*	7.1 ± 4.2	7.0 ± 3.7	0.82
Left Temporal	**No. of vessels= 489**	**No. of vessels= 327**	
Diameter- *μm ± SD*	26.2 ± 8.4	25.7 ± 8.0	0.54
Axial velocity- *mm/s ± SD*	0.54 ± 0.16	0.54 ± 0.15	0.71
Cross-sectional velocity- *mm/s ± SD*	0.37 ± 0.11	0.37 ± 0.10	0.65
Blood flow rate- *pl/s ± SD*	215.3 ± 150.6	210.1 ± 140.4	0.82
Wall shear rate- s^{-1} ± *SD*	128.5 ± 64.9	132.1 ± 69.1	0.50

Wall shear stress- *dynes/cm^2 ± SD*	6.1 ± 3.3	6.5 ± 3.6	0.08
Right Nasal	**No. of vessels= 387**	**No. of vessels= 374**	
Diameter- *µm ± SD*	24.4 ± 7.9	24.8 ± 8.0	0.42
Axial velocity- *mm/s ± SD*	0.58 ± 0.16	0.56 ± 0.14	0.22
Cross-sectional velocity- *mm/s ± SD*	0.40 ± 0.11	0.39 ± 0.10	0.17
Blood flow rate- *pl/s ± SD*	205.1 ± 137.9	209.6 ± 154.6	0.79
Wall shear rate- *s^{-1} ± SD*	149.6 ± 73.4	142.7 ± 70.6	0.15
Wall shear stress- *dynes/cm^2 ± SD*	7.2 ± 3.5	7.0 ± 3.9	0.14
Right Temporal	**No. of vessels= 569**	**No. of vessels= 536**	
Diameter- *µm ± SD*	25.9 ± 8.6	26.1 ± 8.3	0.87
Axial velocity- *mm/s ± SD*	0.54 ± 0.15	0.55 ± 0.14	0.12
Cross-sectional velocity- *mm/s ± SD*	0.37 ± 0.10	0.38 ± 0.09	0.31
Blood flow rate- *pl/s ± SD*	219.1 ± 167.1	223.5 ± 174.7	0.40
Wall shear rate- *s^{-1} ± SD*	132.3 ± 68.9	131.5 ± 65.5	0.71
Wall shear stress- *dynes/cm^2 ± SD*	6.4 ± 3.4	6.4 ± 3.3	0.64

The immediate haemodynamic impact of transcatheter aortic valve implantation on conjunctival microvascular function

All patients included in the SAS cohort underwent successful TAVI for the treatment of their valvular heart disease. No patients had haemodynamically significant aortic regurgitation by fluoroscopic or echocardiographic assessment of valve function. No patients required further valvular intervention during their index hospital admission.

Mean post-TAVI aortic valve peak velocity was 2.1 ± 0.5 m/s, velocity-time integral (VTI) ratio was 0.62 ± 0.17, peak gradient was 17.9 ± 8.2 mmHg, mean gradient was 9.7 ± 5.0 mmHg, valve area was 1.7 ± 0.6 cm^2, invasive peak gradient was 2.7 ± 1.8 mmHg, invasive mean gradient was 2.8 ± 2.6 mmHg and left ventricular end diastolic pressure (LVEDP) was 15.1 ± 7.1 mmHg.

Quantitative conjunctival microvascular analysis was performed in a total of 1945 vessels following TAVI (293 arterioles and 1505 venules). The mean number of vessels analysed per patient was 21.6 ± 11.7 (3.4 ± 3.7 arterioles and 16.6 ± 10.6 venules).

The mean changes in conjunctival parameters were calculated in both arterioles and venules for each patient post-TAVI. In arterioles the mean change in D was -0.39 ± 9.08 µm, V_a was 0.04 ± 0.15 mm/s, V_{cs} was 0.03 ± 0.11 mm/s, Q was 11.5 ± 165.2 pl/s, WSR was 26.9 ± 112.1 s^{-1} and WSS was 0.15 ± 5.16 dynes/cm^2. In venules mean change in D was 0.81

± 4.29 µm, V_a was -0.008 ± 0.08 mm/s, V_{cs} was -0.007 ± 0.06 mm/s, Q was 7.48 ± 80.1 pl/s, WSR was -7.21 ± 34.8 s^{-1} and WSS was -1.10 ± 1.87 dynes/cm^2.

Mean V_a, V_{cs} and WSR significantly increased in conjunctival arterioles post-TAVI. Conversely WSS in all vessels combined was reduced post-TAVI, being driven by a significant reduction in WSS in venules, but not arterioles (see **Table 5.13**)

Table 5.13. Comparison of conjunctival microvascular parameters in patients pre- and post-TAVI

All vessels			
Parameter	**Pre-TAVI (n=90)**	**Post-TAVI (n=90)**	**p-value**
Diameter- *μm ± SD*	25.5 ± 3.6	25.9 ± 3.4	0.43
Axial velocity- *mm/s ± SD*	0.56 ± 0.06	0.56 ± 0.05	0.83
Cross-sectional velocity- *mm/s ± SD*	0.39 ± 0.04	0.39 ± 0.04	0.88
Blood flow rate- *pl/s ± SD*	218.9 ± 64.5	225.2 ± 62.3	0.69
Wall shear rate- s^{-1} ± *SD*	139.0 ± 27.1	138.3 ± 26.5	0.63
Wall shear stress- *dynes/cm^2 ± SD*	6.7 ± 1.8	5.9 ± 1.4	**<0.001**
Arterioles			
Parameter	**Pre-TAVI (n=78)**	**Post-TAVI (n=78)**	**p-value**
Diameter- *μm ± SD*	23.2 ± 6.2	22.2 ± 7.3	0.39
Axial velocity- *mm/s ± SD*	0.57 ± 0.11	0.62 ± 0.12	**0.005**
Cross-sectional velocity- *mm/s ± SD*	0.40 ± 0.08	0.44 ± 0.08	**0.002**
Blood flow rate- *pl/s ± SD*	186.3 ± 99.4	190.7 ± 125.7	0.74
Wall shear rate- s^{-1} ± *SD*	160.8 ± 70.5	194.3 ± 94.2	**0.02**
Wall shear stress- *dynes/cm^2 ± SD*	7.9 ± 3.8	8.4 ± 4.0	0.50

Venules			
Parameter	**Pre-TAVI (n=90)**	**Post-TAVI (n=90)**	**p-value**
Diameter- *μm ± SD*	25.8 ± 3.9	26.6 ± 3.5	0.14
Axial velocity- *mm/s ± SD*	0.56 ± 0.07	0.55 ± 0.06	0.42
Cross-sectional velocity- *mm/s ± SD*	0.39 ± 0.05	0.38 ± 0.04	0.29
Blood flow rate- *pl/s ± SD*	225.1 ± 74.6	232.5 ± 63.5	0.39
Wall shear rate- s^{-1} ± *SD*	137.0 ± 30.3	129.8 ± 26.2	0.07
Wall shear stress- *dynes/cm^2 ± SD*	6.7 ± 1.9	5.6 ± 1.3	**<0.001**

The increases in conjunctival V_a, V_{cs} and WSR seen in arterioles post-TAVI were once again sex specific, with highly significant changes seen in the arterioles of females, but not males (see **Table 5.14**). The reduction in venular WSS occurred independently of sex (males 6.4 to 5.4 dynes/cm^2, p <0.001 and females 6.5 to 5.8 dynes/cm^2, p <0.001). A reduction in mean arteriole Q in males was statistically significant, but this occurred with a reduction in vessel diameter. There was no change in V_a or V_{cs} in male arterioles, and an analysis of grouped arterioles revealed no difference in Q when standardising diameter.

Table 5.14. Comparison of conjunctival microvascular parameters in arterioles of patients pre- and post-TAVI sub-divided by sex

Males			
Parameter	**Pre-TAVI (n=127)**	**Post-TAVI (n=121)**	**p-value**
Diameter- *µm ± SD*	25.7 ± 8.0	22.7 ± 7.5	**0.002**
Axial velocity- *mm/s ± SD*	0.61 ± 0.16	0.60 ± 0.16	0.59
Cross-sectional velocity- *mm/s ± SD*	0.42 ± 0.11	0.42 ± 0.11	0.88
Blood flow rate- *pl/s ± SD*	227.8 ± 132.9	188.1 ± 136.6	**0.006**
Wall shear rate- s^{-1} *± SD*	153.4 ± 87.5	170.5 ± 86.3	0.06
Wall shear stress- *dynes/cm²* ± *SD*	7.1 ± 4.1	7.8 ± 4.1	0.12
Females			
Parameter	**Pre-TAVI (n=219)**	**Post-TAVI (n=172)**	**p-value**
Diameter- *µm ± SD*	23.6 ± 9.0	23.2 ± 8.6	0.80
Axial velocity- *mm/s ± SD*	0.52 ± 0.16	0.59 ± 0.15	**<0.001**
Cross-sectional velocity- *mm/s ± SD*	0.37 ± 0.11	0.42 ± 0.11	**<0.001**
Blood flow rate- *pl/s ± SD*	176.1 ± 132.9	189.3 ± 128.3	0.15
Wall shear rate- s^{-1} *± SD*	147.1 ± 85.6	176.3 ± 116.0	**0.007**
Wall shear stress- *dynes/cm²* ± *SD*	7.1 ± 4.6	7.3 ± 5.1	0.67

DISCUSSION

This study demonstrates sex-specific differences in conjunctival microvascular function in a group of patients with aortic stenosis in comparison to an age- and sex-matched cohort of controls. Similar to the previously reported cohort of patients with coronary microvascular dysfunction, the haemodynamic alterations were most prominent in conjunctival arterioles. Reductions in arteriole V_a and V_{cs} were observed in females with severe aortic stenosis in comparison to controls without haemodynamically significant valvular heart disease. These microvascular alterations appear to be independent of any between-group differences in baseline demographics, co-morbidities, pharmacological therapies or left ventricular function. Following treatment of aortic stenosis with TAVI, significant increases in conjunctival arteriole V_a, V_{cs} and WSR were observed. This finding however was only seen in the female subjects of this study.

Previous studies have highlighted an association between aortic stenosis and coronary microvascular dysfunction, in addition to immediate improvements in invasive measures of microvascular function (CFR and IMR) following TAVI (Rajappan et al, 2003, Hildick-Smith et al, 2000 & McConkey et al, 2019). CFR and IMR are both calculated using standardised thermodilution techniques to assess mean coronary transit time and hence coronary blood flow velocity and rate (Fearon et al, 2017). Increases in mean transit time and hence decreases in hyperaemic blood flow velocity denote impairment in coronary function at a microvascular

level. The reductions in conjunctival arteriole V_a and V_{cs} seen in the severe aortic stenosis population of this study and increases seen following TAVI, therefore correlate to literature associating coronary microvascular dysfunction with aortic stenosis and improvements in indices of microvascular function following treatment. To the best of our knowledge, this is the first study to demonstrate non-invasive evidence of systemic microvascular dysfunction in any sub-group of patients with aortic stenosis or for that matter any form of valvular heart disease.

The sex-specific differences in microvascular function observed in this study are hypothesis generating. Differences between males and females with respect to both the prevalence and clinical outcomes in cardiovascular disease are well reported (Mosca et al, 2011). There is an extensive evidence base that untreated severe aortic stenosis has an adverse prognosis independent of sex. However, studies have reported worse outcomes for females undergoing SAVR in comparison with males. Conversely, women appear to have better outcomes than males undergoing TAVI (Caponcello et al, 2020). The clinical explanations for this are not clear. Possible explanations include; unconscious selection bias within the healthcare system, sex specific anatomical variations and also sex-specific differences in the pathophysiological manifestations of this cardiovascular disease.

There is evidence suggesting a lower burden of epicardial atherosclerotic disease in age-matched females than males (Taqueti et al, 2018),

however the prognosis of cardiovascular disease in females is worse (Coutinho et al, 2018). The incidence of coronary microvascular dysfunction has been consistently shown to be higher in females presenting with ischaemia and non-obstructive coronary arteries (INOCA) (Mileva et al, 2022). CMD is prognostically adverse, and it has been proposed that sex differences in coronary microvascular function are due to females having smaller coronary arteries (Hiteshi et al, 2014) and higher blood flow than males (Gould et al, 2013). This difference in turn leads to greater endothelial shear stress, creating detrimental effects on coronary anatomy and function (Patel et al, 2016).

Hypertension has been linked to microvascular dysfunction due to resulting decreases in arterial compliance (Mitchell, 2014). Lower arterial compliance has in turn been associated with altered coronary microvascular function in females, but not in males (Coutinho et al, 2018). Similar to hypertension, aortic stenosis increases left ventricular afterload, and therefore theoretically produces similar reductions in arterial compliance, and therefore may have similar sex differences with respect to microvascular function.

LIMITATIONS

The target population over the study period were patients' undergoing TAVI as opposed to SAVR for the treatment of severe aortic stenosis. Therefore, the patients were older, with a mean age >80 years. This is in keeping with the established evidence base for this treatment modality.

This may limit the conclusions that can be drawn with respect to microvascular alterations in a younger population. However, age did not correlate with the measured parameters arguing against the findings being different in a younger cohort.

Ideally the same conjunctival vessels in each individual would be chosen for analysis both pre- and post-TAVI, however the imaging platform and software utilised in this study is semi-automated and does not allow for individual vessel selection. The changes in haemodynamics were therefore averaged for each patient, as opposed to reporting the exact change in each individual vessel. This study is therefore limited by the conjunctival imaging platform's inability to identify the same conjunctival vessels for analysis both pre- and post-TAVI.

The prevalence of co-morbidities was high in each cohort, thereby potentially confounding results, in addition to increasing the number of patients on pre-dating pharmacological therapies for the treatment of these co-morbid conditions that may potentially impact microvascular function. However, evaluating these factors in control subjects, there did not appear to be a significant impact on conjunctival microvascular function, and this is therefore unlikely to confound results.

Atrial fibrillation (AF) was prevalent in the entire cohort (38.7%) and no specific adjustments in microvascular measurements were made in these

patients. There is significant beat to beat variation in stroke volume in AF, which in theory could impact the results obtained.

The primary hypothesis of between group differences in systemic microvascular function in patients with severe AS compared to controls was negative. The observation of sex-specific differences in microvascular parameters in this population whilst hypothesis generating must be taken with caution given that this was merely a sub-group analysis of this study.

CONCLUSION

Evidence of conjunctival microvascular dysfunction was demonstrated non-invasively in females with severe aortic stenosis. Following treatment of aortic stenosis with TAVI, significant alterations in conjunctival microvascular function were observed in this sub-group. Following TAVI, indices of conjunctival microvascular function were in fact comparable to the control cohort, suggesting early improvements in systemic microvascular function following treatment of aortic stenosis in this population. These findings are consistent with current literature suggesting both an association between aortic stenosis and coronary microvascular dysfunction; and improvements in microvascular function following aortic valve intervention.

Chapter 6

Project summary and future developments

Project summary

The objectives of this thesis as presented in the previous chapters were as follows:

- To refine the methodology of this modality of conjunctival microvascular assessment, including the development of techniques for vessel differentiation.
- To compare the conjunctival microcirculation in a cohort of patients with a myocardial infarction, to a cohort of controls with no physiologically significant epicardial coronary disease or personal history of major adverse cardiovascular event.
- To compare the conjunctival microcirculation in a cohort of patients with angina, no obstructive epicardial coronary artery disease and evidence of coronary microvascular dysfunction demonstrated by a positive invasive physiological assessment of coronary microvascular function to a cohort of controls with no physiologically significant epicardial or microvascular disease.
- To compare the conjunctival microcirculation in a cohort of patients with severe aortic stenosis to a cohort of control subjects with no haemodynamically significant valvular heart disease.
- To evaluate the impact of transcatheter aortic valve implantation (TAVI) for the treatment of severe aortic stenosis on conjunctival microcirculatory function.

This chapter summarises the results of the experimental chapters of this thesis and therefore defines the achievement of these objectives.

Refinement of non-invasive conjunctival microvascular imaging

Alterations in parameters of conjunctival microcirculatory function have been reported in association with diabetes mellitus (Cheung et al, 1999 & Khansari et al, 2017), sickle cell disease (Kord Valeshabad et al, 2015), stroke (Kord Valeshabad et al, 2015), pregnancy (Moka et al, 2019), myocardial infarction (Brennan et al, 2021 & Awuah et al, 2022) and cyanotic congenital heart disease (Brennan et al, 2021). Reductions in conjunctival vessel axial velocity has also been correlated with CV risk (Karanam et al, 2019). These findings suggest that these conditions are associated with microvascular dysfunction at a systemic level. Microvascular dysfunction has been shown to confer an adverse long-term CV prognosis and therefore conjunctival vascular imaging may have utility in the augmentation of conventional CV risk assessment in a similar manner to non-invasive imaging modalities such as CT cardiac calcium scoring.

In 2019, Brennan et al reported the first combination of a smartphone with slit-lamp biomicroscope to perform conjunctival vascular imaging. Chapter 2 of this thesis describes the refinement of this modality to improve both the imaging quality and enable differentiation of vessels into groups (arterioles and venules) for subsequent analysis. The smartphone used was upgraded in line with temporal technological developments from an

iPhone 6s to an iPhone 11pro. This improved the recordable resolution of videos from 1080 x 1920 pixels to 3840 x 2160 pixels. To enable quantification of conjunctival microvascular parameters, a pixel to millimetre conversion factor was calculated for this new platform using a calibration reticle. Conjunctival imaging was performed in all subjects in this study using a standard operating protocol described in chapter 2. Videos were processed using a semi-automated technique of sequence selection, stabilisation and estimation of vessel diameter and axial velocity based on the automated detection of erythrocyte motion. Other parameters of microvascular function were then calculated using previously defined formulae. Following the selection of vessels, blood flow direction in relation to vascular bifurcations was established to sub-categorise vessels into arterioles and venules.

Assessment of intra-observer variability for image processing and haemodynamic quantification suggested excellent repeatability across all parameters. Agreement between operators with respect to vessel differentiation was only moderate when comparing experienced and inexperienced operators, but this improved significantly when assessing agreement between two experienced operators. Therefore, in this study vessel differentiation was performed by a single operator experienced in vascular imaging.

Assessment of conjunctival microvascular parameters in patients with acute myocardial infarction in comparison to controls

Our research group previously demonstrated significant reductions in conjunctival axial velocity, blood flow and wall shear rate in patients with an acute myocardial infarction (MI), in comparison to a group of controls (Brennan et al, 2021). The control group in this preceding study were defined by conventional CV risk assessment tools. This group's true burden of coronary atherosclerosis was therefore unknown, potentially including subjects with a CV risk that was underestimated using this conventional assessment.

In chapter 3 of this thesis the MI cohort of this previous study were compared to a newly recruited group of subjects with non-obstructive coronary arteries defined both angiographically and physiologically using contemporary pressure wire evaluation of coronary stenosis severity (NO-CAD cohort). This new cohort of controls also had no established history of coronary artery disease, defined by the absence of a history of MI or percutaneous coronary intervention (PCI).

The primary hypothesis that alterations in microcirculatory parameters would be even more pronounced in the MI cohort compared to the NO-CAD cohort was confirmed. The results demonstrated marked reductions in axial/cross-sectional velocity, blood flow and wall shear rate in the MI cohort. The between-group differences met statistical significance across all vessel diameter sub-groupings and were numerically more significant

than the previous study of controls in whom coronary anatomy had not been established. Whilst significant, these differences are interpreted with caution given the comparison of stable and unstable coronary disease.

Assessment of conjunctival microvascular parameters in patients with coronary microvascular disease in comparison to controls

Chapter 4 describes a comparison of patients with invasive evidence of coronary microvascular dysfunction (CMD cohort) to a control cohort with normal indices of coronary microvascular function. Previous literature suggests an association between CMD and broader systemic microvascular dysfunction, but this remains to be definitely proven. All patients recruited to the cohorts described in this chapter underwent invasive coronary angiography and were included only if epicardial coronary arteries were angiographically and physiologically non-obstructive. The primary hypothesis was that the pathophysiological changes associated with CMD would be present in an alternative microvascular network, with resultant microvascular alterations in the conjunctiva. This represents the first description of conjunctival microcirculatory parameters in patients with CMD.

Reductions were observed in axial and cross-sectional velocity, wall shear rate and wall shear stress in the CMD cohort. Numerically the most marked differences in both axial and cross-sectional velocity were observed in conjunctival arterioles, mirroring the site of alterations in the coronary network. Blood flow rate was also significantly reduced in the

conjunctival arterioles of the CMD cohort. To standardise for between group differences in vessel diameter, a sub-analysis was performed in two distinct diameter sub-groups. In 10 - 25 μm and 25 – 40 μm arterioles, reductions were observed in V_a, V_{cs}, Q, WSR and WSS in the CMD cohort. A sub-group analysis of subjects without potentially confounding co-morbidities (coronary artery disease, diabetes mellitus, systemic hypertension and hypercholesterolaemia) revealed significant reductions in V_a, V_{cs}, WSR and WSS in the CMD cohort. This finding suggested that alterations in conjunctival microvascular function were strongly associated with CMD, rather than these potentially confounding co-morbidities.

Assessment of conjunctival microvascular parameters in patients with severe aortic stenosis in comparison to controls

Chapter 5 describes the assessment of conjunctival haemodynamics in patients with severe AS in comparison to a group of age- and sex-matched controls. No haemodynamics differences were observed in either arterioles or venules in the severe AS vs control groups. However, significant differences were observed in arteriole V_a, V_{cs} and Q comparing males to females with severe AS. The suggestion of sex-specific differences in microvascular parameters led to a sub-analysis of both males and females in isolation in comparison to controls. No differences were observed in males, but in females with severe AS, conjunctival arteriole V_a and V_{cs} were significantly reduced in comparison to controls. The numerical reductions in V_a and V_{cs} were observed in females with severe AS across all vessel diameter sub-groups, with statistically

significant reductions in blood flow rate in 15 – 30 μm arterioles. The severity of AS defined both invasively and echocardiographically was not different between males and females with severe AS, suggesting that the sex-specific differences in parameters of conjunctival microvascular function were not the result of differences in valvular heart disease severity.

Assessment of the impact of transcatheter aortic valve implantation on conjunctival microvascular function

All subjects in this study with severe AS underwent TAVI for the treatment of their valve disease. Between 6 and 24 hours following TAVI, repeat conjunctival imaging was performed to assess the immediate haemodynamic impact of relief of LVOT obstruction on the conjunctival microcirculation.

Comparison of all patients revealed increases in arteriole V_a, V_{cs} and WSR following TAVI, in addition to reductions in venular WSS. The reduction in venular WSS post-TAVI occurred independently of sex, but the increases in V_a, V_{cs} and WSR were sex-specific, occurring only in females following TAVI.

The results suggest that systemic microvascular dysfunction is associated with severe AS. However, similar to literature regarding the higher prevalence of coronary microvascular dysfunction in females, there appears to be an underlying pathophysiological mechanism that affects

microvascular function predominantly in females. Much like in INOCA, the mechanism for this is hypothesis generating, but not entirely clear.

In the original design of this study, a repeat conjunctival assessment at 6 to 12 weeks post-TAVI was planned, but given the emerging COVID-19 pandemic this was not possible. It is possible that further systemic microvascular remodelling occurs in the intermediate period following TAVI and the between group differences may have even become more pronounced.

Future technological developments

This study, in addition to previous work from our research group (Brennan et al, 2019, Brennan et al, 2021 & Awuah et al, 2022) have highlighted the ability for this microvascular imaging platform to assess conjunctival haemodynamics both in a safe and non-invasive manner. The haemodynamic differences observed in a variety of CV disorders suggest possible clinical utilities. However, this method of quantification of parameters of microcirculatory function using dedicated software requires ongoing refinement. The current process employed in this project requires manual user input for frame and subsequent vessel selection, in addition to a visual inspection of videos to allow vessel sub-grouping into arterioles and venules. This process is not only time consuming, but introduces inter-observer variability with respect to both the number and type of vessels that are selected for analysis. This variability whilst small influences the mean vessel haemodynamics per subject.

Further validation of conjunctival imaging for the diagnosis of microvascular dysfunction or the assessment of CV risk will require an increased number of study participants. Development of techniques to fully automate the process of post image acquisition processing are therefore key to reduce the human input required for video processing. If such a technique was found to be effective, automation of vessel analysis would be required prior to any institution in clinical practice. Conjunctival haemodynamics have been successfully quantified using an automated approach for both haemodynamic analysis and vessel sub-grouping in previous research (Khansari et al, 2016 and Meyer et al, 2018). Therefore, similar techniques could be employed for this imaging modality.

Future studies that would be of clinical interest in the evaluation of the utility of conjunctival microvascular haemodynamics as a modality of CV risk assessment could include; the correlation of conjunctival haemodynamics to conventional CV risk score calculators such as SCORE, Q-RISK 3 or ASSIGN; or correlation of CT coronary calcium scores in asymptomatic subjects.

Slit-lamp biomicroscopes are used for all routine optometry-based assessments. Previous studies have therefore utilised routine retinal imaging to provide large cohorts of patients to retrospectively identify microvascular anatomical features that may have the ability to differentiate CV risk (Rim et al, 2021). The aforementioned study carried the benefit of

having pre-existing banks of retinal photography with longitudinal follow-up of participants to enable retrospective development of a retinal CV risk score that was then validated using the data on these participants CV risk. Conjunctival imaging may have similar benefits and ideally would be validated in large populations of asymptomatic patients with follow-up periods of 5 to 10 years.

Conclusion

Alterations in conjunctival microvascular haemodynamics can be demonstrated non-invasively in a variety of distinct cardiovascular diseases. These findings suggest an association of myocardial infarction, coronary microvascular disease and severe aortic stenosis with systemic microvascular dysfunction. The conjunctival microvascular changes that occur are similar in all 3 disease states, implying that systemic microvascular dysfunction can be detected regardless of the underlying pathophysiological mechanism that produces dysfunction. Further research is required to determine if this novel imaging modality has a role in either the diagnosis of cardiovascular disease or the enhancement of conventional CV risk assessment.

Bibliography

Acacio I, Goldberg MF. Peripapillary and macular vessel occlusions in sickle cell anaemia. Am J Ophthalmol. 1973 May;75(5):861-6. doi: 10.1016/0002-9394(73)90892-1. PMID: 4706419.

Ahn JH, Kim SM, Park SJ, Jeong DS, Woo MA, Jung SH, Lee SC, Park SW, Choe YH, Park PW, Oh JK. Coronary Microvascular Dysfunction as a Mechanism of Angina in Severe AS: Prospective Adenosine-Stress CMR Study. J Am Coll Cardiol. 2016 Mar 29;67(12):1412-1422. doi: 10.1016/j.jacc.2016.01.013. PMID: 27012401.

Antonios TF, Kaski JC, Hasan KM, Brown SJ, Singer DR. Rarefaction of skin capillaries in patients with anginal chest pain and normal coronary arteriograms. Eur Heart J. 2001;22:1144-8.

Arima M, Majima T, Tsukamoto S, Hara T, Wada I, Nakao S, Sonoda KH. The utility of a new fundus camera using a portable slit-lamp combined with a smartphone. Acta Ophthalmol. 2019 Aug;97(5):e814-e816. doi: 10.1111/aos.14049. Epub 2019 Feb 14. PMID: 30767402; PMCID: PMC6767703.

Aronow WS. Recognition and management of aortic stenosis in the elderly. Geriatrics. 2007 Dec;62(12):23-32. PMID: 18069882.

Aziz A, Hansen HS, Sechtem U, Prescott E, Ong P. Sex-Related Differences in Vasomotor Function in Patients With Angina and Unobstructed Coronary Arteries. J Am Coll Cardiol 2017;70:2349- 2358.

Bachmann JM, Willis BL, Ayers CR, Khera A, Berry JD. Association between family history and coronary heart disease death across long-term follow-up in men: the Cooper Center Longitudinal Study. Circulation 2012;125:3092–3098

Bairey Merz CN, Pepine CJ, Walsh MN, Fleg JL. Ischemia and No Obstructive Coronary Artery Disease (INOCA): Developing Evidence-Based Therapies and Research Agenda for the Next Decade. Circulation. 2017 Mar 14;135(11):1075-1092. doi: 10.1161/CIRCULATIONAHA.116.024534. PMID: 28289007; PMCID: PMC5385930.

Banovic MD, Vujisic-Tesic BD, Kujacic VG, Callahan MJ, Nedeljkovic IP, Trifunovic DD, Aleksandric SB, Petrovic MZ, Obradovic SD, Ostojic MC. Coronary flow reserve in patients with aortic stenosis and nonobstructed coronary arteries. Acta Cardiol. 2011; 66:743–749. doi: 10.2143/AC.66.6.2136958

Baskurt OK, Meiselman HJ (2003). "Blood rheology and hemodynamics". Seminars in Thrombosis and Haemostasis. **29** (5): 435–450. doi:10.1055/s-2003-44551. PMID 14631543. S2CID 17873138.

Berry C, Sidik N, Pereira AC, Ford TJ, Touyz RM, Kaski JC, Hainsworth AH. Small-Vessel Disease in the Heart and Brain: Current Knowledge, Unmet Therapeutic Need, and Future Directions. J Am Heart Assoc. 2019;8(3):e011104.

Bevan GH, Zidar DA, Josephson RA, Al-Kindi SG. Mortality Due to Aortic Stenosis in the United States, 2008-2017. JAMA. 2019 Jun 11;321(22):2236-2238. doi: 10.1001/jama.2019.6292. PMID: 31184728; PMCID: PMC6563552.

Beyerbacht HP, Lamb HJ, van Der Laarse A, Vliegen HW, Leujes F, Hazekamp MG, de Roos A, van Der Wall EE. Aortic valve replacement in patients with aortic valve stenosis improves myocardial metabolism and diastolic function. Radiology. 2001; 219:637–643. doi: 10.1148/radiology.219.3.r01jn25637.

Bhatnagar P, Wickramasinghe K, Wilkins E, Townsend N. Trends in the epidemiology of cardiovascular disease in the UK. Heart. 2016 Dec

15;102(24):1945-1952. doi: 10.1136/heartjnl-2016-309573. Epub 2016 Aug 22. PMID: 27550425; PMCID: PMC5256396.

Birkemeyer R, Maisch L, Dahme T, Spieß J, Althaus K, Schneider S, Ravens U, Haase D, Schotten U. Feasibility of digital atrial fibrillation screening in an elderly population : The Ulm heart rhythm weeks. Herzschrittmacherther Elektrophysiol. 2021 Sep;32(3):346-352. English. doi: 10.1007/s00399-021-00783-2. Epub 2021 Jul 9. PMID: 34241681.

Blann AD, Landray MJ, Lip GY. ABC of antithrombotic therapy: An overview of antithrombotic therapy [published correction appears in BMJ 2002 Nov 23;325(7374):1231]. *BMJ*. 2002;325(7367):762-765. doi:10.1136/bmj.325.7367.762

Bos D, Leening MJ, Kavousi M, et al. Comparison of atherosclerotic calcification in major vessel beds on the risk of all-cause and cause-specific mortality: the Rotterdam Study [published online December 11, 2015]. Circ Cardiovasc Imaging.

Brennan PF, McNeil AJ, Jing M, Awuah A, Moore JS, Mailey J, Finlay DD, Blighe K, McLaughlin JAD, Nesbit MA, Trucco E, Moore TCB, Spence MS. Assessment of the conjunctival microcirculation for patients presenting

with acute myocardial infarction compared to healthy controls. Sci Rep. 2021 Apr 7;11(1):7660. doi: 10.1038/s41598-021-87315-7. PMID: 33828174; PMCID: PMC8027463.

Brennan PF, Jing M, McNeil AJ, Awuah A, Mailey J, Kelly B, Finlay DD, Blighe K, McLaughlin JAD, Nesbit MA, Trucco E, Lockhart CJ, Moore TCB, Spence MS. Assessment of the conjunctival microcirculation in adult patients with cyanotic congenital heart disease compared to healthy controls. Microvasc Res. 2021 Jul;136:104167. doi: 10.1016/j.mvr.2021.104167. Epub 2021 Apr 7. PMID: 33838207.

Camici PG, Crea F. Coronary microvascular dysfunction. N Engl J Med. 2007 Feb 22;356(8):830-40. doi: 10.1056/NEJMra061889. PMID: 17314342.

Caponcello MG, Banderas LM, Ferrero C, Bramlage C, Thoenes M, Bramlage P. Gender differences in aortic valve replacement: is surgical aortic valve replacement riskier and transcatheter aortic valve replacement safer in women than in men? J Thorac Dis. 2020 Jul;12(7):3737-3746. doi: 10.21037/jtd-20-700. PMID: 32802453; PMCID: PMC7399394.

Carabello BA. The relationship of left ventricular geometry and hypertrophy to left ventricular function in valvular heart disease. J Heart Valve Dis. 1995; 4(suppl 2):S132–S138; discussion S138

Chang SM, Nabi F, Xu J, et al. Value of CACS compared with ETT and myocardial perfusion imaging for predicting long-term cardiac outcome in asymptomatic and symptomatic patients at low risk for coronary disease: clinical implications in a multimodality imaging world. JACC Cardiovasc Imaging. 2015;8(2):134-144.

Chen W, Xu Z, Jiang H, Zhou J, Wang L, Wang J. Altered Bulbar Conjunctival Microcirculation in Response to Contact Lens Wear. Eye Contact Lens. 2017 Mar;43(2):95-99. doi: 10.1097/ICL.0000000000000241. PMID: 27078615; PMCID: PMC5063651.

Cheung AT, Perez RV, Chen PC. Improvements in diabetic microangiopathy after successful simultaneous pancreas-kidney transplantation: a computer-assisted intravital microscopy study on the conjunctival microcirculation. Transplantation. 1999 Oct 15;68(7):927-32. doi: 10.1097/00007890-199910150-00005. PMID: 10532529.

Cheung AT, Hu BS, Wong SA, Chow J, Chan MS, To WJ, Li J, Ramanujam S, Chen PC. Microvascular abnormalities in the bulbar conjunctiva of contact lens users. Clin Hemorheol Microcirc. 2012;51(1):77-86. doi: 10.3233/CH-2011-1513. PMID: 22240372.

Coutinho T, Mielniczuk LM, Srivaratharajah K, deKemp R, Wells GA, Beanlands RS. Coronary artery microvascular dysfunction: Role of sex and arterial load. Int J Cardiol. 2018 Nov 1;270:42-47. doi: 10.1016/j.ijcard.2018.06.072. Epub 2018 Jun 20. PMID: 29954671.

Cramariuc D, Gerdts E, Davidsen ES, Segadal L, Matre K. Myocardial deformation in aortic valve stenosis: relation to left ventricular geometry. Heart. 2010; 96:106–112. doi: 10.1136/hrt.2009.172569

Crawshaw J, Auyeung V, Norton S, Weinman J. Identifying psychosocial predictors of medication non-adherence following acute coronary syndrome: A systematic review and meta-analysis. J Psychosom Res 2016;90:10–32

Crea F, Camici PG, Bairey Merz CN. Coronary microvascular dysfunction: an update. Eur Heart J. 2014; 35:1101–1111. doi: 10.1093/eurheartj/eht513.

D'Arcy JL, Coffey S, Loudon MA, Kennedy A, Pearson-Stuttard J, Birks J, Frangou E, Farmer AJ, Mant D, Wilson J, Myerson SG, Prendergast BD. Large-scale community echocardiographic screening reveals a major burden of undiagnosed valvular heart disease in older people: the OxVALVE Population Cohort Study. Eur Heart J 2016;37:3515–3522

Davies JE, Whinnett ZI, Francis DP, Manisty CH, Aguado-Sierra J, Willson K, Foale RA, Malik IS, Hughes AD, Parker KH, Mayet J. Evidence of a dominant backward-propagating "suction" wave responsible for diastolic coronary filling in humans, attenuated in left ventricular hypertrophy. Circulation. 2006; 113:1768–1778. doi: 10.1161/CIRCULATIONAHA.105.603050

Davies JE, Sen S, Broyd C, Hadjiloizou N, Baksi J, Francis DP, Foale RA, Parker KH, Hughes AD, Chukwuemeka A, Casula R, Malik IS, Mikhail GW, Mayet J. Arterial pulse wave dynamics after percutaneous aortic valve replacement: fall in coronary diastolic suction with increasing heart rate as a basis for angina symptoms in aortic stenosis. Circulation. 2011; 124:1565–1572. doi: 10.1161/CIRCULATIONAHA.110.011916

Den Ruijter HM, Peters SA, Anderson TJ, Britton AR, Dekker JM, Eijkemans MJ, Engstrom G, Evans GW, de Graaf J, Grobbee DE, Hedblad B, Hofman A, Holewijn S, Ikeda A, Kavousi M, Kitagawa K, Kitamura A,

Koffijberg H, Lonn EM, Lorenz MW, Mathiesen EB, Nijpels G, Okazaki S, O'Leary DH, Polak JF, Price JF, Robertson C, Rembold CM, Rosvall M, Rundek T, Salonen JT, Sitzer M, Stehouwer CD, Witteman JC, Moons KG, Bots ML. Common carotid intima-media thickness measurements in cardiovascular risk prediction: a meta-analysis. JAMA 2012;308:796–803

Di Angelantonio E, Gao P, Pennells L, Kaptoge S, Caslake M, Thompson A, Butterworth AS, Sarwar N, Wormser D, Saleheen D, Ballantyne CM, Psaty BM, Sundstrom J, Ridker PM, Nagel D, Gillum RF, Ford I, Ducimetiere P, Kiechl S, Koenig W, Dullaart RP, Assmann G, D'Agostino RBSr., Dagenais GR, Cooper JA, Kromhout D, Onat A, Tipping RW, Gomez-de-la-Camara A, Rosengren A, Sutherland SE, Gallacher J, Fowkes FG, Casiglia E, Hofman A, Salomaa V, Barrett-Connor E, Clarke R, Brunner E, Jukema JW, Simons LA, Sandhu M, Wareham NJ, Khaw KT, Kauhanen J, Salonen JT, Howard WJ, Nordestgaard BG, Wood AM, Thompson SG, Boekholdt SM, Sattar N, Packard C, Gudnason V, Danesh J. Lipid-related markers and cardiovascular disease prediction. JAMA 2012;307:2499–2506

Elias-Smale SE, Proenca RV, Koller MT, et al. Coronary calcium score improves classification of coronary heart disease risk in the elderly: the Rotterdam study. J Am Coll Cardiol. 2010;56(17):1407-1414

Fearon WF, Balsam LB, Farouque HM, Caffarelli AD, Robbins RC, Fitzgerald PJ, Yock PG, Yeung AC. Novel index for invasively assessing the coronary microcirculation. Circulation. 2003;107:3129- 32.

Fearon WF, Kobayashi Y. Invasive Assessment of the Coronary Microvasculature: The Index of Microcirculatory Resistance. Circ Cardiovasc Interv. 2017 Dec;10(12). pii: e005361.

Ford TJ, Corcoran D, Berry C. Stable coronary syndromes: pathophysiology, diagnostic advances and therapeutic need. Heart. 2018 Feb;104(4):284-292. doi: 10.1136/heartjnl-2017-311446. Epub 2017 Oct 13. PMID: 29030424; PMCID: PMC5861393.

Ford TJ, Stanley B, Good R, Rocchiccioli P, McEntegart M, Watkins S, Eteiba H, Shaukat A, Lindsay M, Robertson K, Hood S, McGeoch R, McDade R, Yii E, Sidik N, McCartney P, Corcoran D, Collison D, Rush C, McConnachie A, Touyz RM, Oldroyd KG, Berry C. Stratified Medical Therapy Using Invasive Coronary Function Testing in Angina: The CorMicA Trial. J Am Coll Cardiol. 2018 Dec 11;72(23 Pt A):2841-2855. doi: 10.1016/j.jacc.2018.09.006. Epub 2018 Sep 25. PMID: 30266608.

Ford TJ, Yii E, Sidik N, Good R, Rocchiccioli P, McEntegart M, Watkins S, Eteiba H, Shaukat A, Lindsay M, Robertson K, Hood S, McGeoch R, McDade R, McCartney P, Corcoran D, Collison D, Rush C, Stanley B, McConnachie A, Sattar N, Touyz RM, Oldroyd KG, Berry C. Ischemia and No Obstructive Coronary Artery Disease: Prevalence and Correlates of Coronary Vasomotion Disorders. Circ Cardiovasc Interv. 2019 Dec;12(12):e008126.

Ford TJ, Rocchiccioli P, Good R, McEntegart M, Eteiba H, Watkins S, Shaukat A, Lindsay M, Robertson K, Hood S, Yii E, Sidik N, Harvey A, Montezano A, Beattie E, Haddow L, Oldroyd KG, Touyz RM, Berry C. Systemic microvascular dysfunction in microvascular and vasospastic angina. Eur Heart J. 2018 Dec 7;39(46):4086-4097.

Forsberg D. Robust image registration for improved clinical efficiency: Using local structure analysis and model-based processing PhD Thesis, Linkoping University, Medical Informatics, The Institute of Technology, Center for Medical Image Science and Visualisation

Frangi, A.F., Niessen, W.J., Vincken, K.L., Viergever, M.A. (1998). Multiscale vessel enhancement filtering. In: Wells, W.M., Colchester, A., Delp, S. (eds) Medical Image Computing and Computer-Assisted Intervention — MICCAI'98. MICCAI 1998. Lecture Notes in Computer

Science, vol 1496. Springer, Berlin, Heidelberg.
https://doi.org/10.1007/BFb0056195

Fudim M, Zalawadiya S, Patel DK, Egolum UO, Afonso L. Data on coronary artery calcium score performance and cardiovascular risk reclassification across gender and ethnicities. Data Brief. 2016;6:578-581.

Fulton WFM. Arterial anastomoses in the coronary circulation. I. Anatomical features in normal and diseased hearts demonstrated by stereoarteriography. Scot Med J 1963;8:420 –34.

Galiuto L, Lotrionte M, Crea F, Anselmi A, Biondi-Zoccai GG, De Giorgio F, Baldi A, Baldi F, Possati G, Gaudino M, Vetrovec GW, Abbate A. Impaired coronary and myocardial flow in severe aortic stenosis is associated with increased apoptosis: a transthoracic Doppler and myocardial contrast echocardiography study. Heart. 2006; 92:208–212. doi: 10.1136/hrt.2005.062422.

Garabedian LF, Ross-Degnan D, Wharam JF. Mobile Phone and Smartphone Technologies for Diabetes Care and Self-Management. Curr Diab Rep. 2015 Dec;15(12):109. doi: 10.1007/s11892-015-0680-8. PMID: 26458380; PMCID: PMC6525331.

GBD 2015 Mortality and Causes of Death Collaborators. Global, regional, and national life expectancy, all-cause mortality, and cause-specific mortality for 249 causes of death, 1980-2015: a systematic analysis for the Global Burden of Disease Study 2015. Lancet 2016;388:1459–1544.

Geisel MH, Bauer M, Hennig F, et al. Comparison of coronary artery calcification, carotid intima-media thickness and ankle-brachial index for predicting 10-year incident cardiovascular events in the general population. Eur Heart J. 2017;38(23):1815-1822.

George H.F., Qureshi F. (2013) Newton's Law of Viscosity, Newtonian and Non-Newtonian Fluids. In: Wang Q.J., Chung YW. (eds) Encyclopedia of Tribology. Springer, Boston, MA. https://doi.org/10.1007/978-0-387-92897-5_143

Ghekiere O, Salgado R, Buls N, Leiner T, Mancini I, Vanhoenacker P, Dendale P, Nchimi A. Image quality in coronary CT angiography: challenges and technical solutions. Br J Radiol. 2017 Apr;90(1072):20160567. doi: 10.1259/bjr.20160567. Epub 2017 Mar 7. PMID: 28055253; PMCID: PMC5605061.

Gijsen F, Katagiri Y, Barlis P, Bourantas C, Collet C, Coskun U, Daemen J, Dijkstra J, Edelman E, Evans P, van der Heiden K, Hose R, Koo BK, Krams R, Marsden A, Migliavacca F, Onuma Y, Ooi A, Poon E, Samady H, Stone P, Takahashi K, Tang D, Thondapu V, Tenekecioglu E, Timmins L, Torii R, Wentzel J, Serruys P. Expert recommendations on the assessment of wall shear stress in human coronary arteries: existing methodologies, technical considerations, and clinical applications. Eur Heart J. 2019 Nov 1;40(41):3421-3433. doi: 10.1093/eurheartj/ehz551. PMID: 31566246; PMCID: PMC6823616.

Gonçalves A, Marcos-Alberca P, Almeria C, Feltes G, Rodríguez E, Hernández-Antolín RA, Garcia E, Maroto L, Fernandez Perez C, Silva Cardoso JC, Macaya C, Zamorano JL. Acute left ventricle diastolic function improvement after transcatheter aortic valve implantation. Eur J Echocardiogr. 2011; 12:790–797. doi: 10.1093/ejechocard/jer147.

Gould KL, Johnson NP, Bateman TM, Beanlands RS, Bengel FM, Bober R, Camici PG, Cerqueira MD, Chow BJW, Di Carli MF, Dorbala S, Gewirtz H, Gropler RJ, Kaufmann PA, Knaapen P, Knuuti J, Merhige ME, Rentrop KP, Ruddy TD, Schelbert HR, Schindler TH, Schwaiger M, Sdringola S, Vitarello J, Williams KA Sr, Gordon D, Dilsizian V, Narula J. Anatomic versus physiologic assessment of coronary artery disease. Role of coronary flow reserve, fractional flow reserve, and positron emission tomography imaging in revascularization decision-making. J Am Coll

Cardiol. 2013 Oct 29;62(18):1639-1653. doi: 10.1016/j.jacc.2013.07.076. Epub 2013 Aug 28. PMID: 23954338.

Gould KL, Johnson NP. Coronary Physiology Beyond Coronary Flow Reserve in Microvascular Angina: JACC State-of-the-Art Review. J Am Coll Cardiol. 2018;72:2642-2662.

Greenland P, LaBree L, Azen SP, Doherty TM, Detrano RC. Coronary artery calcium score combined with Framingham score for risk prediction in asymptomatic individuals. JAMA. 2004;291(2):210-215

Hadamitzky M, Freissmuth B, Meyer T, Hein F, Kastrati A, Martinoff S, Schomig A, Hausleiter J. Prognostic value of coronary computed tomographic angiography for prediction of cardiac events in patients with suspected coronary artery disease. JACC Cardiovasc Imaging 2009;2:404–411.

Hennekens CH, Gaziano JM. Antioxidants and heart disease: Epidemiology and clinical evidence. *Clin Cardiol.* 1993;16(4 Suppl 1):I10–3

Hildick-Smith DJ, Shapiro LM. Coronary flow reserve improves after aortic valve replacement for aortic stenosis: an adenosine transthoracic echocardiography study. J Am Coll Cardiol. 2000; 36:1889–1896.

Hippisley-Cox J, Coupland C, Brindle P. Development and validation of QRISK3 risk prediction algorithms to estimate future risk of cardiovascular disease: prospective cohort study. BMJ 2017;357:j2099

Hiteshi AK, Li D, Gao Y, Chen A, Flores F, Mao SS, Budoff MJ. Gender differences in coronary artery diameter are not related to body habitus or left ventricular mass. Clin Cardiol. 2014 Oct;37(10):605-9. doi: 10.1002/clc.22310. Epub 2014 Sep 30. PMID: 25269657; PMCID: PMC6649484.

Hoffmann U, Massaro JM, D'Agostino RB Sr, Kathiresan S, Fox CS, O'Donnell CJ. Cardiovascular event prediction and risk reclassification by coronary, aortic, and valvular calcification in the Framingham Heart Study. J Am Heart Assoc. 2016;5(2):e003144

Hu L, Shu XP, Xu YY, Cheng J, Xu ZQ, Wang JH, Lyu F. [Clinical study on microcirculation changes of bulbar conjunctiva after contact lens wear].

Zhonghua Yan Ke Za Zhi. 2019 Feb 11;55(2):98-104. Chinese. doi: 10.3760/cma.j.issn.0412-4081.2019.02.006. PMID: 30772987.

Iung B, Delgado V, Rosenhek R, Price S, Prendergast B, Wendler O, De Bonis M, Tribouilloy C, Evangelista A, Bogachev-Prokophiev A, Apor A, Ince H, Laroche C, Popescu BA, Pierard L, Haude M, Hindricks G, Ruschitzka F, Windecker S, Bax JJ, Maggioni A, Vahanian A, EORP VHD II Investigators. Contemporary presentation and management of valvular heart disease: The EURObservational Research Programme Valvular Heart Disease II Survey. Circulation 2019;140:1156–1169.

Jerman T, Pernuš F, Likar B, Špiclin Ž. Enhancement of vascular structures in 3D and 2D angiographic images. IEEE transactions on medical imaging. 2016 Apr 4;35(9):2107-18.

Jespersen L, Hvelplund A, Abildstrøm SZ, Pedersen F, Galatius S, Madsen JK, Jørgensen E, Kelbæk H, Prescott E. Stable angina pectoris with no obstructive coronary artery disease is associated with increased risks of major adverse cardiovascular events. Eur Heart J. 2012 Mar;33(6):734-44. doi: 10.1093/eurheartj/ehr331. Epub 2011 Sep 11. PMID: 21911339.

Jespersen L, Abildstrøm SZ, Hvelplund A, Prescott E. Persistent angina: highly prevalent and associated with long-term anxiety, depression, low physical functioning, and quality of life in stable angina pectoris. Clin Res Cardiol. 2013 Aug;102(8):571-81. doi: 10.1007/s00392-013-0568-z. Epub 2013 May 1. PMID: 23636227.

Jiang H, Zhong J, DeBuc DC, Tao A, Xu Z, Lam BL, Liu C, Wang J. Functional slit-lamp biomicroscopy for imaging bulbar conjunctival microvasculature in contact lens wearers. Microvasc Res. 2014 Mar;92:62-71. doi: 10.1016/j.mvr.2014.01.005. Epub 2014 Jan 17. PMID: 24444784; PMCID: PMC3960300.

Jo HC, Jeong H, Lee J, Na KS, Kim DY. Quantification of Blood Flow Velocity in the Human Conjunctival Microvessels Using Deep Learning-Based Stabilization Algorithm. Sensors (Basel). 2021 May 6;21(9):3224. doi: 10.3390/s21093224. PMID: 34066590; PMCID: PMC8124391.

Kamstrup PR, Tybjaerg-Hansen A, Nordestgaard BG. Extreme lipoprotein(a) levels and improved cardiovascular risk prediction. J Am Coll Cardiol 2013;61:1146–1156

Karanam VC, Tamariz L, Batawi H, Wang J, Galor A. Functional slit-lamp biomicroscopy metrics correlate with cardiovascular risk. Ocul Surf. 2019 Jan;17(1):64-69. doi: 10.1016/j.jtos.2018.09.002. Epub 2018 Sep 22. PMID: 30253248; PMCID: PMC6340746.

Kaski JC, Crea F, Gersh BJ, Camici PG. Reappraisal of Ischemic Heart Disease. Circulation. 2018 Oct 2;138(14):1463-1480. doi: 10.1161/CIRCULATIONAHA.118.031373. PMID: 30354347.

Kaski JC, Tousoulis D, Gavrielides S, McFadden E, Galassi AR, Crea F, Maseri A. Comparison of epicardial coronary artery tone and reactivity in Prinzmetal's variant angina and chronic stable angina pectoris. J Am Coll Cardiol. 1991;17:1058-62.

Kavousi M, Desai CS, Ayers C, et al. Prevalence and prognostic implications of coronary artery calcification in low-risk women: a meta-analysis. JAMA. 2016;316(20):2126-2134.

Kavousi M, Elias-Smale S, Rutten JH, et al. Evaluation of newer risk markers for coronary heart disease risk classification: a cohort study. Ann Intern Med. 2012;156(6):438-444

Kelshiker MA, Seligman H, Howard JP, Rahman H, Foley M, Nowbar AN, Rajkumar CA, Shun-Shin MJ, Ahmad Y, Sen S, Al-Lamee R, Petraco R. Coronary flow reserve and cardiovascular outcomes: a systematic review and meta-analysis. Eur Heart J. 2022 Apr 19;43(16):1582-1593. doi: 10.1093/eurheartj/ehab775. PMID: 34849697; PMCID: PMC9020988.

Kenny A, Wisbey CR, Shapiro LM. Profiles of coronary blood flow velocity in patients with aortic stenosis and the effect of valve replacement: a transthoracic echocardiographic study. Br Heart J. 1994; 71:57–62. doi: 10.1136/hrt.71.1.57.

Khansari MM, Wanek J, Felder AE, Camardo N, Shahidi M. Automated Assessment of Hemodynamics in the Conjunctival Microvasculature Network. IEEE Trans Med Imaging. 2016 Feb;35(2):605-11. doi: 10.1109/TMI.2015.2486619. Epub 2015 Oct 6. PMID: 26452274; PMCID: PMC4821773.

Khansari MM, Wanek J, Tan M, Joslin CE, Kresovich JK, Camardo N, Blair NP, Shahidi M. Assessment of Conjunctival Microvascular Hemodynamics in Stages of Diabetic Microvasculopathy. Sci Rep. 2017 Apr 7;7:45916. doi: 10.1038/srep45916. PMID: 28387229; PMCID: PMC5384077.

Kim JM, Stewart R, Kang HJ, Kim SY, Kim JW, Lee HJ, Lee JY, Kim SW, Shin IS, Kim MC, Shin HY, Hong YJ, Ahn Y, Jeong MH, Yoon JS. Long-term cardiac outcomes of depression screening, diagnosis and treatment in patients with acute coronary syndrome: the DEPACS study. Psychol Med 2020:1–11

Kim KH, Kerndt CC, Adnan G, Schaller DJ. Nitroglycerin. 2021 Nov 4. In: StatPearls [Internet]. Treasure Island (FL): StatPearls Publishing; 2022 Jan–. PMID: 29494004.

Kivimäki M, Steptoe A. Effects of stress on the development and progression of cardiovascular disease. Nat Rev Cardiol. 2018 Apr;15(4):215-229. doi: 10.1038/nrcardio.2017.189. Epub 2017 Dec 7. PMID: 29213140

Knuuti J, Wijns W, Saraste A, Capodanno D, Barbato E, Funck-Brentano C, Prescott E, Storey RF, Deaton C, Cuisset T, Agewall S, Dickstein K, Edvardsen T, Escaned J, Gersh BJ, Svitil P, Gilard M, Hasdai D, Hatala R, Mahfoud F, Masip J, Muneretto C, Valgimigli M, Achenbach S, Bax JJ; ESC Scientific Document Group. 2019 ESC Guidelines for the diagnosis and management of chronic coronary syndromes. Eur Heart J. 2020 Jan 14;41(3):407-477. doi: 10.1093/eurheartj/ehz425. Erratum in: Eur Heart J. 2020 Nov 21;41(44):4242. PMID:

Kobayashi Y, Fearon WF, Honda Y, Tanaka S, Pargaonkar V, Fitzgerald PJ, Lee DP, Stefanick M, Yeung AC, Tremmel JA. Effect of Sex Differences on Invasive Measures of Coronary Microvascular Dysfunction in Patients With Angina in the Absence of Obstructive Coronary Artery Disease. JACC Cardiovasc Interv. 2015;8:1433-41.

Koide M, Nagatsu M, Zile MR, Hamawaki M, Swindle MM, Keech G, DeFreyte G, Tagawa H, Cooper G, Carabello BA. Premorbid determinants of left ventricular dysfunction in a novel model of gradually induced pressure overload in the adult canine. Circulation. 1997; 95:1601–1610.

Kord Valeshabad A, Wanek J, Mukarram F, Zelkha R, Testai FD, Shahidi M. Feasibility of assessment of conjunctival microvascular hemodynamics in unilateral ischemic stroke. Microvasc Res. 2015 Jul;100:4-8. doi: 10.1016/j.mvr.2015.04.007. Epub 2015 Apr 24. PMID: 25917010; PMCID: PMC4461531.

Kord Valeshabad A, Wanek J, Zelkha R, Lim JI, Camardo N, Gaynes B, Shahidi M. Conjunctival microvascular haemodynamics in sickle cell retinopathy. Acta Ophthalmol. 2015 Jun;93(4):e275-80. doi: 10.1111/aos.12593. Epub 2014 Nov 27. PMID: 25429907; PMCID: PMC4437847.

Koutsiaris AG, Tachmitzi SV, Batis N, Kotoula MG, Karabatsas CH, Tsironi E, Chatzoulis DZ. Volume flow and wall shear stress quantification in the human conjunctival capillaries and post-capillary venules in vivo. Biorheology. 2007;44(5-6):375-86. PMID: 18401076.

Koutsiaris AG, Tachmitzi SV, Papavasileiou P, Batis N, Kotoula MG, Giannoukas AD, Tsironi E. Blood velocity pulse quantification in the human conjunctival pre-capillary arterioles. Microvasc Res. 2010 Sep;80(2):202-8. doi: 10.1016/j.mvr.2010.05.001. Epub 2010 May 18. PMID: 20478318.

Koutsiaris AG, Tachmitzi SV, Batis N. Wall shear stress quantification in the human conjunctival pre-capillary arterioles in vivo. Microvasc Res. 2013 Jan;85:34-9. doi: 10.1016/j.mvr.2012.11.003. Epub 2012 Nov 12. PMID: 23154279.

Koutsiaris AG. Correlation of axial blood velocity to venular and arteriolar diameter in the human eye in vivo. Clin Hemorheol Microcirc. 2015;61(3):429-38. doi: 10.3233/CH-141888. PMID: 25267455.

Kwak BR, Bäck M, Bochaton-Piallat ML, Caligiuri G, Daemen MJ, Davies PF, Hoefer IE, Holvoet P, Jo H, Krams R, Lehoux S, Monaco C, Steffens

S, Virmani R, Weber C, Wentzel JJ, Evans PC. Biomechanical factors in atherosclerosis: mechanisms and clinical implications. Eur Heart J. 2014 Nov 14;35(43):3013-20, 3020a-3020d. doi: 10.1093/eurheartj/ehu353. Epub 2014 Sep 17. PMID: 25230814; PMCID: PMC4810806.

Kwon, G.P., Schroeder, J.L., Amar, M.J., Remaley, A.T. & Balaban, R.S. Contribution of macromolecular structure to the retention of low-density lipoprotein at arterial branch points. *Circulation* **117**, 2919–2927 (2008).

Layland J, Carrick D, McEntegart M, Ahmed N, Payne A, McClure J, Sood A, McGeoch R, MacIsaac A, Whitbourn R, Wilson A, Oldroyd K, Berry C. Vasodilatory capacity of the coronary microcirculation is preserved in selected patients with non-ST-segment-elevation myocardial infarction. Circ Cardiovasc Interv. 2013;6:231-6.

Lei H, Karniadakis GE. Quantifying the rheological and hemodynamic characteristics of sickle cell anemia. Biophys J. 2012 Jan 18;102(2):185-94. doi: 10.1016/j.bpj.2011.12.006. PMID: 22339854; PMCID: PMC3260690.

Leon MB, Smith CR, Mack MJ, et al; PARTNER 2 Investigators. Transcatheter or Surgical Aortic-Valve Replacement in Intermediate-Risk Patients. N Engl J Med. 2016 Apr 28;374(17):1609-20.

Leon MB, Smith CR, Mack M, Miller DC, Moses JW, Svensson LG, Tuzcu EM, Webb JG, Fontana GP, Makkar RR, Brown DL, Block PC, Guyton RA, Pichard AD, Bavaria JE, Herrmann HC, Douglas PS, Petersen JL, Akin JJ, Anderson WN, Wang D, Pocock S; PARTNER Trial Investigators. Transcatheter aortic-valve implantation for aortic stenosis in patients who cannot undergo surgery. N Engl J Med. 2010 Oct 21;363(17):1597-607. doi: 10.1056/NEJMoa1008232. Epub 2010 Sep 22. PMID: 20961243.

Lester SJ, Heilbron B, Gin K, Dodek A, Jue J. The natural history and rate of progression of aortic stenosis. Chest. 1998; 113:1109–1114. doi: 10.1378/chest.113.4.1109.

Lin JS, Evans CV, Johnson E, Redmond N, Coppola EL, Smith N. Nontraditional Risk Factors in Cardiovascular Disease Risk Assessment: Updated Evidence Report and Systematic Review for the US Preventive Services Task Force. JAMA. 2018 Jul 17;320(3):281-297. doi: 10.1001/jama.2018.4242. PMID: 29998301

Lindemann H, Petrovic I, Hill S, Athanasiadis A, Mahrholdt H, Schäufele T, Klingel K, Sechtem U, Ong P. Biopsy-confirmed endothelial cell activation in patients with coronary microvascular dysfunction. Coron Artery Dis. 2018;29:216-222.

Mack MJ, Leon MB, Thourani VH, et al; PARTNER 3 Investigators. Transcatheter Aortic-Valve Replacement with a Balloon-Expandable Valve in Low-Risk Patients. N Engl J Med. 2019 May 2;380(18):1695-1705.

Maddox TM, Stanislawski MA, Grunwald GK, Bradley SM, Ho PM, Tsai TT, Patel MR, Sandhu A, Valle J, Magid DJ, Leon B, Bhatt DL, Fihn SD, Rumsfeld JS. Nonobstructive coronary artery disease and risk of myocardial infarction. JAMA.2014;312:1754-63.

Mahmod M, Francis JM, Pal N, Lewis A, Dass S, De Silva R, Petrou M, Sayeed R, Westaby S, Robson MD, Ashrafian H, Neubauer S, Karamitsos TD. Myocardial perfusion and oxygenation are impaired during stress in severe aortic stenosis and correlate with impaired energetics and subclinical left ventricular dysfunction. J Cardiovasc Magn Reson. 2014; 16:29. doi: 10.1186/1532-429X-16-29.

Malik S, Budoff MJ, Katz R, et al. Impact of subclinical atherosclerosis on cardiovascular disease events in individuals with metabolic syndrome and diabetes: the multi-ethnic study of atherosclerosis. Diabetes Care. 2011;34(10):2285-2290

Marmot MG, Smith GD, Stansfeld S, Patel C, North F, Head J, White I, Brunner E, Feeney A. Health inequalities among British civil servants: the Whitehall II study. Lancet. 1991 Jun 8;337(8754):1387-93. doi: 10.1016/0140-6736(91)93068-k. PMID: 1674771.

Mathew RC, Bourque JM, Salerno M, Kramer CM. Cardiovascular Imaging Techniques to Assess Microvascular Dysfunction. JACC Cardiovasc Imaging. 2020 Jul;13(7):1577-1590. doi: 10.1016/j.jcmg.2019.09.006. Epub 2019 Oct 11. PMID: 31607665; PMCID: PMC7148179.

McConkey HZR, Marber M, Chiribiri A, Pibarot P, Redwood SR, Prendergast BD. Coronary Microcirculation in Aortic Stenosis. Circ Cardiovasc Interv. 2019 Aug;12(8):e007547. doi: 10.1161/CIRCINTERVENTIONS.118.007547. Epub 2019 Aug 16. PMID: 31416359; PMCID: PMC6733603.

Mehta S, Wells S, Grey C, Riddell T, Kerr A, Marshall R, Ameratunga S, Harrison J, Kenealy T, Bramley D, Chan WC, Thornley S, Sundborn G, Jackson R. Initiation and maintenance of cardiovascular medications following cardiovascular risk assessment in a large primary care cohort: PREDICT CVD-16. Eur J Prev Cardiol. 2014 Feb;21(2):192-202. doi: 10.1177/2047487312462150. Epub 2012 Oct 2. PMID: 23033546

Mejía-Rentería H, van der Hoeven N, van de Hoef TP, Heemelaar J, Ryan N, Lerman A, van Royen N, Escaned J. Targeting the dominant mechanism of coronary microvascular dysfunction with intracoronary physiology tests. Int J Cardiovasc Imaging. 2017 Jul;33(7):1041-1059. doi: 10.1007/s10554-017-1136-9. Epub 2017 May 13. PMID: 28501910.

Meyer PA. Patterns of blood flow in episcleral vessels studied by low-dose fluorescein videoangiography. Eye (Lond). 1988;2 (Pt 5):533-46. doi: 10.1038/eye.1988.104. PMID: 3256492.

Meyer PAR. Re-orchestration of blood flow by micro-circulations. Eye (Lond). 2018 Feb;32(2):222-229. doi: 10.1038/eye.2017.315. Epub 2018 Jan 19. PMID: 29350685; PMCID: PMC5811746.

Mileva N, Nagumo S, Mizukami T, Sonck J, Berry C, Gallinoro E, Monizzi G, Candreva A, Munhoz D, Vassilev D, Penicka M, Barbato E, De Bruyne B, Collet C. Prevalence of Coronary Microvascular Disease and Coronary Vasospasm in Patients With Nonobstructive Coronary Artery Disease: Systematic Review and Meta-Analysis. J Am Heart Assoc. 2022 Apr 5;11(7):e023207. doi: 10.1161/JAHA.121.023207. Epub 2022 Mar 18. PMID: 35301851; PMCID: PMC9075440.

Minten L, McCutcheon K, Jentjens S, Vanhaverbeke M, Segers VFM, Bennett J, Dubois C. The coronary and microcirculatory measurements in patients with aortic valve stenosis study: rationale and design. Am J Physiol Heart Circ Physiol. 2021 Dec 1;321(6):H1106-H1116. doi: 10.1152/ajpheart.00541.2021. Epub 2021 Oct 22. PMID: 34676781.

Mitchell G.F. Arterial stiffness and hypertension. Hypertension, 64 (2014), pp. 13-18.

Miyagawa S, Masai T, Fukuda H, Yamauchi T, Iwakura K, Itoh H, Sawa Y. Coronary microcirculatory dysfunction in aortic stenosis: myocardial contrast echocardiography study. Ann Thorac Surg. 2009; 87:715–719. doi: 10.1016/j.athoracsur.2008.11.078

Mohlenkamp S, Moebus S, et al. Coronary risk stratification, discrimination, and reclassification improvement based on quantification of subclinical coronary atherosclerosis: the Heinz Nixdorf Recall Study. J Am Coll Cardiol. 2010;56(17):1397-1406

Mohlenkamp S, Lehmann N, Moebus S, et al. Quantification of coronary atherosclerosis and inflammation to predict coronary events and all-cause mortality. J Am Coll Cardiol. 2011;57(13):1455-1464

Moka S, Koutsiaris AG, Garas A, Messinis I, Tachmitzi SV, Giannoukas A, Tsironi EE. Blood flow velocity comparison in the eye capillaries and postcapillary venules between normal pregnant and non-pregnant women. Microvasc Res. 2020 Jan;127:103926. doi: 10.1016/j.mvr.2019.103926. Epub 2019 Sep 12. PMID: 31521542.

Moore, K.J. & Tabas, I. Macrophages in the pathogenesis of atherosclerosis. *Cell* **145**, 341–355 (2011).

Mosca L, Barrett-Connor E, Wenger NK. Sex/gender differences in cardiovascular disease prevention: what a difference a decade makes. Circulation. 2011;124(19):2145-2154. doi:10.1161/CIRCULATIONAHA.110.968792

Nagpal KC, Goldberg MF, Rabb MF. Ocular manifestations of sickle hemoglobinopathies. Surv Ophthalmol. 1977 Mar-Apr;21(5):391-411. doi: 10.1016/0039-6257(77)90042-x. PMID: 559355.

Nemes A, Balázs E, Csanády M, Forster T. Long-term prognostic role of coronary flow velocity reserve in patients with aortic valve stenosis - insights from the SZEGED Study. Clin Physiol Funct Imaging. 2009 Nov;29(6):447-52. doi: 10.1111/j.1475-097X.2009.00893.x. Epub 2009 Aug 27. PMID: 19712079.

Newby DE, Adamson PD, Berry C, Boon NA, Dweck MR, Flather M, Forbes J, Hunter A, Lewis S, MacLean S, Mills NL, Norrie J, Roditi G, Shah ASV, Timmis AD, van Beek EJR, Williams MC. Coronary CT Angiography and 5-Year Risk of Myocardial Infarction. N Engl J Med 2018;379:924–933

Ng MK, Yeung AC, Fearon WF. Invasive assessment of the coronary microcirculation: superior reproducibility and less hemodynamic dependence of index of microcirculatory resistance compared with coronary flow reserve. Circulation. 2006;113:2054-61.

NICE: Cardiovascular disease: risk assessment and reduction, including lipid modification. London: National Institute for Health and Care Excellence (NICE); 2016 Sep. PMID: 32200592

Ong P, Camici PG, Beltrame JF, Crea F, Shimokawa H, Sechtem U, Kaski JC, Bairey Merz CN; Coronary Vasomotion Disorders International Study Group (COVADIS). International standardization of diagnostic criteria for microvascular angina. Int J Cardiol. 2018 Jan 1;250:16-20. doi: 10.1016/j.ijcard.2017.08.068. Epub 2017 Sep 8. PMID: 29031990.

Osnabrugge RL, Mylotte D, Head SJ, Van Mieghem NM, Nkomo VT, LeReun CM, Bogers AJ, Piazza N, Kappetein AP. Aortic stenosis in the elderly: disease prevalence and number of candidates for transcatheter aortic valve replacement: a meta-analysis and modeling study. J Am Coll Cardiol.2.

Pantely GA, Bristow JD. Adenosine. Renewed interest in an old drug. Circulation. 1990 Nov;82(5):1854-6. doi: 10.1161/01.cir.82.5.1854. PMID: 2225382.

Patel MB, Bui LP, Kirkeeide RL, Gould KL. Imaging Microvascular Dysfunction and Mechanisms for Female-Male Differences in CAD. JACC

Cardiovasc Imaging. 2016 Apr;9(4):465-82. doi: 10.1016/j.jcmg.2016.02.003. PMID: 27056165.

Patel MR, Peterson ED, Dai D, Brennan JM, Redberg RF, Anderson HV, Brindis RG, Douglas PS. Low diagnostic yield of elective coronary angiography. N Engl J Med. 2010 Mar 11;362(10):886-95. doi: 10.1056/NEJMoa0907272. Erratum in: N Engl J Med. 2010 Jul 29;363(5):498. PMID: 20220183; PMCID: PMC3920593.

Patel R, Barnard S, Thompson K, Lagord C, Clegg E, Worrall R, Evans T, Carter S, Flowers J, Roberts D, Nuttall M, Samani NJ, Robson J, Kearney M, Deanfield J, Waterall J. Evaluation of the uptake and delivery of the NHS Health Check programme in England, using primary care data from 9.5 million people: a cross-sectional study. BMJ Open. 2020 Nov 5;10(11):e042963. doi: 10.1136/bmjopen-2020-042963. PMID: 33154064; PMCID: PMC7646358.

Peters SA, den Ruijter HM, Bots ML, Moons KG. Improvements in risk stratification for the occurrence of cardiovascular disease by imaging subclinical atherosclerosis: a systematic review. Heart. 2012 Feb;98(3):177-84. doi: 10.1136/heartjnl-2011-300747. Epub 2011 Nov 17. PMID: 22095617.

Piepoli MF, Hoes AW, Agewall S, Albus C, Brotons C, Catapano AL, Cooney MT, Corrà U, Cosyns B, Deaton C, Graham I, Hall MS, Hobbs FDR, Løchen ML, Löllgen H, Marques-Vidal P, Perk J, Prescott E, Redon J, Richter DJ, Sattar N, Smulders Y, Tiberi M, van der Worp HB, van Dis I, Verschuren WMM, Binno S; ESC Scientific Document Group. 2016 European Guidelines on cardiovascular disease prevention in clinical practice: The Sixth Joint Task Force of the European Society of Cardiology and Other Societies on Cardiovascular Disease Prevention in Clinical Practice (constituted by representatives of 10 societies and by invited experts) Developed with the special contribution of the European Association for Cardiovascular Prevention & Rehabilitation (EACPR). Eur Heart J. 2016 Aug 1;37(29):2315-2381. doi: 10.1093/eurheartj/ehw106. Epub 2016 May 23. PMID: 27222591; PMCID: PMC4986030.

Polak JF, Szklo M, O'Leary DH. Carotid intima-media thickness score, positive coronary artery calcium score, and incident coronary heart disease: the Multi-Ethnic Study of Atherosclerosis. J Am Heart Assoc. 2017;6(1):e004612.

Polonsky TS, McClelland RL, Jorgensen NW, et al. Coronary artery calcium score and risk classification for coronary heart disease prediction. JAMA. 2010;303(16):1610-1616.

Quemada D. A rheological model for studying the hematocrit dependence of red cell-red cell and red cell-protein interactions in blood. Biorheology. 1981;18(3-6):501-16. doi: 10.3233/bir-1981-183-615. PMID: 7326391.

Rafieian-Kopaei M, Setorki M, Doudi M, Baradaran A, Nasri H. Atherosclerosis: process, indicators, risk factors and new hopes. *Int J Prev Med*. 2014;5(8):927-946.

Rahman H, Corcoran D, Aetesam-Ur-Rahman M, Hoole SP, Berry C, Perera D. Diagnosis of patients with angina and non-obstructive coronary disease in the catheter laboratory. Heart. 2019 Jul 31. pii: heartjnl-2019-315042.

Rahman H, Demir OM, Khan F, Ryan M, Ellis H, Mills MT, Chiribiri A, Webb A, Perera D. Physiological Stratification of Patients With Angina Due to Coronary Microvascular Dysfunction. J Am Coll Cardiol. 2020 May 26;75(20):2538-2549. doi: 10.1016/j.jacc.2020.03.051. PMID: 32439003; PMCID: PMC7242900.

Rajalakshmi R, Subashini R, Anjana RM, Mohan V. Automated diabetic retinopathy detection in smartphone-based fundus photography using artificial intelligence. Eye (Lond). 2018 Jun;32(6):1138-1144. doi:

10.1038/s41433-018-0064-9. Epub 2018 Mar 9. PMID: 29520050; PMCID: PMC5997766.

Rajappan K, Rimoldi OE, Dutka DP, Ariff B, Pennell DJ, Sheridan DJ, Camici PG. Mechanisms of coronary microcirculatory dysfunction in patients with aortic stenosis and angiographically normal coronary arteries. Circulation. 2002; 105:470–476. doi: 10.1161/hc0402.102931.

Rajappan K, Bellenger NG, Melina G, Di Terlizzi M, Yacoub MH, Sheridan DJ, Pennell DJ. Assessment of left ventricular mass regression after aortic valve replacement–cardiovascular magnetic resonance versus M-mode echocardiography. Eur J Cardiothorac Surg. 2003; 24:59–65.

Rajappan K, Rimoldi OE, Camici PG, Bellenger NG, Pennell DJ, Sheridan DJ. Functional changes in coronary microcirculation after valve replacement in patients with aortic stenosis. Circulation. 2003; 107:3170–3175. doi: 10.1161/01.CIR.0000074211.28917.31.

Raju B, Raju NS, Akkara JD, Pathengay A. Do it yourself smartphone fundus camera - DIYretCAM. Indian J Ophthalmol. 2016 Sep;64(9):663-667. doi: 10.4103/0301-4738.194325. PMID: 27853015; PMCID: PMC5151157.

Rana JS, Gransar H, Wong ND, et al. Comparative value of coronary artery calcium and multiple blood biomarkers for prognostication of cardiovascular events. Am J Cardiol. 2012;109(10):1449-1453

Rassi AN, Pibarot P, Elmariah S. Left ventricular remodelling in aortic stenosis. Can J Cardiol. 2014 Sep;30(9):1004-11. doi: 10.1016/j.cjca.2014.04.026. Epub 2014 Apr 30. PMID: 25151283.

Reardon MJ, Van Mieghem NM, Popma JJ, et al; SURTAVI Investigators. Surgical or Transcatheter Aortic-Valve Replacement in Intermediate-Risk Patients. N Engl J Med. 2017 Apr 6;376(14):1321-1331.

Rim TH, Lee CJ, Tham YC, Cheung N, Yu M, Lee G, Kim Y, Ting DSW, Chong CCY, Choi YS, Yoo TK, Ryu IH, Baik SJ, Kim YA, Kim SK, Lee SH, Lee BK, Kang SM, Wong EYM, Kim HC, Kim SS, Park S, Cheng CY, Wong TY. Deep-learning-based cardiovascular risk stratification using coronary artery calcium scores predicted from retinal photographs. Lancet Digit Health. 2021 May;3(5):e306-e316. doi: 10.1016/S2589-7500(21)00043-1. PMID: 33890578.

Rosengren A, Hawken S, Ounpuu S, Sliwa K, Zubaid M, Almahmeed WA, Blackett KN, Sitthi-amorn C, Sato H, Yusuf S, INTERHEART investigators.

Association of psychosocial risk factors with risk of acute myocardial infarction in 11119 cases and 13648 controls from 52 countries (the INTERHEART study): case-control study. Lancet 2004;364:953–962

Ross J, Braunwald E. Aortic stenosis. Circulation. 1968; 38(1suppl):61–67. doi: 10.1161/01.cir.38.1s5.v-61.

Rozanski A, Gransar H, Shaw LJ, et al. Impact of coronary artery calcium scanning on coronary risk factors and downstream testing: the EISNER (Early Identification of Subclinical Atherosclerosis by Noninvasive Imaging Research) prospective randomized trial. J Am Coll Cardiol. 2011;57(15):1622-1632

Rozanski A. Behavioral cardiology: current advances and future directions. J Am Coll Cardiol 2014;64:100–110.

Russo A, Morescalchi F, Costagliola C, Delcassi L, Semeraro F. A Novel Device to Exploit the Smartphone Camera for Fundus Photography. J Ophthalmol. 2015;2015:823139. doi: 10.1155/2015/823139. Epub 2015 Jun 2. PMID: 26137320; PMCID: PMC4468345.

Samady H, Eshtehardi P, McDaniel MC, Suo J, Dhawan SS, Maynard C, Timmins LH, Quyyumi AA, Giddens DP. Coronary artery wall shear stress is associated with progression and transformation of atherosclerotic plaque and arterial remodeling in patients with coronary artery disease. Circulation. 2011 Aug 16;124(7):779-88. doi: 10.1161/CIRCULATIONAHA.111.021824. Epub 2011 Jul 25. PMID: 21788584.

Sara JD, Widmer RJ, Matsuzawa Y, Lennon RJ, Lerman LO, Lerman A. Prevalence of Coronary Microvascular Dysfunction Among Patients With Chest Pain and Nonobstructive Coronary Artery Disease. JACC Cardiovasc Interv 2015;8:1445-53.

Sax FL, Cannon RO 3rd, Hanson C, Epstein SE. Impaired forearm vasodilator reserve in patients with microvascular angina. Evidence of a generalized disorder of vascular function? N Engl J Med. 1987;317:1366-70.

Schattke S, Baldenhofer G, Prauka I, Zhang K, Laule M, Stangl V, Sanad W, Spethmann S, Borges AC, Baumann G, Stangl K, Knebel F. Acute regional improvement of myocardial function after interventional transfemoral aortic valve replacement in aortic stenosis: a speckle tracking

echocardiography study. Cardiovasc Ultrasound. 2012; 10:15. doi: 10.1186/1476-7120-10-15.13.

Schwarz F, Baumann P, Manthey J, Hoffmann M, Schuler G, Mehmel HC, Schmitz W, Kübler W. The effect of aortic valve replacement on survival. Circulation. 1982; 66:1105–1110. doi: 10.1161/01.cir.66.5.1105.

Shahidi M, Wanek J, Gaynes B, Wu T. Quantitative assessment of conjunctival microvascular circulation of the human eye. Microvasc Res. 2010 Mar;79(2):109-13. doi: 10.1016/j.mvr.2009.12.003. Epub 2010 Jan 4. PMID: 20053367; PMCID: PMC3253734.

Shi C, Jiang H, Gameiro GR, Wang J. Microcirculation in the conjunctiva and retina in healthy subjects. Eye Vis (Lond). 2019 Apr 6;6:11. doi: 10.1186/s40662-019-0136-3. PMID: 30993144; PMCID: PMC6451216.

Shumway CL, Motlagh M, Wade M. Anatomy, Head and Neck, Eye Conjunctiva. 2021 Jul 26. In: StatPearls [Internet]. Treasure Island (FL): StatPearls Publishing; 2021 Jan–. PMID: 30137787.

Si S, Moss JR, Sullivan TR, Newton SS, Stocks NP. Effectiveness of general practice-based health checks: a systematic review and meta-

analysis. Br J Gen Pract. 2014 Jan;64(618):e47-53. doi: 10.3399/bjgp14X676456. PMID: 24567582; PMCID: PMC3876170.

Siasos G, Sara JD, Zaromytidou M, Park KH, Coskun AU, Lerman LO, Oikonomou E, Maynard CC, Fotiadis D, Stefanou K, Papafaklis M, Michalis L, Feldman C, Lerman A, Stone PH. Local Low Shear Stress and Endothelial Dysfunction in Patients With Nonobstructive Coronary Atherosclerosis. J Am Coll Cardiol. 2018;71:2092-2102.

Sivapalaratnam S, Boekholdt SM, Trip MD, Sandhu MS, Luben R, Kastelein JJ, Wareham NJ, Khaw KT. Family history of premature coronary heart disease and risk prediction in the EPIC-Norfolk prospective population study. Heart 2010;96:1985–1989.

Smith CR, Leon MB, Mack MJ, et al; PARTNER Trial Investigators. Transcatheter versus surgical aortic-valve replacement in high-risk patients. N Engl J Med. 2011 Jun 9;364(23):2187-98.

Stein JH, Korcarz CE, Hurst RT, Lonn E, Kendall CB, Mohler ER, Najjar SS, Rembold CM, Post WS, American Society of Echocardiography Carotid Intima-Media Thickness Task Force. Use of carotid ultrasound to identify subclinical vascular disease and evaluate cardiovascular disease

risk: a consensus statement from the American Society of Echocardiography Carotid Intima-Media Thickness Task Force. Endorsed by the Society for Vascular Medicine. J Am Soc Echocardiogr 2008;21:93–111; quiz 189-190

Steinberg ML, Williams JM, Li Y. Poor Mental Health and Reduced Decline in Smoking Prevalence. Am J Prev Med 2015;49:362–369

Stokes KY, Granger DN. The microcirculation: A motor for the systemic inflammatory response and large vessel disease induced by hypercholesterolaemia? *J. Physiol.* 2005;**562**:647–653. doi: 10.1113/jphysiol.2004.079640

Stone PH, Maehara A, Coskun AU, Maynard CC, Zaromytidou M, Siasos G, Andreou I, Fotiadis D, Stefanou K, Papafaklis M, Michalis L, Lansky AJ, Mintz GS, Serruys PW, Feldman CL, Stone GW. Role of Low Endothelial Shear Stress and Plaque Characteristics in the Prediction of Nonculprit Major Adverse Cardiac Events: The PROSPECT Study. JACC Cardiovasc Imaging. 2018;11:462-471.

Taqueti VR, Di Carli MF. Coronary Microvascular Disease Pathogenic Mechanisms and Therapeutic Options: JACC State-of-the-Art Review. J Am Coll Cardiol. 2018;72:2625-2641.

Taqueti VR. Sex Differences in the Coronary System. Adv Exp Med Biol. 2018;1065:257-278. doi: 10.1007/978-3-319-77932-4_17. PMID: 30051390; PMCID: PMC6467060.

Tavakol M, Ashraf S, Brener SJ. Risks and complications of coronary angiography: a comprehensive review. Glob J Health Sci. 2012 Jan 1;4(1):65-93. doi: 10.5539/gjhs.v4n1p65. PMID: 22980117; PMCID: PMC4777042.

Tavella R, Cutri N, Tucker G, Adams R, Spertus J, Beltrame JF. Natural history of patients with insignificant coronary artery disease. Eur Heart J Qual Care Clin Outcomes 2016;2:117-124.

Thygesen K, Alpert JS, Jaffe AS, Chaitman BR, Bax JJ, Morrow DA, White HD; Executive Group on behalf of the Joint European Society of Cardiology (ESC)/American College of Cardiology (ACC)/American Heart Association (AHA)/World Heart Federation (WHF) Task Force for the Universal Definition of Myocardial Infarction. Fourth Universal Definition of

Myocardial Infarction (2018). J Am Coll Cardiol. 2018 Oct 30;72(18):2231-2264. doi: 10.1016/j.jacc.2018.08.1038. Epub 2018 Aug 25. PMID: 30153967.

Townsend N, Bhatnagar P, Wilkins E, et al*. Cardiovascular disease statistics 2015. London: British Heart Foundation, 2015.*

Vaccarino V, Badimon L, Bremner JD, Cenko E, Cubedo J, Dorobantu M, Duncker DJ, Koller A, Manfrini O, Milicic D, Padro T, Pries AR, Quyyumi AA, Tousoulis D, Trifunovic D, Vasiljevic Z, de Wit C, Bugiardini R; ESC Scientific Document Group Reviewers. Depression and coronary heart disease: 2018 position paper of the ESC working group on coronary pathophysiology and microcirculation. Eur Heart J. 2020 May 1;41(17):1687-1696. doi: 10.1093/eurheartj/ehy913. Erratum in: Eur Heart J. 2020 May 1;41(17):1696. PMID: 30698764.

Vahanian A, Beyersdorf F, Praz F, Milojevic M, Baldus S, Bauersachs J, Capodanno D, Conradi L, De Bonis M, De Paulis R, Delgado V, Freemantle N, Gilard M, Haugaa KH, Jeppsson A, Jüni P, Pierard L, Prendergast BD, Sádaba JR, Tribouilloy C, Wojakowski W; ESC/EACTS Scientific Document Group; ESC Scientific Document Group. 2021 ESC/EACTS Guidelines for the management of valvular heart disease.

Eur Heart J. 2021 Aug 28:ehab395. doi: 10.1093/eurheartj/ehab395. Epub ahead of print. PMID: 34453165.

Veronesi G, Gianfagna F, Giampaoli S, Chambless LE, Mancia G, Cesana G, Ferrario MM. Improving long-term prediction of first cardiovascular event: the contribution of family history of coronary heart disease and social status. Prev Med 2014;64:75–80.

Visseren FLJ, Mach F, Smulders YM, Carballo D, Koskinas KC, Bäck M, Benetos A, Biffi A, Boavida JM, Capodanno D, Cosyns B, Crawford C, Davos CH, Desormais I, Di Angelantonio E, Franco OH, Halvorsen S, Hobbs FDR, Hollander M, Jankowska EA, Michal M, Sacco S, Sattar N, Tokgozoglu L, Tonstad S, Tsioufis KP, van Dis I, van Gelder IC, Wanner C, Williams B; ESC Scientific Document Group. 2021 ESC Guidelines on cardiovascular disease prevention in clinical practice. Eur Heart J. 2021 Sep 7;42(34):3227-3337. doi: 10.1093/eurheartj/ehab484. PMID: 34458905.

Vlachopoulos C, Aznaouridis K, Stefanadis C. Prediction of cardiovascular events and all-cause mortality with arterial stiffness: a systematic review and meta-analysis. J Am Coll Cardiol 2010;55:1318–1327

Wang L, Yuan J, Jiang H, Yan W, Cintrón-Colón HR, Perez VL, DeBuc DC, Feuer WJ, Wang J. Vessel Sampling and Blood Flow Velocity Distribution With Vessel Diameter for Characterizing the Human Bulbar Conjunctival Microvasculature. Eye Contact Lens. 2016 Mar;42(2):135-40. doi: 10.1097/ICL.0000000000000146. PMID: 25839347; PMCID: PMC4591084.

Wiegerinck EM, van de Hoef TP, Rolandi MC, Yong Z, van Kesteren F, Koch KT, Vis MM, de Mol BA, Piek JJ, Baan J. Impact of aortic valve stenosis on coronary hemodynamics and the instantaneous effect of transcatheter aortic valve implantation. Circ Cardiovasc Interv. 2015; 8:e002443. doi: 10.1161/CIRCINTERVENTIONS.114.002443.

Willeit P, Kaptoge S, Welsh P, Butterworth AS, Chowdhury R, Spackman SA, Pennells L, Gao P, Burgess S, Freitag DF, Sweeting M, Wood AM, Cook NR, Judd S, Trompet S, Nambi V, Olsen MH, Everett BM, Kee F, Arnlov J, Salomaa V, Levy D, Kauhanen J, Laukkanen JA, Kavousi M, Ninomiya T, Casas JP, Daniels LB, Lind L, Kistorp CN, Rosenberg J, Mueller T, Rubattu S, Panagiotakos DB, Franco OH, de Lemos JA, Luchner A, Kizer JR, Kiechl S, Salonen JT, Goya Wannamethee S, de Boer RA, Nordestgaard BG, Andersson J, Jorgensen T, Melander O, Ballantyne Ch M, DeFilippi C, Ridker PM, Cushman M, Rosamond WD, Thompson SG, Gudnason V, Sattar N, Danesh J, Di Angelantonio E. Natriuretic peptides and integrated risk assessment for cardiovascular

disease: an individual-participant-data meta-analysis. Lancet Diabetes Endocrinol 2016;4:840–849.

Willeit P, Welsh P, Evans JDW, Tschiderer L, Boachie C, Jukema JW, Ford I, Trompet S, Stott DJ, Kearney PM, Mooijaart SP, Kiechl S, Di Angelantonio E, Sattar N. High-Sensitivity Cardiac Troponin Concentration and Risk of First-Ever Cardiovascular Outcomes in 154,052 Participants. J Am Coll Cardiol 2017;70:558–568.

Wong ND, Gransar H, Shaw L, et al. Thoracic aortic calcium versus coronary artery calcium for the prediction of coronary heart disease and cardiovascular disease events. JACC Cardiovasc Imaging. 2009;2(3):319-326.

World health statistics 2020: monitoring health for the SDGs, sustainable development goals. Geneva: World Health Organization; 2020.Licence: CC BY-NC-SA 3.0 IGO.

Wormser D, Kaptoge S, Di Angelantonio E, Wood AM, Pennells L, Thompson A, Sarwar N, Kizer JR, Lawlor DA, Nordestgaard BG, Ridker P, Salomaa V, Stevens J, Woodward M, Sattar N, Collins R, Thompson SG, Whitlock G, Danesh J. Separate and combined associations of body-mass

index and abdominal adiposity with cardiovascular disease: collaborative analysis of 58 prospective studies. Lancet 2011;377:1085–1095

Xu Z, Jiang H, Tao A, Wu S, Yan W, Yuan J, Liu C, DeBuc DC, Wang J. Measurement variability of the bulbar conjunctival microvasculature in healthy subjects using functional slit-lamp biomicroscopy (FSLB). Microvasc Res. 2015 Sep;101:15-9. doi: 10.1016/j.mvr.2015.05.003. Epub 2015 Jun 16. PMID: 26092682; PMCID: PMC4537817.

Yadgir S, Johnson CO, Aboyans V, Adebayo OM, Adedoyin RA, Afarideh M, Alahdab F, Alashi A, Alipour V, Arabloo J, Azari S, Barthelemy CM, Benziger CP, Berman AE, Bijani A, Carrero JJ, Carvalho F, Daryani A, Duraes AR, Esteghamati A, Farid TA, Farzadfar F, Fernandes E, Filip I, Gad MM, Hamidi S, Hay SI, Ilesanmi OS, Naghibi Irvani SS, Jurisson M, Kasaeian A, Kengne AP, Khan AR, Kisa A, Kisa S, Kolte D, Manafi N, Manafi A, Mensah GA, Mirrakhimov EM, Mohammad Y, Mokdad AH, Negoi RI, Thi Nguyen HL, Nguyen TH, Nixon MR, Otto CM, Patel S, Pilgrim T, Radfar A, Rawaf DL, Rawaf S, Rawasia WF, Rezapour A, Roever L, Saad AM, Saadatagah S, Senthilkumaran S, Sliwa K, Tesfay BE, Tran BX, Ullah I, Vaduganathan M, Vasankari TJ, Wolfe CDA, Yonemoto N, Roth GA, Global Burden of Disease Study Nonrheumatic Valve Disease Collaborators. Global, regional, and national burden of calcific aortic valve and degenerative mitral valve diseases, 1990-2017. Circulation 2020;141:1670–1680.

Yarbrough WM, Mukherjee R, Ikonomidis JS, Zile MR, Spinale FG. Myocardial remodeling with aortic stenosis and after aortic valve replacement: mechanisms and future prognostic implications. J Thorac Cardiovasc Surg. 2012 Mar;143(3):656-64. doi: 10.1016/j.jtcvs.2011.04.044. Epub 2011 Jul 16. PMID: 21762938; PMCID: PMC3210937.

Yeboah J, Erbel R, Delaney JC, et al. Development of a new diabetes risk prediction tool for incident coronary heart disease events: the Multi-Ethnic Study of Atherosclerosis and the Heinz Nixdorf Recall Study. Atherosclerosis. 2014;236(2):411-417.

Yeboah J, McClelland RL, Polonsky TS, Burke GL, Sibley CT, O'Leary D, Carr JJ, Goff DC, Greenland P, Herrington DM. Comparison of novel risk markers for improvement in cardiovascular risk assessment in intermediate-risk individuals. JAMA 2012;308:788–795.

Yeboah J, Young R, McClelland RL, et al. Utility of nontraditional risk markers in atherosclerotic cardiovascular disease risk assessment. J Am Coll Cardiol. 2016;67(2):139-147